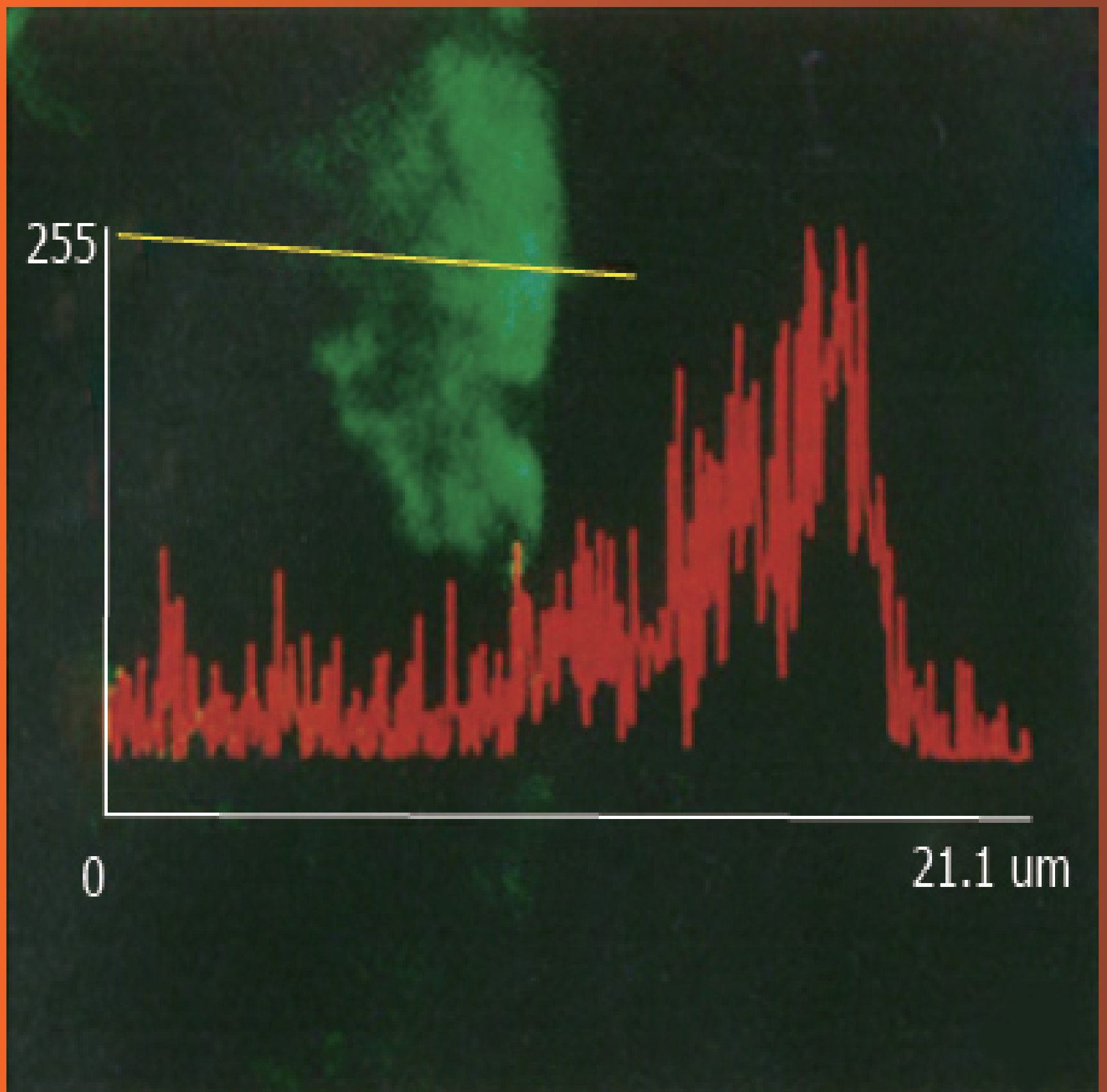


World Journal of *Gastroenterology*

World J Gastroenterol 1996 September 15; 2(3): 125-186



**EXPERIMENTAL PAPERS**

- 125 Mucosal permeability to lipopolysaccharides in the colon in chronic alcoholic rats
Chen XM, Xu RL, Ma XH, Zhou YC, Han DW
- 128 Expression of vascular endothelial growth factor and its prognostic significance in gastric carcinoma
Tao HQ, Qin LF, Lin YZ, Wang RN
- 131 Structure-activity relationship of pituitary adenylate cyclase activating polypeptide
Wei MX, Naruse S, Nokihara K, Ozaki T, Ando E, Wray V
- 134 Prevention of liver metastasis by intraperitoneal 5-FU chemotherapy in nude mice inoculated with human colon cancer cells
Feng GG, Zhou XG, Yu BM
- 136 Pharmacology of novel Chinese medicines screened for treatment of severe acute pancreatitis
Zhao LG, Wu XX, Zhu ZM, Chen YL, Liu FS, Chen JT
- 139 Effects of basic fibroblast growth factor on ischemic gut and liver injuries
Fu XB, Sheng ZY, Wang YP, Ye YX, Sun TZ, Ma NS, Chang GY, Xu MH, Zhou BT

CLINICAL ARTICLES

- 141 Study on traditional Chinese Medicine Syndrome-typing of chronic ulcerative colitis
Chen ZS, Zhou CM, Lu Y, Nie ZW, Sun QL, Wang YX, Chi Y
- 144 Radiological diagnosis of inflammatory ulcerative diseases of the small bowel
Lu Y, Duan JY, Gao Y
- 146 An epidemiologic study of *Helicobacter pylori* infection in three areas with high, moderate or low incidences of gastric carcinoma
Zhang WD, Wu Y, Liu GL, Yang HT, Zhou DY
- 149 Metal stent implantation for palliation of malignant biliary obstruction: A report of 57 cases
Hu B, Zhou DY, Gong B, Zhang FM, Wang SZ, Cheng HY, Wu MC
- 152 Ultrastructural observation of *Helicobacter pylori* to the gastric epithelia in chronic gastritis and peptic ulcers
Yang SM, Lin BZ, Fang Y, Zheng Y
- 155 Quantitative ultrastructure analysis of neuroendocrine cells of gastric mucosa in normal and pathological conditions
Yu JY, Adda T
- 158 Comparative study on the effects of hepatic arterial embolization with *Bletilla striata* or Gelfoam in treatment of primary hepatic carcinoma
Feng GS, Kramann B, Zheng CS, Zhou RM, Liang B, Zhang YF

- 161 Overexpression and mutations of tumor suppressor gene *p53* in hepatocellular carcinoma
Wang D, Shi JQ
- 165 Clinical use of hepatic carcinoma associated membrane protein antigen (HAg18-1) for detection of primary hepatocellular carcinoma
Hu SX, Fang GY
- 167 Magnetic resonance imaging of portal vein invasion in hepatocellular carcinoma: Results from 25 cases
Zhu XX, Chen JK, Lu GM
- 171 Evaluation of the IL-2/IL-2R system in patients with liver cirrhosis or carcinoma
Wang XZ, Lin GZ
- 173 Assessment of natural and interleukin-2-induced production of interferon-gamma in patients with liver diseases
Chen SB, Miao XH, Du P, Wu QX
- 176 Effects of acute hepatic damage on natriuresis and water excretion after acute normal saline loading in rats
Liu HQ, Ren CY, Jia LS, Yao XX, Ren XL
- 179 Effect of interferon in combination with ribavirin on the plus and minus strands of HCV RNA in patients with chronic hepatitis C
He YW, Liu W, Zen LL, Xiong KJ, Luo DD

REVIEW

- 182 Recent advances in the application of cultured hepatocytes into bioartificial liver
Xu XP, Yang JZ, Gao Y

BRIEF REPORT

- 185 Combination assay for serum tumor markers in patients with hepatic carcinoma
Zhao SL, Pan XF, Li SX, Liu DG

ABOUT COVER

Chen XM, Xu RL, Ma XH, Zhou YC, Han DW. Mucosal permeability to lipopolysaccharides in the colon in chronic alcoholic rats. *World J Gastroenterol* 1996; 2(3): 125-127

AIMS AND SCOPE

World Journal of Gastroenterology (*World J Gastroenterol*, *WJG*, print ISSN 1007-9327, online ISSN 2219-2840, DOI: 10.3748) is a peer-reviewed open access journal. *WJG* was established on October 1, 1995.

The primary task of *WJG* is to rapidly publish high-quality original articles, reviews, and commentaries in the fields of gastroenterology, hepatology, gastrointestinal endoscopy, gastrointestinal surgery, hepatobiliary surgery, gastrointestinal oncology, gastrointestinal radiation oncology, gastrointestinal imaging, gastrointestinal interventional therapy, gastrointestinal infectious diseases, gastrointestinal pharmacology, gastrointestinal pathophysiology, gastrointestinal pathology, evidence-based medicine in gastroenterology, pancreatology, gastrointestinal laboratory medicine, gastrointestinal molecular biology, gastrointestinal immunology, gastrointestinal microbiology, gastrointestinal genetics, gastrointestinal translational medicine, gastrointestinal diagnostics, and gastrointestinal therapeutics. *WJG* is dedicated to become an influential and prestigious journal in gastroenterology and hepatology, to promote the development of above disciplines, and to improve the diagnostic and therapeutic skill and expertise of clinicians.

INDEXING/ABSTRACTING

World Journal of Gastroenterology is now indexed in Current Contents[®]/Clinical Medicine, Science Citation Index Expanded (also known as SciSearch[®]), Journal Citation Reports[®], Index Medicus, MEDLINE, PubMed, PubMed Central.

EDITORS FOR
THIS ISSUE

Responsible Assistant Editor: *Xiang Li*
Responsible Electronic Editor: *Rui-Fang Li*
Proofing Editor-in-Chief: *Lian-Sheng Ma*

Responsible Science Editor: *Ze-Mao Gong*
Proofing Editorial Office Director: *Jin-Lei Wang*

NAME OF JOURNAL
World Journal of Gastroenterology

ISSN
ISSN 1007-9327 (print)
ISSN 2219-2840 (online)

LAUNCH DATE
October 1, 1995

FREQUENCY
Quarterly

EDITORS-IN-CHIEF
Bo-Yong Pan, President of China Speciality Council of Gastrology and China Association of Huatuo Medicine, Room 12, Building 621, the Fourth Military Medical University, Xi'an 710033, Shaanxi Province, China

Lian-Sheng Ma, Member of the Speciality Committee of Digestive Diseases, Chinese Association of Combined Traditional Chinese and Western Medicine, Taiyuan Research & Treatment Centre for Digestive Diseases, Taiyuan 030001, Shanxi Province, China

EDITORIAL OFFICE
Jin-Lei Wang, Director
Xiu-Xia Song, Vice Director
World Journal of Gastroenterology
Room 903, Building D, Ocean International Center,
No. 62 Dongsihuan Zhonglu, Chaoyang District,
Beijing 100025, China
Telephone: +86-10-59080039
Fax: +86-10-85381893
E-mail: editorialoffice@wjgnet.com
Help Desk: <http://www.wjgnet.com/esps/helpdesk.aspx>
<http://www.wjgnet.com>

PUBLISHER
Baishideng Publishing Group Inc
8226 Regency Drive,
Pleasanton, CA 94588, USA
Telephone: +1-925-223-8242
Fax: +1-925-223-8243
E-mail: bpgoffice@wjgnet.com
Help Desk: <http://www.wjgnet.com/esps/helpdesk.aspx>
<http://www.wjgnet.com>

PUBLICATION DATE
September 15, 1996

COPYRIGHT
© 1996 Baishideng Publishing Group Inc. Articles published by this Open-Access journal are distributed under the terms of the Creative Commons Attribution Non-commercial License, which permits use, distribution, and reproduction in any medium, provided the original work is properly cited, the use is non commercial and is otherwise in compliance with the license.

SPECIAL STATEMENT
All articles published in journals owned by the Baishideng Publishing Group (BPG) represent the views and opinions of their authors, and not the views, opinions or policies of the BPG, except where otherwise explicitly indicated.

INSTRUCTIONS TO AUTHORS
Full instructions are available online at http://www.wjgnet.com/bpg/g_info_19970116143427.htm

ONLINE SUBMISSION
<http://www.wjgnet.com/esps/>

Mucosal permeability to lipopolysaccharides in the colon in chronic alcoholic rats

Xian-Ming Chen, Rei-Ling Xu, Xiao-Hui Ma, Yuan-Chang Zhou, De-Wu Han

Xian-Ming Chen, Rei-Ling Xu, Xiao-Hui Ma, Yuan-Chang Zhou, De-Wu Han, Department of Pathophysiology, Shanxi Medical University, Taiyuan 030001 Shanxi Province, China

Xian-Ming Chen, male, born on 1964-04-21 in Chongyang City, Hubei Province, Han nationality, graduated from Shanxi Medical University as a postgraduate in 1988, associate professor of pathophysiology, major in hepatic pathophysiology, having 15 papers published.

Author contributions: All authors contributed equally to the work.

Presented at the Symposium on Alcoholic Liver Diseases and Cirrhosis, Nanjing, 26-28 July 1995.

Supported by the Natural Science Foundation for Youth of Shanxi Province No.93017, 95013.

Original title: *China National Journal of New Gastroenterology* (1995-1997) renamed *World Journal of Gastroenterology* (1998-).

Correspondence to: Dr. Xian-Ming Chen, Associate Professor, Department of Pathophysiology, Shanxi Medical University, Taiyuan 030001 Shanxi Province, China

Telephone: +86-351-4135067
Fax: +86-351-2024239

Received: July 21, 1996
Revised: August 14, 1996
Accepted: August 29, 1996
Published online: September 15, 1996

Abstract

AIM: To evaluate the effects of chronic alcohol abuse on the mucosal permeability to lipopolysaccharide in the colon in rats.

METHODS: *Escherichia coli* lipopolysaccharide (LPS, 20 µg/mL) was injected into the colon of chronic alcoholic rats ($n = 10$) and the rats were supplied with Lieber diets every other day for 6 weeks. Before LPS injection and 5, 10, 20, 30 min after injection, blood samples from the portal vein were obtained and contents of LPS in the blood were measured. The distribution of LPS in the colon tissues was observed with a confocal laser scanning microscope by immunofluorescent technique using a monoclonal antibody specific to the lipid A region of LPS. Normal rats were used as controls ($n = 6$).

RESULTS: Before LPS injection into the colon, LPS levels in the blood of portal vein of chronic alcoholic rats were significantly higher than those of normal controls (3.56 ± 0.67 pg/mLaa, vs 2.45 ± 0.15 pg/mLaa, $P < 0.01$). At 5, 10, 20, 30 min after injection of LPS, LPS contents were significantly higher than those before LPS injection (173.56 ± 23.45 pg/mLaa, 154.78 ± 20.57 pg/mLaa, 43.89 pg/mLaa ± 8.67 pg/mLaa, 45.38 ± 7.89 pg/mLaa vs 3.56 ± 0.67 pg/mLaa, $P < 0.01$ respectively). Most mucosal cells showed strong

positive reactions to LPS in the rats of chronic alcohol abuse, but no significant changes of LPS contents in blood from the portal vein and fluorescent reactions to LPS in mucosal cells of normal rats were found after LPS injection.

CONCLUSION: Chronic alcohol abuse resulted in a significant increase of permeability to LPS in colon mucosal cells in rats.

Key words: Colon; Alcohol; Ethyl polysaccharides; Bacterial; *Escherichia coli*

© The Author(s) 1996. Published by Baishideng Publishing Group Inc. All rights reserved.

Chen XM, Xu RL, Ma XH, Zhou YC, Han DW. Mucosal permeability to lipopolysaccharides in the colon in chronic alcoholic rats. *World J Gastroenterol* 1996; 2(3): 125-127 Available from: URL: <http://www.wjgnet.com/1007-9327/full/v2/i3/125.htm> DOI: <http://dx.doi.org/10.3748/wjg.v2.i3.125>

INTRODUCTION

Endotoxins are potent biological moieties from the outer membrane of Gram-negative bacteria and mainly composed of lipopolysaccharides (LPS) and proteins^[1]. LPS causes all the toxic actions endotoxin inflicts^[2]. Endotoxemia is a common complication in patients with alcoholic hepatitis, and the liver injury was associated with the development of endotoxemia. Normally, a lot of endotoxins present in the gut and nonpathogenic amounts of this toxic macromolecule material are absorbed through the intestinal wall, reaching the liver^[3]. The sinusoidal cell is the key to the uptake and detoxication of endotoxins in the liver^[4]. Under pathological conditions, such as alcoholic hepatitis, endotoxins in the portal vein may enter the peripheral blood (known as endogenous endotoxemia) as a result of depression of Kupffer cells, or portal systemic circulation^[5,6]. However, there is little information concerning the permeability mechanism of LPS in the gut under those pathological conditions. In the present study, by using a monoclonal antibody specific to the lipid A region of endotoxin, the distribution and localization of endotoxins in the colon in rats of chronic alcohol abuse was observed with confocal laser scanning microscopy. LPS concentrations in the portal vein were measured.

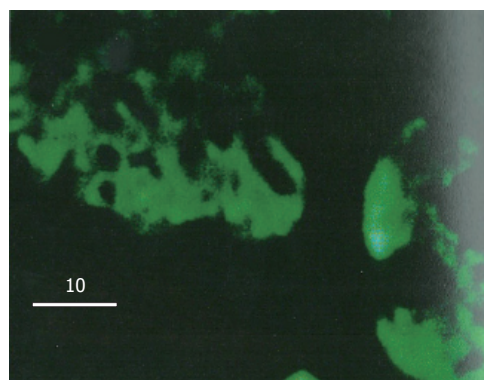
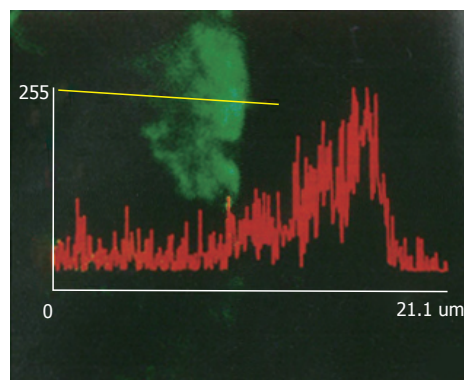
MATERIALS AND METHODS

Animals

Thirty male Wistar rats were divided into two groups: chronic alcoholic group and control group. Rats were fed on a complete liquid diet with the Lieber protocol^[7] in chronic alcoholic group. Diets were supplied every other day with homogenation and administered through Richter feeding tubes for 6 wk. Rats in control group ($n = 6$) were fed ad libitum with ordinary rat chow. Under the anaesthesia

Table 1 lipopolysaccharides contents in blood from the portal vein (pg/mL, $\bar{x} \pm s$)

	<i>n</i>	Before LPS injection	Time points after LPS injection			
			5	10	20	30
Normal control	6	2.45 ± 0.15	3.04 ± 0.98	3.56 ± 1.65	3.05 ± 0.97	2.37 ± 0.56
Alcoholic group	10	3.56 ± 0.67 ^b	173.56 ± 23.45 ^b	154.78 ± 20.57 ^b	43.89 ± 8.67 ^b	45.38 ± 7.89 ^b

^b*P* < 0.01, *vs* normal control at the same time point.**Figure 1** Fluorescent reactions to LPS in the colon mucosa in chronic alcoholic rats 30 min after LPS injection. Those positive reactions were found in the cytoplasm of mucosal cells, tissues under the basement membrane, but not found in the nuclei of the mucosal cells.**Figure 2** Fluorescent reactions to LPS in the colon mucosa in chronic alcoholic rats 30 min after LPS injection. No significant increases of fluorescent reactions were found between the membrane of those mucosal cells.

by intraperitoneal injection of sodium pentobarbital (50 mg/kg body weight), abdomens of rats of both groups were opened. The colons about 1.5 cm-2.0 cm long were ligated at two ends without interruption to their blood circulation. After being washed with sterile saline, the colon was injected *Escherichia coli* LPS. LPS was diluted with sterile saline to 20 μg/mL and the amount of the injected LPS corresponded to the pressure in the colon which was maintained to 10 cm/H₂O. About 0.5 mL-1.0 mL of LPS was injected in to each rat. Before LPS injection and 5, 10, 20, 30 min after the injection of LPS into the colon, blood samples about 0.5 mL were obtained from the portal vein for the determination of LPS in the blood. At 30 min after LPS injection, the colon was taken and washed. Tissue specimens were fixed in buffered formalin, embedded in paraffin and 4 μm sections were cut. The sections were then performed for immunofluorescent staining.

Immunofluorescence staining

As for location of LPS in tissues and cells, the indirect immunofluorescence staining technique was used. Briefly, sections (4 μm thick) were dewaxed with xylene and washed successively with 100%, 96%, 70% aqueous ethanol. After being washed with phosphate buffered saline (PBS), each section was treated with 1% normal goat serum (Vectastain, Vector Laboratories, Inc. Burlingame) for 30 min to cover possible nonspecific sites. Then, all the sections were washed and incubated with the monoclonal antibody against LPS (a gift from Dr. Noguchi) for 60 min at 37 °C. After washing with PBS for three times, fluorescein isothiocyanate (FITC) conjugated goat anti mouse IgM (H&L) F(ab')₂ fragments (1:30, O.E.M. Concepts Inc.) was added for 60 min at 37 °C. Excess conjugate was removed by washing with PBS. Then the sections were mounted with VECTASHIELD mounting medium (Vector Laboratories, North Chicago) for fluorescence under coverslip and ready for observation with Confocal Laser Scanning Microscopy. For the sake of negative controls, sections were incubated with PBS omitting the first antibody or FITC conjugated secondary antibody.

Confocal laser scanning microscopy

Sections were observed within 2 h after immunofluorescence staining. With a confocal laser scanning microscope (LSM-GB200, Olympus, Japan), cellular localization and distribution of LPS in the mucosal cells of the colon were observed.

Statistical analysis

All data were expressed as $\bar{x} \pm s$, and were analyzed with the Stat View Statistical Program. Student's *t* and Anova *F* test were

employed where appropriated.

RESULTS

Changes of LPS concentration in portal vein blood

In rat of chronic alcohol abuse for 6 weeks, LPS concentration in portal vein blood was significantly higher than that of control even before LPS injection into the colon. At 5 min after the injection of LPS, LPS level in the portal vein blood increased markedly and reached the peak point. At 10 min after LPS injection, LPS level in the blood decreased a little but even at 30 min after LPS injection, the LPS level was still significantly higher than that of the normal control. For the rats of normal control, LPS levels in the portal vein blood increased a little after LPS injection, but no significant difference was found in comparison with that before LPS injection (Table 1).

Observation by confocal laser scanning microscopy

In normal control rats after LPS injection, colon mucosal cells showed no obvious FITC fluorescence reaction to LPS except membrane cells on the cavity side of the mucosa which showed slight fluorescence. In the rats of chronic alcoholic abuse, nearly all the mucosal cells showed strong FITC fluorescent reactions to LPS 30 min after LPS injection. The fluorescent reactions were found in the cytoplasm of mucosal cells, tissues under the basement membrane, but not found in the nuclei of the mucosal cells (Figure 1). Fluorescent reactions did not significantly increase between the membrane of the mucosal cells (Figure 2). The positive fluorescent reactions to LPS were evenly scattered, not in spot or particulate form. No fluorescence was detected in negative control tissues using only the monoclonal antibody or FITC labelled secondary antibody.

DISCUSSION

Confocal laser scanning microscopy can scan tissues or cells at thickness as thin as 1 μm, and can actually reflect the FITC fluorescent distribution in tissues and cells. For the location and distribution of LPS in tissues and cells, the monoclonal antibody specific to the lipid A region of LPS is more specific than antibody against the polysaccharide chain of LPS by the immunohistochemical technique, because the antigen is characterized by the fact that the polysaccharide chain of LPS might be changed or separated from lipid A part after LPS enter cells^[8]. Most of the toxic effects of LPS, if not all, reside in the core lipid A part^[9]. No fluorescence was detected in negative controls using only the monoclonal antibody or FITC labelled secondary antibody, and it was reasonable to estimate that the fluorescence reaction detected was specific for the location

and distribution of LPS in tissues and cells.

Endotoxins are mainly composed of lipopolysaccharides and proteins^[1]. There is good evidence that portal vein endotoxemia is in a normal state^[3]. It is generally known that the liver, mainly by Kupffer cells and hepatocytes, is responsible for the clearance of endotoxins in the portal vein blood^[4]. In patients with alcoholic hepatitis, endotoxemia is a common complication^[5,6] and the endotoxins are affirmed primarily from the gut by the portal vein^[10] and the lymphatic vessels^[11] in intestine. The liver injury due to alcohol and its clinical manifestation were confirmed to be associated with the development of endotoxemia^[12], suggesting that endotoxin might play a role in hepatic injury induced by alcohol. In the rats of chronic alcohol abuse with Lieber diets for 6 wk, we found that endotoxin concentration in the portal vein blood was markedly higher than that of the control, and the level increased progressively at various time point after LPS injection, suggesting that the permeability to LPS in the intestine increased after the stimulation by alcohol abuse, a phenomenon which might be critical to the development of endotoxemia in alcoholic hepatitis.

Two different mechanisms, namely specific and non-specific, are suggested to be involved in the initial interaction of LPS with cells^[13]. Specific interactions result from the binding of LPS to a specific receptor on the plasma membrane, and, on the other hand, non-specific interactions result from the binding of LPS macromolecule to any membrane constituents other than the receptors. Both mechanisms are involved in the uptake procedure of LPS by cells^[14,15]. A number of receptors specific to different regions of LPS were recently reported. By using a LPS derivative as a probe to define LPS specific binding structures, Lei MG *et al.*^[16] identified a 73 kDa membrane-localized protein which existed in almost all the mammalian cell subpopulations and was lipid A specific. LPS was found in the cytoplasm of macrophages in spot and particulate form after phagocytized by those cells^[17]. In the present study, the positive reactions to LPS were found in nearly all the mucosal cells in chronic alcoholic rats, indicating that there was no cellular specificity to the permeability of LPS in the colon. There were no positive reactions to LPS among those mucosal cells membranes also suggested that the permeability to LPS in the colon may be through the cells, not through the injection between cells. The positive fluorescent reactions to LPS in the cytoplasm of mucosal cells were evenly distributed, not in spot or particulate form. This phenomenon suggested that the uptake mechanism of LPS by those mucosal cells might not be through phagocytic procedure.

REFERENCES

- 1 Rietschel ET, Brade H. Bacterial endotoxins. *Sci Am* 1992; **267**: 54-61 [PMID: 1641625]
- 2 Morrison DC, Ulevitch RJ. The effects of bacterial endotoxins on host mediation systems. A review. *Am J Pathol* 1978; **93**: 526-618 [PMID: 362943]
- 3 Jacob AI, Goldberg PK, Bloom N, Degenshein GA, Kozinn PJ. Endotoxin and bacteria in portal blood. *Gastroenterology* 1977; **72**: 1268-1270 [PMID: 858472]
- 4 Freudenberg N, Piotraschke J, Galanos C, Sorg C, Askaryar FA, Klosa B, Usener HU, Freudenberg MA. The role of macrophages in the uptake of endotoxin by the mouse liver. *Virchows Arch B Cell Pathol Incl Mol Pathol* 1992; **61**: 343-349 [PMID: 1348896 DOI: 10.1007/BF02890437]
- 5 Bradfield JW. Control of spillover. The importance of Kupffer-cell function in clinical medicine. *Lancet* 1974; **2**: 883-886 [PMID: 4137592]
- 6 Mathison JC, Ulevitch RJ. The clearance, tissue distribution, and cellular localization of intravenously injected lipopolysaccharide in rabbits. *J Immunol* 1979; **123**: 2133-2143 [PMID: 489976]
- 7 Lieber CS, DeCarli LM. The feeding of alcohol in liquid diets: two decades of applications and 1982 update. *Alcohol Clin Exp Res* 1982; **6**: 523-531 [PMID: 6758624 DOI: 10.1111/j.1530-0277.1982.tb05017.x]
- 8 Freudenberg M, Galanos C. Metabolic fate of endotoxin in rat. *Adv Exp Med Biol* 1990; **256**: 499-509 [PMID: 2183561 DOI: 10.1007/978-1-4757-5140-6_44]
- 9 Moldow CF, Bach RR, Staskus K, Rick PD. Induction of endothelial tissue factor by endotoxin and its precursors. *Thromb Haemost* 1993; **70**: 702-706 [PMID: 8116000]
- 10 Nolan JP, Hare DK, McDevitt JJ, Ali MV. In vitro studies of intestinal endotoxin absorption. I. Kinetics of absorption in the isolated everted gut sac. *Gastroenterology* 1977; **72**: 434-439 [PMID: 319036]
- 11 Daniele R, Singh H, Appert HE, Pairent FW, Howard JM. Lymphatic absorption of intraperitoneal endotoxin in the dog. *Surgery* 1970; **67**: 484-487 [PMID: 4905117]
- 12 Bhagwande BS, Apte M, Manwarring L, Dickeson J. Endotoxin induced hepatic necrosis in rats on an alcohol diet. *J Pathol* 1987; **152**: 47-53 [PMID: 3305847 DOI: 10.1002/path.1711520107]
- 13 Morrison DC. Nonspecific interactions of bacterial lipopolysaccharides with membranes and membrane components. In: Berry IJ, eds. *Cellular biology of endotoxin*. New York: Elsevier, 1985: 25-30
- 14 Kriegsmann J, Gay S, Bräuer R. Endocytosis of lipopolysaccharide in mouse macrophages. *Cell Mol Biol (Noisy-le-grand)* 1993; **39**: 791-800 [PMID: 8268763]
- 15 Fox ES, Thomas P, Broitman SA. Comparative studies of endotoxin uptake by isolated rat Kupffer and peritoneal cells. *Infect Immun* 1987; **55**: 2962-2966 [PMID: 2824379]
- 16 Lei MG, Stimpson SA, Morrison DC. Specific endotoxic lipopolysaccharide-binding receptors on murine splenocytes. III. Binding specificity and characterization. *J Immunol* 1991; **147**: 1925-1932 [PMID: 1716286]
- 17 Kang YH, Dwivedi RS, Lee CH. Ultrastructural and immunocytochemical study of the uptake and distribution of bacterial lipopolysaccharide in human monocytes. *J Leukoc Biol* 1990; **48**: 316-332 [PMID: 2118560]

S- Editor: Yang ZD L- Editor: Filipodia E- Editor: Li RF

Expression of vascular endothelial growth factor and its prognostic significance in gastric carcinoma

Hou-Quan Tao, Lan-Fang Qin, Yan-Zhen Lin, Rui-Nian Wang

Hou-Quan Tao, Yan-Zhen Lin, Department of Surgery, Ruijin Hospital, Shanghai Second Medical University, Shanghai 200025, China

Lan-Fang Qin, Rui-Nian Wang, Department of Pathology, Shanghai Second Medical University, Shanghai 200025, China

Author contributions: All authors contributed equally to the work.

Original title: *China National Journal of New Gastroenterology* (1995-1997) renamed *World Journal of Gastroenterology* (1998-).

Correspondence to: Dr. Hou-Quan Tao, Department of Surgery, Ruijin Hospital, Shanghai Second Medical University, Shanghai 200025, China
Telephone: +86-21-64370045

Received: June 1, 1996
Revised: July 3, 1996
Accepted: August 11, 1996
Published online: September 15, 1996

Abstract

AIM: The aim was to investigate the clinical significance of vascular endothelial growth factor (VEGF) expression in gastric carcinoma.

METHODS: The expression of VEGF in 128 gastric carcinomas was investigated by immunohistochemical staining with an anti-VEGF polyclonal antibody. Correlations between VEGF expression and various clinicopathological factors and prognosis were studied.

RESULTS: The overall VEGF-rich expression rate was 64.1% in gastric carcinoma tissue, and was significantly higher in patients with stage III and IV disease than in those with stage I disease ($P < 0.05$). Significant differences in expression rate were related to growth pattern, serosal invasion, and lymph node metastasis. VEGF-rich expression was much higher in tumors with an expanding growth pattern (71.8%) or serosal invasion (73.5%) than in those with an infiltrative growth pattern (52.0%) or nonserosal invasion (53.3%) ($P < 0.025$, respectively). Expression was also significantly higher in patients with lymph node metastases (75.0%) than in those without such metastases (50.0%, $P < 0.05$). A postoperative survey of 86 patients who had been followed for at least 5 years found that the 5-year survival rate of patients with VEGF-rich tumors was significantly lower than that of patients with VEGF-poor tumors ($P < 0.05$).

CONCLUSION: VEGF expression may be associated with invasion and metastasis and may also be a useful indicator of gastric carcinoma prognosis.

Key words: Stomach neoplasms/pathology; Endothelial growth factors; Prognosis

© The Author(s) 1996. Published by Baishideng Publishing Group Inc. All rights reserved.

Tao HQ, Qin LF, Lin YZ, Wang RN. Expression of vascular endothelial growth factor and its prognostic significance in gastric carcinoma. *World J Gastroenterol* 1996; 2(3): 128-130 Available from: URL: <http://www.wjgnet.com/1007-9327/full/v2/i3/125.htm> DOI: <http://dx.doi.org/10.3748/wjg.v2.i3.128>

INTRODUCTION

Solid tumors require neovascularization for growth and metastasis. Experimental evidence shows that endothelial growth factors, such as basic fibroblastic growth factor (bFGF), transforming growth factor (TGF), and vascular endothelial growth factor (VEGF) secreted by tumor cells play a crucial role in tumor angiogenesis^[1]. VEGF regulates microvasculature permeability and is an endothelial cell-specific mitogen^[2,3], and is likely to play an important role in both tumor angiogenesis and generation of tumor stroma^[4]. Results obtained with monoclonal neutralizing antibodies to VEGF have produced strong evidence that VEGF contributes to the progression and metastasis of solid tumors by promoting angiogenesis^[5,6]. We used immunohistochemical staining of gastric carcinoma tissue with an anti-VEGF polyclonal antibody to investigate the correlations between VEGF expression, various clinicopathological factors, and prognosis.

MATERIALS AND METHODS

Clinical material

Resected specimens from 128 patients with gastric carcinoma who underwent gastrectomy at Ruijin Hospital were studied. The patients were 38 to 78 years of age (mean: 58.7 years), 86 were men, and 42 were women. No patient had received chemotherapy or radiation therapy before surgery. The Guidelines of National Gastric Cancer Association were used for pathologic diagnosis and classification of variables, and histologic staging was determined according to the TNM criteria (Table 1). In this study, tumors were divided into two histologic subgroups, a differentiated type including of papillary and tubular adenocarcinomas, and an undifferentiated type including poorly differentiated adenocarcinomas, signet ring cell carcinomas, and mucinous adenocarcinomas. Curative resection was performed in 109 patients, 86 of whom were followed for at least 5 years after surgery; 19 patients underwent noncurative surgical procedures.

For pathological evaluation and immunohistochemistry, tissue specimens were fixed in a 10% formaldehyde solution, embedded in paraffin, sectioned at 4 μ m, and mounted on glass slides.

Antibodies and reagents

Rabbit polyclonal antibody to VEGF was purchased from Santa Cruz Inc. Recombinant human VEGF was a kind gift from Genentech Ltd. (CA). Labeled streptavidin-biotin (LSAB) staining kits were produced by DAKO Inc.

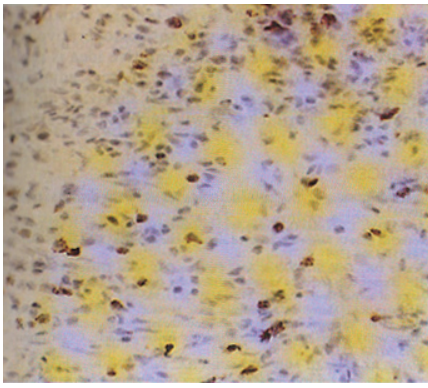


Figure 1 Poorly differentiated adenocarcinoma tissue with VEGF++ staining. Cytoplasmic VEGF staining was seen in tumor cells and diffuse distribution of VEGF-positive tumor cells is apparent. (original magnification $\times 200$)

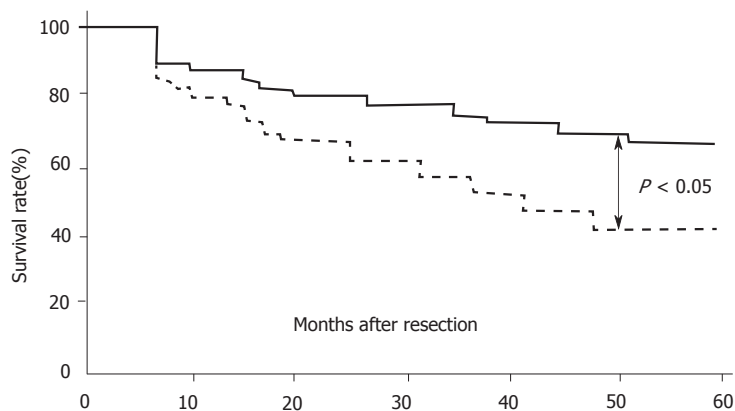


Figure 2 Survival rate after curative resection of VEGF-poor ($n = 30$) and VEGF-rich tumors ($n = 56$)

Immunohistochemical study

Immunohistochemical staining was performed by the immunoperoxidase technique following predigestion and trypsinization. Anti-VEGF polyclonal antibodies were used at a 1:20 dilution. Normal rabbit immunoglobulin G was substituted for primary antibody as the negative control. Immunoreactivity was graded as (-), (\pm), (+) and (++) by the staining intensity. Tumors graded as (+) or (++) were designated as VEGF-rich and those with (-) or (\pm) staining were VEGF-poor. Tumors including both VEGF-positive and VEGF-negative subpopulations were graded as (+). The evaluations were done by an observer completely blinded to the patient characteristics.

Statistical methods

The significance of relationships between VEGF expression and clinicopathological factors was tested by the chi-square method. Survival curves were calculated using the Kaplan-Meier method and analyzed by the log rank test. Statistical significance was defined as $P < 0.05$.

RESULTS

VEGF Expression

The expression of VEGF was observed mainly in the cytoplasm of tumor cells. A representative case of VEGF (++) staining is shown in Figure 1. VEGF staining was blocked by pretreatment with an antibody to recombinant human VEGF (data not shown). Weakly positive VEGF staining was seen in endothelial cells, no direct correlation was found between the staining intensity of tumor cells and that of endothelial cells. A heterogeneous distribution of VEGF-stained tumor cells was seen in tissue from several of the tumors. Of 128 tumors, 82 (64.1%) were VEGF-rich; faint staining was seen in the cells of most VEGF-poor tumors.

Correlation between VEGF expression and tumor histologic stage

Table 1 shows the correlation between VEGF expression and tumor histologic stage. The VEGF-rich expression rates in patients with

Table 1 Correlation between vascular endothelial growth factor expression and TNM stage

TNM stage	n	VEGF-poor rate (%)	VEGF-rich rate (%)
I	39	48.7	51.3
II	27	37.0	63.0
III	48	27.1	72.9 ^a
IV	14	28.6	71.4 ^a

^a $P < 0.05$, compared with stage I.

Table 2 Correlation between clinicopathologic factors and vascular endothelial growth factor expression

Variable	Patients (n)	VEGF-poor rate (%)	VEGF-rich rate (%)	P value
Histologic type				
Differentiated	50	36.0	64.0	> 0.05
Undifferentiated	78	35.9	64.1	
Serosal invasion				
Positive	68	26.5	73.5	< 0.025
Negative	60	46.7	53.3	
Growth pattern				
Expanding	50	48.0	52.0	< 0.025
Infiltrative	78	28.2	71.8	
Lymph node metastasis				
Negative	50	25.6	74.4	< 0.05
Positive	78	52.0	48.0	

stage III and IV disease was significantly higher than that in patients with stage I disease.

Relationship between VEGF expression and clinicopathological factors

Table 2 shows the relationships of VEGF expression with various clinicopathologic factors. There was a statistically significant association between VEGF-rich expression and growth pattern, depth of invasion, and lymph node metastasis. However, expression rate was not significantly correlated with histologic type.

Survival

Of the 86 patients who underwent curative resection and were followed for at least 5 years, 42 died following tumor recurrence. Postoperative analysis demonstrated that the 5-year survival rate of patients with VEGF-rich tumors (42.8%, 24/56) was significantly lower than that of patients with VEGF-poor tumors (66.7%, 20/30; (Figure 2, $P < 0.05$, log-rank test).

DISCUSSION

VEGF is an endothelial cell-specific mitogen and an *in vivo* inducer of tumor angiogenesis. It has also been purified and shown to act independently as a tumor-derived vascular permeability factor promoting the extravasation of plasma proteins, including fibrinogen^[2,3]. VEGF thus has important biological significance for the generation of vascularized tumor stroma. VEGF is known to be expressed in a variety of tumor cell types and in tumor tissues that have are characterized clinically by their neovascularization. In this study, we investigated the expression of VEGF in gastric cancer and observed a significant correlation between VEGF expression and tumor growth pattern, invasion depth, and lymph node metastasis. Melnyk *et al.*^[8] investigated the effect of VEGF inhibition on growth of primary tumors and on micrometastasis in experimental animals, and found that anti-VEGF antibodies not only inhibited growth of primary tumors but also suppressed metastasis to distant sites. This suggests that VEGF may have a clinically important effect on tumor growth and distant metastasis. We noted that the VEGF expression rate in patients with stage III and stage IV gastric carcinoma was significantly higher than that in patients with stage I disease, which supports the view that VEGF has a direct effect on tumor growth and metastasis. Many studies have suggested that VEGF contributes to tumor growth and invasion by promoting angiogenesis, which increases the tumor blood supply. Moreover, newly formed tumor capillaries have fragmented basement membranes and leak, making it easier for tumor cells to enter the circulation and form metastases.

VEGF expression level may thus predict the biological behavior of gastric carcinoma.

Although angiogenesis is seen as an increase in blood vessel formation, some studies have found that it is also correlated with increased lymph node metastasis. Smith and Basu demonstrated that neovascularization of rabbit corneas following injection of India ink led to the appearance of ink particles in ipsilateral lymph nodes. These findings indicate that lymphocapillary anastomoses are present and/or that angiogenesis correlates with the formation of new lymphatic vessels. Therefore, we consider that VEGF not only promotes angiogenesis but also induces the formation of new lymphatic vessels, increasing the opportunity for tumor cells to enter lymphatic vessels and form lymph node metastases.

With regard to prognosis, Toi *et al.*^[7] have shown that VEGF expression is closely associated with early relapse after surgery for primary breast cancer. The relapse-free survival rate of patients with VEGF-rich tumors was significantly lower than that of patients with VEGF-poor tumors, and VEGF status was found to be an independent prognostic indicator. Our study confirmed these findings in gastric carcinoma. We observed a significantly worse prognosis in patients with VEGF-rich compared with VEGF-poor tumors. This result suggests that VEGF expression status is a useful prognostic indicator in gastric carcinoma. Recently, it was reported that administration of a neutralizing monoclonal antibody against human VEGF inhibited the growth and metastasis of human tumor xenografts in nude mouse^[5,6]. Millauer *et al.*^[9] reported that growth of C6 rat glioblastoma cells in nude mice was suppressed after local administration of retrovirus expressing a dominant negative mutant of flk-1, the receptor of VEGF. These results provided a scientific rationale for studying the effect of VEGF on human tumorigenesis, invasion and metastasis, and for adopting treatment strategies targeting VEGF.

Gastric carcinoma is one of the most common human malignant tumors. Our study showed that 64.1% of patients had tumors with VEGF-rich expression, and that the prognosis of patients with VEGF-rich tumors was significantly worse than that of patients with VEGF-

poor tumors. We conclude that assay of VEGF expression in gastric carcinoma, and treating patients with VEGF-rich tumors with anti-VEGF antibodies may help prevent postoperative recurrence and metastasis. If this proposed treatment is applied in combination with other adjuvant therapies, the postoperative overall survival rate of patients with gastric cancer would increase.

REFERENCES

- 1 Folkman J, Shing Y. Angiogenesis. *J Biol Chem* 1992; **267**: 10931-10934 [PMID: 1375931]
- 2 Leung DW, Cachianes G, Kuang WJ, Goeddel DV, Ferrara N. Vascular endothelial growth factor is a secreted angiogenic mitogen. *Science* 1989; **246**: 1306-1309 [PMID: 2479986 DOI: 10.1126/science.2479986]
- 3 Senger DR, Galli SJ, Dvorak AM, Perruzzi CA, Harvey VS, Dvorak HF. Tumor cells secrete a vascular permeability factor that promotes accumulation of ascites fluid. *Science* 1983; **219**: 983-985 [PMID: 6823562 DOI: 10.1126/science.6823562]
- 4 Berkman RA, Merrill MJ, Reinhold WC, Monacci WT, Saxena A, Clark WC, Robertson JT, Ali IU, Oldfield EH. Expression of the vascular permeability factor/vascular endothelial growth factor gene in central nervous system neoplasms. *J Clin Invest* 1993; **91**: 153-159 [PMID: 8380810 DOI: 10.1172/JCI116165]
- 5 Warren RS, Yuan H, Matli MR, Gillett NA, Ferrara N. Regulation by vascular endothelial growth factor of human colon cancer tumorigenesis in a mouse model of experimental liver metastasis. *J Clin Invest* 1995; **95**: 1789-1797 [PMID: 7535799 DOI: 10.1172/JCI117857]
- 6 Kim KJ, Li B, Winer J, Armanini M, Gillett N, Phillips HS, Ferrara N. Inhibition of vascular endothelial growth factor-induced angiogenesis suppresses tumour growth in vivo. *Nature* 1993; **362**: 841-844 [PMID: 7683111 DOI: 10.1038/362841a0]
- 7 Toi M, Hoshina S, Takayanagi T, Tominaga T. Association of vascular endothelial growth factor expression with tumor angiogenesis and with early relapse in primary breast cancer. *Jpn J Cancer Res* 1994; **85**: 1045-1049 [PMID: 7525523 DOI: 10.1111/j.1349-7006.1994.tb02904.x]
- 8 Melnyk O, Shuman MA, Kim KJ. Vascular endothelial growth factor promotes tumor dissemination by a mechanism distinct from its effect on primary tumor growth. *Cancer Res* 1996; **56**: 921-924 [PMID: 8631034]
- 9 Millauer B, Shawver LK, Plate KH, Risau W, Ullrich A. Glioblastoma growth inhibited in vivo by a dominant-negative Flk-1 mutant. *Nature* 1994; **367**: 576-579 [PMID: 8107827 DOI: 10.1038/367576a0]

S- Editor: Tao T L- Editor: Filipodia E- Editor: Li RF



Structure-activity relationship of pituitary adenylate cyclase activating polypeptide

Mu-Xin Wei, S Naruse, K Nokihara, T Ozaki, E Ando, V Wray

Mu-Xin Wei, Department of TCM, 1st College of Clinical Medicine, Nanjing Medical University, Nanjing 210029, Jiangsu Province, China

S Naruse, Department of Internal Medicine 2, Nagoya University School of Medicine, Nagoya 466, Japan

K Nokihara, E Ando, Biotechnology Instruments Department, Shimadzu Corp., Kyoto 604, Japan

T Ozaki, National Institute for Physiological Sciences, Okazaki 444, Japan

V Wray, Gesellschaft Für Biotechnologische Forschung, Braunschweig D 38124, Germany

Mu-Xin Wei, Associate Professor of TCM, a visiting scientist of National Institute for Physiological Sciences in Japan 1992-1996, having 40 papers published.

Author contributions: All authors contributed equally to the work.

Supported by Monbusho international scientific research program and a grant from the Ministry of Education, Science and Culture, Japan to Dr. Naruse S.

Original title: *China National Journal of New Gastroenterology* (1995-1997) renamed *World Journal of Gastroenterology* (1998-).

Correspondence to: Dr. Mu-Xin Wei, Associate Professor, Department of TCM, 1st College of Clinical Medicine, Nanjing Medical University, Nanjing 210029, Jiangsu Province, China
Telephone: +86-25-6600261
Fax: +86-25-6508960

Received: July 28, 1996
Revised: August 13, 1996
Accepted: September 2, 1996
Published online: September 15, 1996

Abstract

AIM: To investigate the structure-activity relationship of pituitary adenylate cyclase activating polypeptide (PACAP) in guinea pig gallbladder using a synthetic PACAP/vasoactive intestinal peptide (VIP) hybrid.

METHODS: We synthesized PACAP-VIP hybrid peptides using the Fmoc strategy and a simultaneous multiple solid-phase peptide synthesizer. The peptides were tested in isolated guinea pig gallbladders using an improved horizontal type organ bath.

RESULTS: VIP induced relaxation of gallbladder smooth muscle strips, while PACAP27 contracted them. Amino acids at positions 4, 5, 9, and 24-26 were replaced without significant loss of activity. [Leu¹³]-PACAP27, a substitution in the α -helix domain, also had no significant loss in activity ($P < 0.05$). It was more potent than [Gly⁸]- and [DAsp⁸]-PACAP27 and could substitute peptides at position 21. Des-[His¹] and [Ala⁶]-PACAP27 had no activity at 10^{-7} mol/L. [Gly⁸]-

[DAsp⁸]-, [Phe²¹]- and [Pro²¹]-PACAP27 at 10^{-7} mol/L had about 25% of the activity of PACAP27 at 10^{-7} mol/L ($P < 0.05$).

CONCLUSION: The N-terminal disordered region is more important than other regions for determining the physiological activity of PACAP in the guinea pig gallbladder.

Key words: Gallbladder; Vasoactive intestinal peptide; Pituitary adenylate cyclase activating polypeptide; Amino acids

© The Author(s) 1996. Published by Baishideng Publishing Group Inc. All rights reserved.

Wei MX, Naruse S, Nokihara K, Ozaki T, Ando E, Wray V. Structure-activity relationship of pituitary adenylate cyclase activating polypeptide. *World J Gastroenterol* 1996; 2(3): 131-133 Available from: URL: <http://www.wjgnet.com/1007-9327/full/v2/i3/131.htm> DOI: <http://dx.doi.org/10.3748/wjg.v2.i3.131>

INTRODUCTION

Pituitary adenylate cyclase activating polypeptide (PACAP) is a neuropeptide structurally related to vasoactive intestinal polypeptide (VIP)^[1]. It exists in the ovine hypothalamus in two molecular forms, PACAP38 and PACAP27. The terminal amino acid 27 residue of PACAP38 (PACAP27) has high sequence homology (68%) with VIP. Many biological actions of PACAP are very similar to those of VIP^[1-3]; but we recently found that PACAP contracts the guinea pig gallbladder, while VIP relaxes it^[4]. The guinea pig gallbladder is a good animal model system to study the structure-activity relationship of PACAP and VIP. In this investigation, we synthesized PACAP-VIP hybrid peptides using the Fmoc strategy and a simultaneous multiple solid phase peptide synthesizer, and we compared the effects of the peptides on gallbladder smooth muscle *in vitro*.

MATERIALS AND METHODS

Peptide Synthesis

Considering the sequence homology of VIP-PACAP, NMR data, and computer-aided molecular graphics^[5], positions 4, 5, 6, 8, 9, 10, 21 and 24-26 were selected as mutation points in this study (Figure 1). Peptides were synthesized using the Fmoc strategy and a simultaneous multiple solid phase peptide synthesizer (Model PSSM 8M, Shimadzu Corp.). After simultaneous cleavage with a trifluoroacetic acid (TFA) cocktail, the desired crude peptides were easily purified by single step reversed phase-high performance liquid chromatography (RP-HPLC), and then characterized and shown to be homogeneous by HPLC, sequencing, amino acid analysis and liquid secondary ion mass spectrometry (LSIMS).

Biological Methods

The peptides were tested in isolated guinea pig gallbladders using an improved horizontal type organ bath. Thirty male Hartley

VIP: HSDAVFTDNY TRLRKQMAVK KYLNSILN-NH₂
 PACAO27: HSDGIFTDSY SRYRKQMAVK KYLAACL-NH₂
 Des-[His¹] PACAO27: SDGIFTDSY SRYRKQMAVK KYLAACL-NH₂
 [Ala⁴]-PACAP27: HSDAIFTDSY SRYRKQMAVK KYLAACL-NH₂
 [Val⁵]-PACAP27: HSDGVFTDSY SRYRKQMAVK KYLAACL-NH₂
 [Ala⁶]-PACAP27: HSDGIATDSY SRYRKQMAVK KYLAACL-NH₂
 [Gly⁶]-PACAP27: HSDGIFTGSY SRYRKQMAVK KYLAACL-NH₂
 [DAsp⁸]-PACAP27: HSDGIFTDSY SRYRKQMAVK KYLAACL-NH₂
 [Asn⁹]-PACAP27: HSDGIFTDNY SRYRKQMAVK KYLAACL-NH₂
 [Leu¹³]-PACAP27: HSDGIFTDSY SRYRKQMAVK KYLAACL-NH₂
 [Ala²¹]-PACAP27: HSDGIFTDSY SRYRKQMAVK AYLAACL-NH₂
 [Phe²¹]-PACAP27: HSDGIFTDSY SRYRKQMAVK FYLAACL-NH₂
 [Pro²¹]-PACAP27: HSDGIFTDSY SRYRKQMAVK PYLAACL-NH₂
 [Asn²⁴, Ser²⁵, Ile²⁶]-PACAP27: HSDGIFTDSY SRYRKQMAVK KYLNSIL-NH₂

Figure 1 Amino acid sequences of the synthetic PACAP-VIP peptides

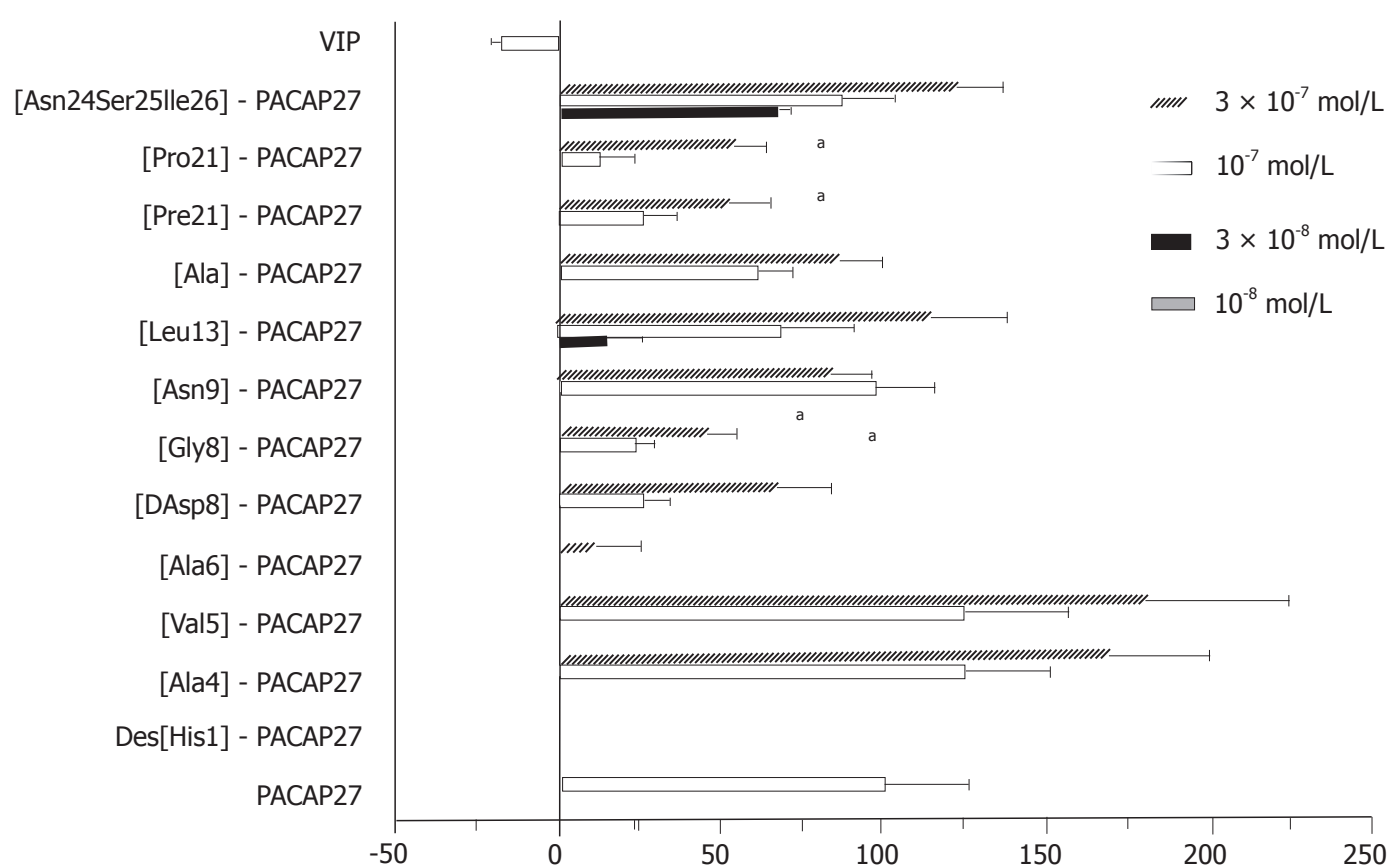


Figure 2 The effect of PACAP-VIP analogues on isolated guinea pig gallbladder. Data are shown as $\bar{x} \pm s$ ($n = 5$). ^a $P < 0.05$ vs PACAP27 at 10⁻⁷ mol/L.

strain guinea pigs (450–580 g) were killed by exsanguination. The gallbladders were excised and four 1.2 mm × 10 mm smooth muscle strips were prepared with the aid of a binocular microscope. The strips were suspended in an organ bath containing (4 mL) Krebs-Ringer solution (pH 7.4), maintained at 37 ± 5 °C, aerated with 95% O₂ and 5% CO₂, and connected to an isotonic displacement transducer. After setting the initial tension at 500 mg, the muscle strips were allowed to equilibrate for 60 min. The length of the strips was recorded using a pen recorder and a computer-controlled data acquisition system. An acetylcholine (Sigma, St. Louis.) control (10⁻⁸–10⁻⁴ mol/L), synthetic PACAP27, VIP, or the hybrid peptides were added to the organ bath at a concentration of 10⁻⁸, 3 × 10⁻⁸, 10⁻⁷, or 3 × 10⁻⁷ mol/L. The gallbladder response to the peptides and control solution were standardized to the PACAP27 response. The maximal contraction induced by PACAP27 (10⁻⁷ mol/L) was taken as 100% contraction and the resting length as 0%.

Statistical analysis

The data (Figure 2) were expressed as means ± standard deviation ($\bar{x} \pm$

s). One way factorial analysis of variance (ANOVA) and Fisher's protected least significant difference (PLSD) multiple comparison test were used to compare the peak responses after adding the peptides. $P < 0.05$ was taken as the level of significance with n equal to the number of animals.

RESULTS

VIP induced relaxation of gallbladder smooth muscle strips, while PACAP27 contracted them. Positions 4, 5, 9, and 24–26 could be replaced without significant loss in activity. [Leu¹³]-PACAP27, a substitution in the α -helix domain, also had no significant loss in activity ($P > 0.05$), was more potent than [Gly⁸]- or [DAsp⁸]-PACAP27, and could substitute peptides at position 21. Des-[His¹]- and [Ala⁶]-PACAP27 had no activity at 10⁻⁷ mol/L. [Gly⁸]-, [DAsp⁸]-, [Phe²¹]-, and [Pro²¹]-PACAP27 at 10⁻⁷ mol/L had about 25% of the activity of PACAP27 at 10⁻⁷ mol/L ($P < 0.05$).

DISCUSSION

The N-terminus of PACAP has a high sequence homology with VIP.

At least two types of PACAP binding sites have been demonstrated in rat tissues. One is a type 1 site that is the dominant site in the hypothalamus, and is highly specific for PACAP. The other is a type 2 site that is the dominant site in the lungs and liver, and has almost equal affinities for both PACAP and VIP^[6,7]. The action of PACAP on guinea pig gallbladder smooth muscle seemed to be directly via the activation of type 1 PACAP receptors because tetrodotoxin, atropine, and CCK antagonists failed to block it.

In our previous studies, the C-terminus (positions 9–26) of PACAP27, similar to VIP, had a propensity for α -helix formation in a hydrophobic environment, but the N-terminus from positions 1 to 8 did not have a well defined helical or strand structure^[5]. PACAP substitutions in this region had a greater loss in activity than was seen with substitutions in other regions. These data suggest that the disordered region from positions 1 to 8 is very important for the recognition of PACAP by its receptor. Position 21 is also important, although it showed no significant loss in activity at a higher dose (3×10^{-7} mol/L).

In conclusion, the N-terminal disordered region is more important than other regions for the physiological activity of PACAP in guinea pig gallbladder.

REFERENCES

- 1 **Arimura A.** Pituitary adenylate cyclase activating polypeptide (PACAP): discovery and current status of research. *Regul Pept* 1992; **37**: 287-303 [PMID: 1313597 DOI: 10.1016/0167-0115(92)90621-Z]
- 2 **Naruse S, Suzuki T, Ozaki T.** The effect of pituitary adenylate cyclase activating polypeptide (PACAP) on exocrine pancreatic secretion in dogs. *Pancreas* 1992; **7**: 543-547 [PMID: 1513802 DOI: 10.1097/00006676-199209000-00006]
- 3 **Naruse S, Suzuki T, Ozaki T, Nokihara K.** Vasodilator effect of pituitary adenylate cyclase activating polypeptide (PACAP) on femoral blood flow in dogs. *Peptides* 1993; **14**: 505-510 [PMID: 8101368 DOI: 10.1016/0196-9781(93)90139-8]
- 4 **Wei MX, Naruse S, Nakamura T, Nokihara K, Ozaki T.** The effect of pituitary adenylate cyclase activating polypeptide (PACAP) 38 on gallbladder smooth muscle in vitro. *Biomed Res* 1994; **15** (Suppl 2): 221-223
- 5 **Wray V, Kakoschke C, Nokihara K, Naruse S.** Solution structure of pituitary adenylate cyclase activating polypeptide by nuclear magnetic resonance spectroscopy. *Biochemistry* 1993; **32**: 5832-5841 [PMID: 8504103 DOI: 10.1021/bi00073a016]
- 6 **Gottschall PE, Tatsuno I, Miyata A, Arimura A.** Characterization and distribution of binding sites for the hypothalamic peptide, pituitary adenylate cyclase-activating polypeptide. *Endocrinology* 1990; **127**: 272-277 [PMID: 2361473 DOI: 10.1210/endo-127-1-272]
- 7 **Shivers BD, Görös TJ, Gottschall PE, Arimura A.** Two high affinity binding sites for pituitary adenylate cyclase-activating polypeptide have different tissue distributions. *Endocrinology* 1991; **128**: 3055-3065 [PMID: 2036976 DOI: 10.1210/endo-128-6-3055]

S- Editor: Cao LB L- Editor: Filipodia E- Editor: Li RF



Prevention of liver metastasis by intraperitoneal 5-FU chemotherapy in nude mice inoculated with human colon cancer cells

Guo-Guang Feng, Xi-Geng Zhou, Bao-Ming Yu

Guo-Guang Feng, Xi-Geng Zhou, Bao-Ming Yu, Department of Surgery, Ruijin Hospital, Shanghai Second Medical University, Shanghai 200025, China

Guo-Guang Feng, Associate Professor of Surgery has published seven papers.

Author contributions: All authors contributed equally to the work.

Supported by the National Science Foundation of China, No.39270650

Original title: *China National Journal of New Gastroenterology* (1995-1997) renamed *World Journal of Gastroenterology* (1998-).

Correspondence to: Dr. Guo-Guang Feng, Associate Professor, Department of Surgery, Ruijin Hospital, Shanghai Second Medical University, Shanghai 200025, China
Telephone: +86-21-64370045-6151

Received: July 29, 1996
Revised: August 9, 1996
Accepted: August 23, 1996
Published online: September 15, 1996

Abstract

AIM: To prevent hepatic metastasis by regional adjuvant chemotherapy after radical surgery for colon cancer.

METHODS: A nude mouse model of human colon cancer (HCC) was used to evaluate the prevention of metastasis of HCC cells following the application of early postoperative intraperitoneal (IP) high-dose 5-fluorouracil chemotherapy.

RESULTS: The incidence of liver metastasis was decreased by 40%, and the mean number of metastatic liver nodules was reduced by 50.89%. Compared with controls, 5-FU 40 mg in NS 40 mL/kg IP for 2 consecutive days prolonged mean survival by 48.21%.

CONCLUSION: IP is a promising and effective novel regional adjuvant chemotherapy for the prevention of liver metastasis of HCC cells after radical surgery for colon cancer.

Key words: Colonic neoplasms/surgery; Liver neoplasms/drug therapy; Fluorouracil/therapeutic use; Liver neoplasms/secondary

© The Author(s) 1996. Published by Baishideng Publishing Group Inc. All rights reserved.

Feng GG, Zhou XG, Yu BM. Prevention of liver metastasis by intraperitoneal 5-FU chemotherapy in nude mice inoculated with human colon cancer cells. *World J Gastroenterol* 1996; 2(3): 134-135 Available from: URL: <http://www.wjgnet.com/1007-9327/full/v2/i3/134.htm> DOI: <http://dx.doi.org/10.3748/wjg.v2.i3.134>

INTRODUCTION

The incidence of liver metastasis after radical surgery for colon cancer is very high and significantly shortens the survival of patients. Intravenous (IV) 5-FU chemotherapy is often not effective for the prevention of liver metastasis. Therefore, early postoperative intraperitoneal (IP) chemotherapy with high-dose 5-FU was evaluated for prevention of liver metastasis by human colonic cancer (HCC) cells in a nude mouse model. HCC cells were inoculated via the spleen.

MATERIALS AND METHODS

Animals

Thirty athymic BALB/c nude mice 5-6 wk of age were provided by the Shanghai Cancer Institute. During the conduct of the study procedures, mice were maintained in a laminar flow cabinet under specific pathogen free conditions.

Cell lines

Colon cancer cell lines derived from human colonic adenocarcinoma were provided by Shanghai Immunology Institute^[1]. The cells were cultured and maintained with more than 95% viability in RPMI 1640 medium with 10% fetal calf serum, penicillin (100 µg/mL), and streptomycin (100 µg/mL) at 37 °C in a 5% CO₂ atmosphere. Aliquots of 1×10^6 cells were suspended in 0.03 mL in normal saline (NS) prior to use.

Splenic injection

Mice were anesthetized by intraperitoneal (IP) injection of phenobarbital and the spleen was exposed under sterile conditions by an incision in the left side of the animal. A 0.03 mL volume of NS containing 1×10^6 cells was slowly injected into the splenic pulp over 1 min, then the spleen was replaced in position and the incision was closed^[2]. The mice were randomly assigned to three groups of 10 each. Group A was given 5-Fu 40 mg in NS 40 mL⁻¹·kg⁻¹, for 2 consecutive days, group B was given 5-Fu 20 mg in NS 40 mL⁻¹·kg⁻¹, for 5 consecutive days, and group C (controls) was given NS 40 mL/kg. Animals were treated 24 h after tumor inoculation and followed-up to determine survival time. The animals were killed 60 days after tumor inoculation, the liver was removed and the tumor nodules were counted.

Statistics

Results were expressed as means \pm standard deviation ($\bar{x} \pm s$). Data were analyzed by analysis of variance (ANOVA) and the chi-square test. $P \leq 0.05$ was considered statistically significant.

RESULTS

The incidence of metastasis in groups A, B and C was 60% (6/10), 70% (7/10), and 100% (10/10), respectively. The 40% difference

Table 1 Metastatic nodules in the livers of experimental and control groups and controls ($\bar{x} \pm s$, nodule)

Group	Liver metastatic nodules (<i>n</i>)					liver nodules ($\bar{x} \pm s$)
	0	1-20	21-40	41-60	61-80	
5-FU 40 mg ^a	4	2	1	1	2	24.80 ± 8.64
5-FU 20 mg	3	1	2	1	3	31.50 ± 8.68
Controls	0	2	1	3	4	50.50 ± 7.32

^a*P* < 0.05, *vs* controls

Table 2 Survival of mice in experimental and control groups

Group	Survival time (d)				Mean survival (d)
	21-30	31-40	41-50	51-60	
5-FU 40 mg	3	1	0	6	45.50 ± 5.12 ^a
5-FU 20 mg	3	1	2	4	43.90 ± 4.77 ^a
Controls	6	2	2	0	30.70 ± 2.59

^a*P* < 0.05, *vs* controls

between group A and 30% difference between group B and controls were not statistically significant (*P* > 0.05).The mean number of metastatic liver nodules was 24.80 ± 8.64 in group A, 31.50 ± 8.68 in group B, and 50.50 ± 7.32 in group C. The differences of 50.89% between group A and controls and 37.62% between group B and controls were both significant (*P* < 0.05, Table 1).

The mean survival times were 45.50 ± 5.12 days in group A, 43.90 ± 4.77 days in group B, and 30.70 ± 2.59 days in the control mice. Survival was prolonged by 48.21% and 43% in groups A and B, respectively (*P* < 0.05, Table 2). surgery

DISCUSSION

Previous studies reported high concentrations of antineoplastic agents in the abdominal cavity, portal vein, and liver after

IP administration, but low concentrations in the systemic circulation, indicating a pharmacokinetic advantage of IP over IV chemotherapy^[3-6]. We reported in our previous studies that HCC cells survived, grew, and disseminated following IP injection, and that chemically induced peritonitis, peritoneal adhesion, and nephrotoxicity were not induced by early postoperative IP chemotherapy with 5-Fu 40 mg in NS, 40 mL⁻¹·kg⁻¹ for 2 consecutive days^[7]. We used a nude mouse model of HCC cell metastasis to evaluate the effects of early postoperative IP chemotherapy with high-dose, large-volume 5-FU chemotherapy. We found a 40% reduction in the incidence of liver metastasis and a decrease in 50.89% in the mean number metastatic liver nodules. The mean survival time was prolonged by 48.21% compared with control mice. The results obtained in this experimental animal model suggest that IP chemotherapy has potential as an effective adjuvant approach in prevention of hepatic metastases in colon cancer .

REFERENCES

1 Drewinko B, Romsdahl MM, Yang LY, Ahearn MJ, Trujillo JM. Establishment of a human carcinoembryonic antigen-producing colon adenocarcinoma cell line. *Cancer Res* 1976; **36**: 467-475 [PMID: 1260746]

2 Feng GG, Zhou XG, Yu BM. Nude mouse model of human colonic cancer hepatic metastasis and its biologic characteristics. *Zhonghua Shiyan Waike Zazhi* 1993; **10**: 147-148

3 Qin SH, Zhou XG. Determination of the concentration of 5-FU in the blood, body fluids and various tissues with high pressure liquid chromatography. *Zhongliuxue* (Shanghai) 1990; **10**: 168-169

4 Qin SH, Zhou XG. Pharmacokinetic studies of 5-fluorouracil intraperitoneal administration. *Weichangbingxue* 1990; **10**: 322-324

5 Qing SH. [Pharmacokinetic comparison of intraperitoneal and intravenous 5-Fu administration]. *Zhonghua Zhongliu Zazhi* 1991; **13**: 340-342 [PMID: 1782844]

6 Speyer JL. The rationale behind intraperitoneal chemotherapy in gastrointestinal malignancies. *Semin Oncol* 1985; **12**: 23-28 [PMID: 4048973]

7 Feng GG, Zhou XG, Yu BM. Chemoprevention of cancer cell growth with intraperitoneal 5-FU in nude mice. *Shanghai Dier Yike Daxue Xuebao* 1993; **13**: 265-266

S- Editor: Yang RC L- Editor: Filipodia E- Editor: Li RF

Pharmacology of novel Chinese medicines screened for treatment of severe acute pancreatitis

Lian-Gen Zhao, Xiao-Xian Wu, Zuo-Ming Zhu, Yu-Ling Chen, Fu-Sen Liu, Jia-Tong Chen

Lian-Gen Zhao, Xiao-Xian Wu, Yu-Ling Chen, Institute of Acute Abdomen, Tianjin 300100, China

Zuo-Ming Zhu, Fu-Sen Liu, Jia-Tong Chen, Nankai University, Tianjin 300100, China

Lian-Gen Zhao, Director of Laboratory of Surgical Research, Institute of Acute Abdomen, Tianjin, conducts research in experimental treatment of acute pancreatitis and the therapeutic principle of Huoxue Huayu. He has published 40 articles and 3 books. Born in 1938, Tangshan, Hebei province, Graduated in 1962 from Pathophysiology Department of the Chinese Medical University.

Author contributions: All authors contributed equally to the work.

Original title: *China National Journal of New Gastroenterology* (1995-1997) renamed *World Journal of Gastroenterology* (1998-).

Correspondence to: Dr. Lian-Gen Zhao, Professor, Institute of Acute Abdomen, Tianjin 300100, China
Telephone: +86-22-7300021

Received: June 2, 1996
Revised: July 26, 1996
Accepted: August 6, 1996
Published online: September 15, 1996

Abstract

AIM: To screen the enzyme-inhibition and observe the pharmacologic effects of circulation-improving Chinese medicines on intestinal and pancreatic hemodynamics.

METHODS: *In vitro* screening of the amylase-and lipase-inhibiting effects of nine Chinese traditional medicines was carried out. Each extract was prepared following methods described by LIN Qi-Shou. Tests of the inhibition of trypsin and elastase activity were carried out by following methods described by ZHANG Tian-Min s and JIANG Chuan-Kui. A Modified Leslie method was used to determine the effects of the best circulation-improving Chinese herb, Tao-Ren (*Semen Persicae*), and its extract (HHI-I), on intestinal hemodynamics. An electromagnetic flowmeter was used to measure intestinal blood flow and a blood oxygen meter was used to measure oxygen consumption. A laser Doppler microcirculation dynamic analyzer was used for to measurement the effect of HHI-I on pancreatic microcirculation, and a tissue oxygen meter was used to measure changes of pancreatic oxygen partial pressure.

RESULTS: Of the nine Chinese traditional medicines, Yuan-Hu (*Rhizome Corydalis*) had the most potent inhibitory activity on both amylase and lipase activity, followed by Da Huang, Zhi Zi, Huang Qin, and Hang Shao. Canine experiments found that Huoxue Huayu (HHI-I) improved intestinal hemodynamics. Intestinal blood flow 20 min after infusion of HHI-I, was 225.0 ± 68.51 mL/min, which was significantly higher than that before infusion (201.34 ± 70.21 mL/min, $P < 0.05$).

Blood flow increased to 245.40 ± 82.78 mL/min ($P < 0.05$) at 40 min and 252.20 ± 82.41 mL/min ($P < 0.01$). 60 min after infusion. Intestinal oxygen consumption also increased significantly, to 5.33 ± 2.57 mL/min at 60 min after infusion, compared with (2.72 ± 1.09 mL/min ($P < 0.05$) at baseline. HHI-I improved pancreatic microcirculation and tissue oxygen partial pressure. The basal microcirculatory blood flow of 20.4 ± 5.0 mL/min/100 g body weight increased to 49.0 ± 9.0 mL/min/100g body weight 20 min after administration ($P < 0.05$). Blood flow increase further to 51.0 ± 7.97 mL/min/100 g body weight ($P < 0.01$) at 40 min and 54.8 ± 15.51 mL/min/100 g body weight ($P < 0.01$) at 60 min. Pancreatic oxygen partial pressure was 6.21 ± 0.94 kPa at baseline, rose to 7.55 ± 1.40 kPa at 20 min ($P < 0.01$), 7.65 ± 1.76 kPa ($P < 0.05$) at 40 min, and 7.67 ± 1.64 kPa ($P < 0.01$) at 60 min after HHI-I administration. In the control group, saline administration had no significant effect of the indices.

CONCLUSION: Yuan-Hu and Tao-Ren used together have the potential to become novel, effective medicines

Key words: Pancreatitis treatment; Yuan hu; Tao ren

© The Author(s) 1996. Published by Baishideng Publishing Group Inc. All rights reserved.

Zhao LG, Wu XX, Zhu ZM, Chen YL, Liu FS, Chen JT. Pharmacology of novel Chinese medicines screened for treatment of severe acute pancreatitis. *World J Gastroenterol* 1996; 2(3): 136-138 Available from: URL: <http://www.wjgnet.com/1007-9327/full/v2/i3/136.htm> DOI: <http://dx.doi.org/10.3748/wjg.v2.i3.136>

INTRODUCTION

The mortality of severe acute pancreatitis (SAP) is high, and there are no specific treatments. The development of effective SAP therapy is a worldwide priority. Inhibition of pancreatic enzymes and improving pancreatic blood circulation are potential treatment approach. There have been many reports of successful treatment of SAP with Chinese medicines. Treating SAP with the most effective enzyme-inhibiting and circulation-improving herbs may result in decreased in SAP mortality. In this study, we screened nine enzyme-inhibiting herbs and evaluated the hemodynamic effects of the most effective circulation-improving Chinese medicinal herbs.

MATERIALS AND METHODS

Inhibitory effect on trypsin activity

Method Extracts of each herb were prepared following methods previously described by Lin Qi-Shou^[1]. The anti-trypsin inhibitory activity of 300 μ L samples of each extract were tested and compared with control reactions that proceeded without inhibitors^[2].

Results All nine herbal extracts inhibited trypsin activity, but they

Table 1 Effect of nine of Chinese herbal extracts on trypsin activity

Herbs	1	2	3	4	5	6	7	8	9
Activity change (± %)	-0.3	-6	-26	-12	-25	-17	-11	-5.1	-77

1: Chai Hu (Radix Bupleuri), 2: Bin Lang (Semen Arecae), 3: Da Huang, 4: Hu Lian (Rhizoma Picrorhizae), 5: Zhi Zi, 6: Huang Qin (Radix Scutellariae), 7: Hang Shao (Radix paeoniae Alba), 8: Mu Xiang (Radix Aucklandiae), 9: Yuan Hu

Table 2 Effect of nine of Chinese herbal extracts on elastase activity

Herbs	1	2	3	4	5	6	7	8	9
Activity change (± %)	-6	-6	13	5	-19	-26	-25	19	-90

Table 3 Effect of HHI-I on intestinal hemodynamics

	Before infusion	After infusion (min)		
		20	40	60
BF (mL/min)	201.34 ± 70.21	225.00 ± 68.51 ^a	245.40 ± 82.78 ^b	252.20 ± 82.41 ^b
OC (mL/min)	2.72 ± 1.09	4.92 ± 3.39	5.03 ± 2.55	5.33 ± 2.57 ^a
(A-V)O ₂ (mL/100 mL)	1.47 ± 0.68	1.21 ± 1.34	2.16 ± 1.11 ^a	2.29 ± 1.31
VR (kPa/mL/min)	0.10 ± 0.04	0.09 ± 0.04	0.08 ± 0.03 ^a	0.08 ± 0.03 ^a
HCT (%)	46.85 ± 10.58	47.73 ± 11.10	46.25 ± 10.47	45.20 ± 12.30

Five animals were tested. Data are expressed as ($\bar{x} \pm s_x$); ^a*P* < 0.05, ^b*P* ≤ 0.01 vs. controls.

Table 4 Effect of HHI-I on pancreatic oxygen tension and microcirculation

	Group	Before HHI-I	After HHI-I (min)		
			20	40	60
Microcirculation (mL/min/100 g)	HHI-I	20.4 ± 5.0	49.0 ± 9.0 ^a	51.0 ± 7.97 ^b	54.8 ± 15.51 ^b
	Control	32.4 ± 6.35	34.6 ± 3.65	34.2 ± 4.02	31.2 ± 5.71
Oxygen tension (kPa)	HHI-I	6.21 ± 0.94	7.55 ± 1.40 ^b	7.65 ± 1.76 ^a	7.67 ± 1.64 ^b
	Control	5.60 ± 0.97	5.76 ± 1.07	5.49 ± 0.93	5.52 ± 0.79

Data are expressed as ($\bar{x} \pm s_x$); ^a*P* < 0.05; ^b*P* < 0.01 vs controls

differed in effectiveness (Table 1), which may have been related to differences in the concentrations of active substance in each herb. Yuan Hu was the most effective followed by Da Huang (Radix et Rhizoma Rhei), and Zhi Zi (Fructus Gardeniae) (Table 1).

Inhibitory effect on elastase activity

Method The *in vitro* test followed a method previously described by Chuan-Rui Jiang^[3]. Anti-elastase activity was tested in 200 μL sample of each extract.

Results Most of the nine extracts inhibited elastase activity, but a few had an activating effect (Table 2). Yuan Hu was the most effective inhibitor, followed by Huang Qin and Hang Shao.

Effect of HHI I on intestinal hemodynamics in dogs

Method Intestinal hemodynamics were evaluated following a method previously described by Leslie^[5]. Blood flow was measured in the superior mesenteric artery with an electromagnetic flowmeter. Blood samples were obtained from femoral artery and superior mesenteric vein, and the oxygen consumption of intestine was calculated. Five dogs with mean body weight of 19.2 ± 3.96 kg were used. A solution of Huoxue Huayu (HHI-I) was infused intravenously at a dose of 2.0 mL/kg of body weight.

Results HHI-I increased intestinal blood flow and oxygen consumption (Table 3, Figure 1). It also increased oxygen extraction (A-V)O₂ and decreased vascular resistance. No effect of HHI-I on hematocrit was observed. No effects were observed in a control group given an intravenous infusion of saline.

Effect of HHI I on microcirculation and pancreatic tissue oxygenation in dogs

Experimental methods Five healthy male and female dogs weighing 18.9 ± 2.61 kg were anesthetized, and the pancreas was exposed. An oxygen meter (POG-5000, Japan) electrode was inserted into the pancreatic tissue to measure tissue oxygen tension,

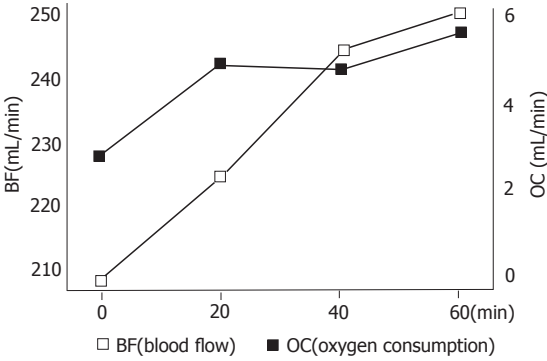


Figure 1 Effect of HHI-I on intestinal hemodynamics

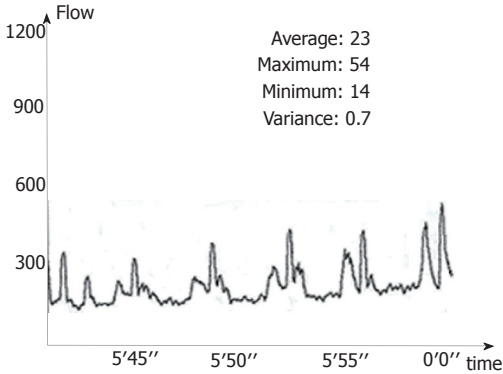


Figure 2 Effect of HHI-I on pancreatic microcirculation before administration

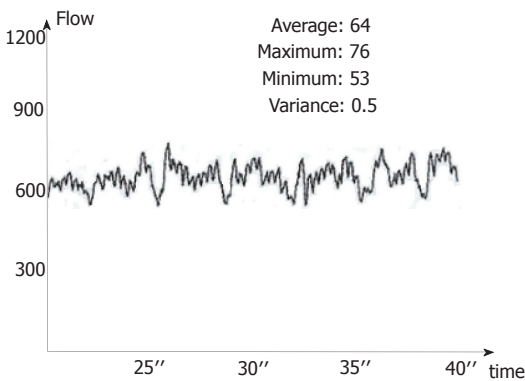


Figure 3 Effect of HHI-I on pancreatic microcirculation at 40 min

and pancreatic microcirculation was measured by a dynamic laser Doppler microcirculation analyzer (JI-200, Tianjin). The dose of HHI I used in this experiment was the same as that used to evaluate the effect on intestinal hemodynamics.

Results Blood microcirculation in pancreatic tissue significantly increased 10 min after HHI-I infusion, and the increase was maintained during the whole period of infusion. The oxygen tension of pancreas increased at the same time. The two indices did not change in control animals (Table 4, Figures 2 and 3).

DISCUSSION

Even though aprotinin has shown disappointing results in experimental and clinical treatment of SAP, inhibition of pancreatic enzymes should not be ignored as a possible treatment. In addition to trypsin, gabexate mesilate (417 Daltons) also inhibits phospholipase A2 and has shown satisfactory therapeutic effects in the preclinical studies and clinical trials. Camostatate (FOY-305, 494.5 Daltons) having a more extensive spectrum of enzyme inhibition, and has markedly increased SAP survival rates in animal models^[6,7]. Because it contains agglutinin and native antiproteases, human plasma can significantly improve survival time in rats with SAP caused by 5% sodium taurocholate compared with control animals. In a rat SAP model caused by caerulein infusion (5 μg/kg of body weight per hour), urinastatin, a protease inhibitor extracted from human urine, had protective

effects on serum amylase, pancreatic water content, amylase content of pancreatic tissue, lysosome distribution, and fragility of acinar cells and lysosomes^[8]. ON03307, a synthetic antiprotease with low molecular weight and high activity, was effective against SAP when administered with allopurinol^[9]. Combination treatment increased release of amylase and cathepsin by pancreatic juice and increased the proportion of zymogen-containing lysosomes. Combined administration of a protease inhibitor and a xanthine oxygenase inhibitor thus improved SAP treatment. In the pathogenesis of SAP, elastase digests elastin in blood vessel walls playing a pivotal role in the conversion of mild into severe hemorrhagic and necrotic pancreatitis. A synthetic, low molecular weight inhibitor of pancreatic elastase would be of great value, and glutaryl-trialanin-ethylamide a competitive inhibitor of pancreatic elastase, has been shown to slow the progress of SAP in a rat model^[10].

There have been many reports of the enzyme inhibitory activity of Chinese herbs, including Ban Xia (*Rhizoma Pinelliae*), Da Huang, Huang Qin, Hu Lian, and Bai Shao^[11]. This study found Yuan Hu to be the strongest inhibitor of trypsin and elastase; and in our laboratory, the injectable form is called YHI. It has also been found that combined treatment with YHI and HHI-I reduces the severity of experimental SAP rabbits (unpublished data).

Many experimental studies and clinical trials have found that pancreatic ischemia in the early stage of AP is an important step in the development of necrosis^[12,13]. In dogs, occlusion of small pancreatic arterioles by 8–20 μ m microsphere induced hemorrhagic and necrotic pancreatitis; pancreatic edema superimposed on pancreatic ischemia can lead to necrotic pancreatitis. The effectiveness of low molecular weight dextran for prevention and treatment of pancreatic ischemia has been reported in experimental animal models of AP. Dextran has specific effects on pancreatic microcirculation, and isovolemic hemodilution with dextran 60 at a dose of 10 ± 1.3 mL/kg body weight reduced vacuolization of acinar cells and parenchymal edema compared with controls^[14]. In a clinical trial including 13 SAP patients (mean Ranson score of 4.6). The average time from symptom appearance to dextran hemodilution was 38 h (range 19–90 h). Hematocrit decreased from $50\% \pm 6\%$ to $34\% \pm 3\%$ in the first hour and $31\% \pm 4\%$ in the second hour. The volume exchanged was 750–1700 mL, and the mortality rate was only 7.7%^[15]. HHI-I, Tao Ren injection, is the most effective herb selected from the HuoXue HuaYu decoction used in our hospital for improving blood circulation and increasing oxygen consumption^[4]. This study provides additional evidence of the positive effect of HHI-I on intestinal hemodynamics

and pancreatic oxygen supply, and microcirculation in this dog model. HHI-I has potential as an effective medicine to improving blood circulation and to treat SAP.

REFERENCES

- 1 **Lien QS.** Constituent chemistry of Chinese traditional herbs. Scientific Press 1977: 343-346
- 2 **Zhang TM.** Biochemical pharmaceuticals for animals. People's Health Press 1982: 138-169
- 3 **Jiang CK.** Activity measurement of instrument enzymes. Shanghai Scientific and Technologic Press 1982: 107-110
- 4 **Wu XX, Zhao LG.** Research for constituents of Huoxue Huayu injection with optimized experiment. *Zhongguo Zhongxiyi Jiehe Zazhi* 1991; **11**(suppl): 335-337
- 5 **Zhao LG, Zhang H, Meng QZ.** [Effect of injections of huoxue huayu on hemodynamics of the canine small intestine]. *Zhongxiyi Jiehe Zazhi* 1989; **9**: 731-733 [PMID: 2624989]
- 6 **Zhao LG.** [The clinical and experimental research on acute pancreatitis]. *Zhonghua Waike Zazhi* 1992; **30**: 58-60 [PMID: 1499431]
- 7 **Büchler M, Malfertheiner P, Uhl W, Schölmerich J, Stöckmann F, Adler G, Gaus W, Rolfe K, Beger HG.** Gabexate mesilate in human acute pancreatitis. German Pancreatitis Study Group. *Gastroenterology* 1993; **104**: 1165-1170 [PMID: 8462805]
- 8 **Hirano T, Manabe T, Tobe T.** Effect of urinary trypsin inhibitor on pancreatic cellular and lysosomal fragility in cerulein-induced acute pancreatitis in rats. *Dig Dis Sci* 1993; **38**: 660-664 [PMID: 7681748 DOI: 10.1007/BF01316797]
- 9 **Hirano T, Manabe T, Steer M, Printz H, Calne R, Tobe T.** Protective effects of therapy with a protease and xanthine oxidase inhibitor in short form pancreatic biliary obstruction and ischemia in rats. *Surg Gynecol Obstet* 1993; **176**: 371-381 [PMID: 8460415]
- 10 **Fric P, Slabý J, Kasářík E, Kocná P, Marek J.** Effective peritoneal therapy of acute pancreatitis in the rat with glutaryl-trialanin-ethylamide: a novel inhibitor of pancreatic elastase. *Gut* 1992; **33**: 701-706 [PMID: 1377154 DOI: 10.1136/gut.33.5.701]
- 11 **Yao GQ.** Progress of treatment in acute pancreatitis with integrated Chinese and western medicine. *Zhongguo Zhongxiyi Jiehe Waike Zazhi* 1995; **1**: 190-192
- 12 **Klar E, Messmer K, Warshaw AL, Herfarth C.** Pancreatic ischaemia in experimental acute pancreatitis: mechanism, significance and therapy. *Br J Surg* 1990; **77**: 1205-1210 [PMID: 2252994 DOI: 10.1002/bjs.1800771104]
- 13 **Printz H, Saluja A, Leli U, Sengupta A, Steer M.** Effects of hemorrhagic shock, aspirin, and ethanol on secretagogue-induced experimental pancreatitis. *Int J Pancreatol* 1990; **6**: 207-217 [PMID: 1697883]
- 14 **Klar E, Mall G, Messmer K, Herfarth C, Rattner DW, Warshaw AL.** Improvement of impaired pancreatic microcirculation by isovolemic hemodilution protects pancreatic morphology in acute biliary pancreatitis. *Surg Gynecol Obstet* 1993; **176**: 144-150 [PMID: 8421802]
- 15 **Klar E, Foitzik T, Buhr H, Messmer K, Herfarth C.** Isovolemic hemodilution with dextran 60 as treatment of pancreatic ischemia in acute pancreatitis. Clinical practicability of an experimental concept. *Ann Surg* 1993; **217**: 369-374 [PMID: 7682053 DOI: 10.1097/00000658-199304000-00008]

S- Editor: Cao LB L- Editor: Filipodia E- Editor: Li RF

Effects of basic fibroblast growth factor on ischemic gut and liver injuries

Xiao-Bing Fu, Zhi-Yong Sheng, Ya-Ping Wang, Yi-Xiu Ye, Tong-Zhu Sun, Nuo-Shan Ma, Guo-You Chang, Ming-Huo Xu, Bao-Tong Zhou

Xiao-Bing Fu, Zhi-Yong Sheng, Ya-Ping Wang, Yi-Xiu Ye, Tong-Zhu Sun, Nuo-Shan Ma, Guo-You Chang, Ming-Huo Xu, Bao-Tong Zhou, Trauma Center, Postgraduate Military Medical College, 304th Hospital, Beijing 100037, China

Xiao-Bing Fu, has published 85 papers and 7 books; is associate professor and deputy director of the research department.

Author contributions: All authors contributed equally to the work.

Supported by the National Natural Science Foundation of China, No.39470706.

Original title: *China National Journal of New Gastroenterology* (1995-1997) renamed *World Journal of Gastroenterology* (1998-).

Correspondence to: Dr. Xiao-Bing Fu, Trauma Center of Postgraduate Military Medical College, 304th Hospital, Beijing 100037, China
Telephone: +86-10-66843129-41396
Fax: +86-10-68429998

Received: July 15, 1996

Revised: August 6, 1996

Accepted: August 26, 1996

Published online: September 15, 1996

Abstract

AIM: To explore the effects of basic fibroblast growth factor (bFGF) on ischemic gut and liver injuries following trauma.

METHODS: An animal model of superior mesenteric artery (SMA) occlusion was used. Seventy-two male Wistar rats were randomized equally to three treatment groups of 24 each. Group 1 was injected with 4 μ g of bFGF in 0.15 mL of normal saline solution containing 0.1% (w/v) heparin through the jugular vein at the onset of reperfusion. Group 2 received normal saline without bFGF. Group 3 was treated was given a sham operation without SMA occlusion. Liver function, serum tumor necrosis factor (TNF) α , bacterial cultures, and pathological evaluations were carried out.

RESULTS: In group 1, alanine transaminase (ALT), aspartate transaminase (AST), and serum TNF α were significantly reduced at 6, 24 and 48 h compared with group 2. Bacterial cultures showed that the bacterial translocation from gut to liver, spleen, and mesenteric lymph nodes (MLN) was significantly lower in group 1 than in group 2. Pathological evaluation was consistent with a significant protective effect of bFGF.

CONCLUSION: Venous administration of bFGF may help reduce gut and liver ischemia/reperfusion injury through its mitogenic and nonmitogenic hormone-like effects.

Key words: Intestine; Liver; Fibroblast growth factor; Mesenteric arteries

© The Author(s) 1996. Published by Baishideng Publishing Group Inc. All rights reserved.

Fu XB, Sheng ZY, Wang YP, Ye YX, Sun TZ, Ma NS, Chang GY, Xu MH, Zhou BT. Effects of basic fibroblast growth factor on ischemic gut and liver injuries. *World J Gastroenterol* 1996; 2(3): 139-140 Available from: URL: <http://www.wjgnet.com/1007-9327/full/v2/i3/139.htm> DOI: <http://dx.doi.org/10.3748/wjg.v2.i3.139>

INTRODUCTION

Gut ischemia/reperfusion injury after serious trauma is an important problem in the clinic. Damage to gut barrier function may lead to translocation of bacteria from the gut to internal organs, resulting in organ impairment. Preservation of the gut barrier is thus a key step in preventing multiple organ failure after trauma^[1]. The involvement of growth factors and their effects on ischemic injury to internal organs is an area of active research^[2]. We evaluated systemic administration of basic fibroblast growth factor (bFGF) for prevention of serious gut and liver injury after occlusion of the superior mesenteric artery (SMA) and investigated its mechanism of action.

MATERIALS AND METHODS

Animal model

Seventy-two male Wistar rats weighing 200–250 grams were housed in the laboratory for 1 wk prior to use in the study, and had free access to food and water. Occlusion of the superior mesenteric artery (SMA) was done under intravenous anesthesia with sodium pentothal (40 mg/kg). A midabdominal incision was made, and the SMA was identified and isolated by blunt dissection. Blood flow was completely blocked by a microvascular clamp placed on the root of SMA. The clamp was removed after 45 min, and return of blood flow to the gut was confirmed visually. The incision was then closed in two layers, animals were allowed to recover spontaneously and were observed for 3 d. All operations were performed under aseptic conditions.

Animals were randomly allocated to three groups of 24 each. At the onset of reperfusion, rats in Group 1 were given 4 μ g of bFGF in 0.15 mL of normal saline containing 0.1% (w/v) heparin intravenously through the jugular vein. Animals in Group 2 were given the same volume of normal saline plus heparin, but not bFGF. Animals in Group 3 were given sham-operation consisting of a laparotomy without SMA occlusion and reperfusion.

Liver function tests and cytokine measurement

Serum alanine transaminase (ALT) and aspartate aminotransferase (AST) were assayed with an automatic biochemistry analyzer (Monarch, United States) before ischemia and 6, 24 and 48 h respectively after ischemia. Serum tumor necrosis factor α (TNF α) was determined with a radioassay kit (Hun Qun Co., Beijing) following the same schedule.

Bacterial cultures

A midabdominal incision was made under sterile conditions at 6, 24, and 48 h after ischemia, and swabs of the peritoneal cavity were obtained for aerobic culture. The mesenteric lymph nodes

Table 1 Changes in alanine transaminase in the three study groups

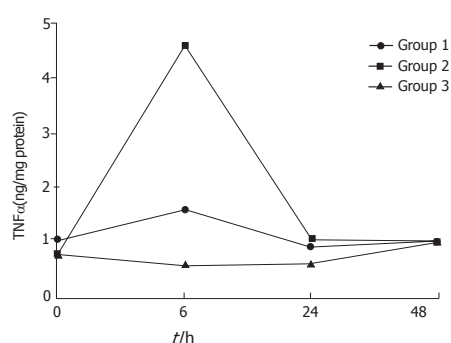
Group	ALT (nmol/L)			
	0 h	6 h	24 h	48 h
1	792.7 ± 97.0	850.2 ± 498.1 ^b	786.3 ± 308.6 ^a	622.3 ± 134.9
2	925.2 ± 68.8	4777.6 ± 710.6	2771.2 ± 646.6	969.0 ± 105.7
3	1100.2 ± 148.5	858.5 ± 257.4	919.4 ± 170.0	923.5 ± 116.0

Data are expressed as ($\bar{x} \pm s$). ^a $P < 0.05$; ^b $P < 0.01$ vs Group 2

Table 2 Changes of aspartate transaminase in the three study groups

Group	ALT (nmol/L)			
	0 h	6 h	24 h	48 h
1	2130.9 ± 217.9	3453.5 ± 1532.1 ^b	2155.9 ± 946.0 ^a	2125.4 ± 437.6
2	2352.6 ± 281.2	7988.3 ± 1087.6	5845.7 ± 1274.8	3627.4 ± 695.3
3	3386.3 ± 587.5	3717.4 ± 1147.9	6079.0 ± 1464.0	2353.8 ± 242.9

Data are expressed as ($\bar{x} \pm s$). ^a $P < 0.05$, ^b $P < 0.01$, vs Group 2.

**Figure 1** Changes of plasma TNF α after ischemia.

(MLN), liver, and spleen were removed, weighed, and homogenized in sterile grinding tubes. The samples were plated for quantitative culture and incubated at 37 °C for 48 h before reading.

Histopathological examination

Specimens of gut and liver tissue were taken for examination by light microscopy at 6, 24 and 48 h after ischemia.

Statistical analysis

Student's-*t* test was used to determine the significance of changes before and after ischemia and the significance of between-group differences. Statistical significance was defined as $P < 0.05$. Data were expressed as means \pm standard deviation ($\bar{x} \pm s$).

RESULTS

Organ function and serum TNF α

In group 2, serum ALT and AST were increased at 6, 24, and 48 h, both were significantly higher than before injury ($P < 0.05$) and were higher than in group 1 ($P < 0.01$). In group 1, all values were increased at 6 h, but were not significantly different than preinjury values or the group 3 values (Tables 1 and 2).

In groups 1 and 2, serum TNF α concentrations rose and fell, with a peak at 6 h, but declined at 24 and 48 h. No significant changes in serum TN were found at all times (Figure 1).

Bacterial study and pathologic examination

At 6 h after ischemia, MLN, liver, and spleen tissue samples in groups 1 and 2 had positive bacterial cultures, but the proportion of positive cultures was lower in group 1 than in group 2. In group 3, positive bacterial cultures were obtained only from MLN. The calculated bacteria per gram of tissue in the three groups differed (Tables 3 and 4).

Pathologic examination found that the proportion of intestine and liver tissue samples with subepithelial edema, hemorrhage, erosion, or neutrophilic and lymphocytic infiltration was much larger in saline-treated than in bFGF-treated rats. No changes in tissue structure were observed in sham operated rats.

DISCUSSION

Mucosal injuries that lead to translocation of bacteria or endotoxins from the gut to other tissues and organs are the primary factor in the pathogenesis of multiple organ injury or failure after serious trauma^[1,2].

Table 3 Positive bacterial cultures from organs in the three study groups

Group	Positive bacterial cultures (%)		
	Liver	Spleen	MLN
1	12.5 ^a (1/8)	12.5 ^a (1/8)	75.0 (6/8)
2	62.5 (5/8)	57.1 (4/7)	62.5 (5/8)
3	0.0 (0/8)	0.0 (0/8)	50.0 (4/8)

^a $P < 0.05$ vs Group 2.

Table 4 Bacteria cultured from organ samples

Group	Organs sampled (n)	Positive (n)	Bacteria ¹ (log CFU/g tissue)
1	33	30	3.70 ± 0.91
2	9	8	4.06 ± 1.19
3	18	7	3.42 ± 0.50

¹Data expressed as $\bar{x} \pm s$. CFU, colony forming unit

Resuscitation and anti-oxidation treatment are effective in reducing multiple organ injury and mortality^[3], but the traditional methods can only block the cycle of tissue injury. They do not accelerate the repair of damaged tissues. From what is known of the pathogenesis of multiple organ failure, we considered that the mitogenic effects and nonmitogenic hormone-like activity of bFGF, might be protective against ischemic organ injuries^[4-6]. The study data showed that systemic administration of bFGF at the onset of reperfusion reduced the functional and morphological changes of the gut and liver and reduced bacterial translocation from the gut to the liver and spleen. Moreover, inflammatory factors such as TNF α were reduced by bFGF treatment. In a model of stomach ischemia, Ishikawa *et al.*^[7] observed that the administration of epidermal growth factor (EGF) reduced mucosal edema and necrosis. It follows that growth factors may be useful in promoting internal organ repair after trauma.

Possible mechanisms of bFGF's protection against ischemic injury may its vasodilator activity, which may help open microvascular beds and ameliorate the "no reflow" phenomenon that occurs after ischemia^[8]. It has been found that the longer ischemia persists, the more serious the gut and liver damage and the higher the mortality. Increased intracellular calcium and redistribution of intracellular calcium pools may result in cell injury and contribute to cell death. Because bFGF can trigger the influx and intracellular release of Ca²⁺, it may have a role in regulating extracellular and intracellular Ca²⁺ balance and modulate transduction of transmembrane signals to inhibit Ca²⁺-dependent ATPase and other mitochondrial enzyme activity associated with ischemia/reperfusion^[9]. Finally, signal transduction by bFGF and its interactions with other enzymes might also be involved in the protective effect of bFGF on ischemia/reperfusion injury. Further study is needed.

REFERENCES

- Zhi-Yong S, Dong YL, Wang XH. Bacterial translocation and multiple system organ failure in bowel ischemia and reperfusion. *J Trauma* 1992; **32**: 148-153 [PMID: 1740793 DOI: 10.1097/00005373-199202000-00006]
- Yu Y, Shi ZG, Zhu XF. The observation of gut bacterial translocation and endotoxin after shock in rats. *Basic Med Clinic* 1993; **13**: 48-50
- Sheng ZY, Dong YL, Guo ZY. Protective effects of antioxidants in hepatic and pulmonary injuries subsequent to bowel ischemia. *Zhonghua Yixue Zazhi* 1988; **64**: 183-187
- Gospodarowicz D, Ferrara N, Schweigerer L, Neufeld G. Structural characterization and biological functions of fibroblast growth factor. *Endocr Rev* 1987; **8**: 95-114 [PMID: 2440668 DOI: 10.1210/edrv-8-2-95]
- Fu XB, Cuevas P, Tian HM, Sheng ZY. Tissue damage due to acute ischemia and reperfusion can be reduced by acidic fibroblast growth factor (aFGF). *Jiefangjun Yixue Zazhi* 1995; **20**: 95-97
- Fu XB, Cuevas P, Tian HM, Sheng ZY. Therapeutic effects of acidic fibroblast growth factor on postischemic renal injury. *Zhonghua Weizhongzheng Yixue Zazhi* 1995; **7**: 8-11
- Ishikawa T, Tarnawski A, Sarfeh IJ, Stachura J. Epidermal growth factor protects gastric mucosa against ischemia-reperfusion injury. *J Clin Gastroenterol* 1993; **17** Suppl 1: S104-S110 [PMID: 8283003 DOI: 10.1097/00004836-199312001-00019]
- Cuevas P, Carceller F, Ortega S, Zazo M, Nieto I, Giménez-Gallego G. Hypotensive activity of fibroblast growth factor. *Science* 1991; **254**: 1208-1210 [PMID: 1957172]
- Fu XB. Fibroblast growth factor and its non-mitogenic effects. *Pathophysiol Rev* 1994; **14**: 221-222

S- Editor: Tao T L- Editor: Filipodia E- Editor: Li RF

Study on traditional Chinese Medicine Syndrome-typing of chronic ulcerative colitis

Zhi-Shui Chen, Chun-Mei Zhou, Yao Lu, Zhi-Wei Nie, Qi-Li Sun, Yun-Xiang Wang, Yong Chi

Zhi-Shui Chen, Chun-Mei Zhou, Yao Lu, Zhi-Wei Nie, Qi-Li Sun, Yun-Xiang Wang, Yong Chi, Department of TCM, 211 Hospital of the PLA, Harbin 150080, Heilongjiang Province, China

Zhi-Shui Chen, male, born in Guang Han of Sichuan Province in July 1952, graduated from the TCM Department of Heilongjiang Traditional Chinese Medical College in 1975. He is the head of the Department of TCM, 211 Hospital of the PLA, Chief Physician, mainly devoted to the studies of diagnosis and treatment of digestive diseases with integrated Chinese Western therapy. He has 103 papers and 3 books published.

Author contributions: All authors contributed equally to the work.

Original title: *China National Journal of New Gastroenterology* (1995-1997) renamed *World Journal of Gastroenterology* (1998-).

Correspondence to: Dr. Zhi-Shui Chen, Chief Physician, Department of TCM, 211 Hospital of the PLA, Harbin 150080, Heilongjiang Province, China
Telephone: +86-451-6666491-2501

Received: June 2, 1996
Revised: July 29, 1996
Accepted: August 14, 1996
Published online: September 15, 1996

Abstract

AIM: To study the relationship between the modern clinical and pathohistological classification and the traditional Chinese Medicine (TCM) Syndrome-typing of chronic ulcerative colitis (CUC).

METHODS: In total, 452 patients with CUC were classified according to the standards of the TCM Syndrome-typing set up by the Conference of the Combination of the Chinese-Western Medicine on Digestive Diseases in Linfen. The relevant changes between both classifications were analyzed and compared through the colonofiberscopic and pathohistological examination.

RESULTS: The type of retention of interior damp-heat is more commonly seen at the initial onset of disease ($P < 0.01$). No significant differences among other TCM Syndrome-typing groups in patients with persistent disease and with recurrent disease ($P > 0.05$) were observed. The congestion, edema, reduction of goblet cells and the infiltration of neutrophils are pathologically common to all TCM Syndrome-typing groups. Mucosal ulcers were dominant in damp-heat syndrome while crypt ulcers were dominant in spleen-stomach asthenia and spleen-kidney Yang deficiency ($P < 0.01$).

CONCLUSION: There appeared to be a certain relationship between the TCM syndrome-typing and pathohistological changes of the colon mucosa of CUC.

Key words: Ulcerative colitis/pathology; Zheng differentiation classification

© The Author(s) 1996. Published by Baishideng Publishing Group Inc. All rights reserved.

Chen ZS, Zhou CM, Lu Y, Nie ZW, Sun QL, Wang YX, Chi Y. Study on traditional Chinese Medicine Syndrome-typing of chronic ulcerative colitis. *World J Gastroenterol* 1996; 2(3): 141-143 Available from: URL: <http://www.wjgnet.com/1007-9327/full/v2/i3/141.htm> DOI: <http://dx.doi.org/10.3748/wjg.v2.i3.143>

INTRODUCTION

In recent years, both Chinese and Western specialists have been studied the pathogenesis and treatment methods of chronic ulcerative colitis (CUC). However, the relationships between traditional Chinese Medicine (TCM) Syndrome-typing and pathohistological changes of western medicine have not yet been extensively reported. In this study of 452 patients with CUC, we analyzed this relationship and report the results.

MATERIALS AND METHODS

Clinical materials

In total, 452 patients, including 263 males and 189 females were observed in our study. The age range was from 17 years to 65 years, with an average age of 37.8 ± 9.1 . The duration of illness varied between 5 months to 23 years, with an average time of 5.6 ± 4.1 years. The rectum and sigmoid were affected in 215 patients. The left half of the colon was affected in 179 patients. The right half of the colon was affected in 17 patients. The whole colon was affected in 41 patients. The number of patients with mild, moderate and severe disease was 179, 205 and 68, respectively.

Diagnosis

All patients were diagnosed in accordance with the criteria set up in the 1987 Conference of Digestive Diseases in Hangzhou^[1]. The standards of the TCM Syndrome-typing were the same as those set up in the 1992 Conference of Combination of Chinese Western Medicine on Digestive Diseases in Linfen^[2].

Methods

Colonofiberscope, biopsy and the relevant pathohistological observations were carried out in all patients. Two doctors classified the TCM Syndrome-typing. The χ^2 test was used to analyze the data statistically.

RESULTS

The relationship between the TCM Syndrome-typing and the duration of CUC is shown in Table 1. Patients who have had CUC for less than a year were more likely to have damp-heat syndrome. Patients who have had CUC for one year to ten years were more

Table 1 The relationship between the traditional Chinese Medicine Syndrome-typing and the duration of chronic ulcerative colitis *n* (%)

TCM Syndrome-typing	Number	Duration (yr)			
		< 1	1-5	6-10	> 10
Spleen-stomach asthenia	185	23 (12.4) ¹	81 (43.8)	46 (24.9)	35 (18.9)
Spleen-kidney Yang deficiency	81	3 (3.7)	19 (23.4)	26 (32.1)	33 (40.7)
Yin and blood asthenia	46	9 (19.6)	13 (28.3)	14 (30.4)	10 (21.7)
Liver stagnation and spleen deficiency	55	15 (27.3)	17 (30.9)	18 (32.7)	5 (9.1)
Vital energy stagnation and blood stasis	33	6 (18.2)	8 (24.2)	10 (30.3)	9 (27.3)
Damp-heat	52	27 (51.9)	18 (34.6)	5 (9.6)	2 (3.8)

¹Data in parentheses denotes the percentage.**Table 2 Relationship between the traditional Chinese Medicine Syndrome-typing and clinical types *n* (%)**

TCM Syndrome-typing	Number	Clinical types			
		Initial	Persistent	Recurrent	Onset
Spleen-stomach asthenia	185	12 (6.5) ¹	59 (31.9)	114 (61.6)	
Spleen-kidney Yang deficiency	81	2 (2.5)	37 (45.7)	41 (50.6)	1 (1.2)
Yin and blood asthenia	46	1 (2.2)	25 (54.3)	20 (43.5)	
Liver stagnation and spleen deficiency	55	8 (14.5)	17 (30.9)	30 (54.5)	
Vital energy stagnation and blood stasis	33	2 (6.1)	15 (45.5)	16 (48.5)	
Damp-heat retention	52	39 (75.0)	3 (5.8)	8 (15.4)	2 (3.8)

¹Data in parentheses denotes the percentage.**Table 3 Relationship between the traditional Chinese Medicine Syndrome-typing and mucosal changes *n* (%)**

Mucosal changes	Number	Spleen stomach deficiency (<i>n</i> = 185)	Spleen-kidney deficiency (<i>n</i> = 81)	Yin-blood deficiency (<i>n</i> = 46)	Liver stagnation spleen deficiency (<i>n</i> = 55)	Vital energy stagnation and blood stasis (<i>n</i> = 33)	Damp-heat retention (<i>n</i> = 52)	<i>p</i> value
Mild congestion and edema	166	71 (38.4) ¹	12 (14.8)	35 (76.1)	37 (67.3)	9 (27.3)	2 (3.8)	< 0.01
Moderate congestion and edema	184	83 (44.9)	30 (37.0)	11 (23.9)	18 (32.7)	21 (63.6)	21 (40.4)	< 0.01
Severe congestion and edema	102	31 (16.7)	39 (48.1)			3 (9.1)	29 (55.8)	< 0.01
Erosion	304	152 (82.2)	75 (92.6)	7 (15.2)	9 (16.4)	12 (36.4)	49 (94.2)	< 0.01
Ulcer	383	163 (88.1)	79 (97.5)	31 (67.4)	36 (65.5)	23 (69.7)	51 (98.1)	< 0.01
Bleeding	147	61 (33.0)	45 (55.6)	2 (4.3)	3 (5.5)	7 (21.2)	29 (55.8)	< 0.01
Granulation	179	77 (41.6)	47 (58.0)	19 (41.3)	5 (9.1)	29 (87.8)	2 (3.8)	< 0.01
Atrophy	55	11 (5.9)	9 (11.1)	27 (58.7)	1 (1.8)	7 (21.2)		< 0.01
Polyp proliferation	67	27 (14.6)	19 (23.5)	1 (2.2)	2 (3.6)	17 (51.5)	1 (1.9)	< 0.01

¹Data in parentheses denotes the percentage.**Table 4 Relationship between the traditional Chinese Medicine Syndrome-typing and pathohistological changes *n* (%)**

Pathological change	Number	Spleen stomach deficiency (<i>n</i> = 185)	Spleen kidney Yang deficiency (<i>n</i> = 81)	Yin blood deficiency (<i>n</i> = 46)	Liver stagnation spleen deficiency (<i>n</i> = 55)	Vital energy stagnation, blood stasis (<i>n</i> = 33)	Damp-heat retention (<i>n</i> = 52)	<i>p</i> value
Goblet cell reduction	444	182 (98.4) ¹	81 (100.0)	44 (95.6)	53 (96.4)	32 (97.0)	52 (100.0)	> 0.05
Neutrophil infiltration	421	171 (92.4)	79 (97.5)	41 (89.1)	47 (85.5)	31 (93.9)	52 (100.0)	< 0.05
Lymphocyte infiltration	248	127 (68.6)	52 (64.2)	15 (32.6)	41 (74.5)	10 (30.0)	3 (5.7)	< 0.01
Angiitis of small vessels	295	121 (65.4)	54 (66.7)	23 (50.0)	36 (65.5)	24 (72.7)	37 (71.2)	> 0.05
Crypt abscess	395	161 (87.0)	72 (88.9)	40 (87.0)	44 (80.0)	29 (87.9)	49 (94.2)	> 0.05
Mucosal ulcer	188	68 (38.8)	32 (39.5)	11 (23.9)	13 (23.6)	10 (30.0)	34 (65.4)	< 0.01
Crypt ulcer	311	142 (76.8)	59 (72.8)	24 (52.2)	28 (50.9)	21 (63.6)	37 (71.2)	< 0.01
Abnormal epitheliosis	63	27 (14.6)	19 (23.5)	3 (6.5)	4 (7.3)	9 (27.3)	1 (1.9)	< 0.01

¹Data in parentheses denotes the percentage.

likely to have the spleen-stomach asthenia syndrome. Patients who have had CUC for more than ten years were more likely to have the spleen-kidney Yang deficiency. The other three TCM types (asthenia of Yin, asthenia of blood, liver stagnation and spleen deficiency, and stagnation of vital energy and blood stasis) had no definite relationship with the duration of the disease.

The relationship between the TCM Syndrome-typing and the clinical classification of CUC is shown in Table 2. The occurrence of damp-heat was more common in the initially affected patients ($p < 0.01$) and less common in the persistent and recurrent cases. There is no significant difference among the other TCM Syndrome-typing groups in the persistent and recurrent patients ($p > 0.05$).

The relationship between the TCM Syndrome-typing and the changes of the colon mucosa is shown in Table 3. The congestion and edema found in all of the TCM Syndrome-typing groups had different severity levels in the different groups. Damp-heat, spleen-kidney Yang deficiency, and spleen-stomach asthenia syndrome were characterized by erosion, ulcers and bleeding. Stagnation of vital energy and blood stasis were characterized by granulation and

polyp proliferation. Both Yin and blood deficiency were characterized by atrophy.

The relationship between the TCM Syndrome-typing and the pathohistological changes of the colon mucosa is shown in Table 4. The reduction of goblet cells and the infiltration of neutrophils are pathological features common to all groups. However, neutrophil infiltration was prevalent in damp-heat syndrome, while lymphocyte infiltration was prevalent in spleen-stomach asthenia, spleen-kidney Yang deficiency, and stagnation of liver and deficiency of spleen. Mucosal ulcers were prevalent in damp-heat, while crypt ulcers were prevalent in spleen-stomach asthenia and spleen-kidney Yang deficiency. Abnormal epithelial proliferation was prevalent both in stagnation of vital energy and blood, and in spleen-kidney Yang deficiency.

DISCUSSION

Chronic and non-specific ulcerative colitis has been under investigation for more than 100 years. The etiology and pathogenesis, according to modern medicine are associated with

many factors such as the immune system, heredity, intestinal infection, mental stress, food sensitivity, and intestinal bacteriolysis. The etiology and pathogenesis, according to TCM, are associated with many factors including mental injury, disorder of diet rhythms, invasion of outside pathogenic evils, and spleen-kidney asthenia. In this series of 452 patients, 40.9% of cases were spleen-stomach asthenia, 17.9% of cases were spleen kidney Yang deficiency, 12.1% of cases were stagnation of liver and deficiency of spleen, 11.5% of cases were for damp-heat retention, 10.1% of cases were deficiency of both Yin and blood, and 7.3% of cases were stagnation of vital energy and blood. The cases involving spleen-kidney asthenia account for more than 50% and the cases involving sthenia syndromes (damp-heat and stagnation of vital energy and blood stasis) account for less than 20%. We theorized that the spleen kidney asthenia could be the prevalent syndromes in CUC, while the damp-heat is superficial. Though the lesion is located in the large intestine, the effects of the lesion could extend to the spleen, kidney and liver.

In order to investigate some objective rules of the TCM Syndrome-typing, we carried out systematic observations through clinical, pathological and laboratory examinations. After analysis of the data from 452 patients, there is a clear relationship between the TCM Syndrome-typing and the duration of CUC. The sequence of progression tended to begin with damp-heat, then to spleen asthenia, and further to kidney asthenia. This indicated that damp-heat was more common in cases with a shorter duration. The pathogenic damp may stay in the spleen as the duration of illness was prolonged. This can lead to injury of the organ and its vital energy. The disease may further progress to spleen-stomach asthenia syndrome. Moreover, the kidney could be affected by the spleen distress. Therefore, the spleen kidney Yang asthenia results.

Currently, there are no studies investigating the relationship between the TCM Syndrome-typing and the pathological change of the colon mucosa. Dai *et al.*^[3] hypothesized that the body of the tongue had significant influence on an endoscopy diagnosis. This alludes to a relationship between Chinese glossoscopy and intestinal diseases. Our study elucidated the relationship between the TCM Syndrome-typing and pathological changes of the colon mucosa, as observed by the naked eye or by micro-pathohistological

examination. For example, mild congestion and edema are prevalent in cases of asthenia of both Yin and blood, and the stagnation of liver and deficiency of spleen. Moderate congestion and edema are prevalent in cases of spleen-stomach asthenia, and stagnation of vital energy and stasis of blood. Severe congestion and edema are prevalent in cases of damp-heat retention and spleen-kidney Yang deficiency.

Although cellular infiltration and ulcerative changes of the colon mucosa are features common to all of the TCM Syndrome-typings, the types of infiltrating cells and the sites of the ulcers are different. The nature of spleen-kidney Yang deficiency is opposite to that of damp-heat. The former belongs to the syndrome of Yin, deficiency and cold, while the latter belongs to the syndrome of Yang, sthenic and heat. All of the TCM Syndrome-typings have the same notable congestion, edema, and ulcers. Therefore, further studies are required to investigate the pathogenesis. Notably, we observed several differences. In the cases of spleen-kidney Yang deficiency, the mucosal edema was more apparent than congestion, there was no marked swelling around the ulcer, and a white secretion covered the surface. In the cases of damp-heat, the mucosal edema was more apparent than congestion, there was marked swelling around the ulcer, and a yellow purulent secretion covered the surface. Taken together, there are internal relationships between the TCM Syndrome-typing and pathological changes in CUC.

Our study is only a preliminary investigation of the relationships between the TCM Syndrome-typing and the pathological, pathohistological, and clinical classification of modern medicine. Further study is required for understanding the pathogenesis of CUC and establishing objective parameters of the TCM Syndrome-typing.

REFERENCES

- 1 **The Chinese Conference of Digestive Diseases.** The standards of diagnosis and treatment of non-specific ulcerative colitis. Abstracts of the Conference abstract 1978: 217-217
- 2 **Chen ZS, We BH, Chen ZM.** The standards of diagnosis: typing and treating of chronic non-specific ulcerative colitis using Chinese-western medicine combination method (draft). *Zhongguo Zhongxiyi Jiehe Zazhi* 1994; **4**: 239-240
- 3 **Dai WZ, Dai HL, Zhang JW.** The significance of the Chinese glossoscopy contrasting to endoscopy in diagnosing diseases of the lower digestive tract. *Zhongguo Yiyao Xuebao* 1994; **35**: 43-45

S- Editor: Yang RC L- Editor: Filipodia E- Editor: Li RF



Radiological diagnosis of inflammatory ulcerative diseases of the small bowel

Yan Lu, Jian-Ying Duan, Yu Gao

Yan Lu, Jian-Ying Duan, Yu Gao, Department of Radiology, Sino Japan Friendship Hospital, Beijing 100029, China

Yan Lu, Professor of Radiology, having 56 papers and two books published. Born on June 24, 1934 in Fujian. Graduated from Tongji Medical University in 1957.

Author contributions: All authors contributed equally to the work.

Original title: *China National Journal of New Gastroenterology* (1995-1997) renamed *World Journal of Gastroenterology* (1998-).

Correspondence to: Dr. Yan Lu, Professor, Department of Radiology, Sino Japan Friendship Hospital, Beijing 100029, China
Telephone: +86-10-64222963

Received: Jun 2, 1996
Revised: July 4, 1996
Accepted: August 10, 1996
Published online: September 15, 1996

Abstract

AIM: To analyze the radiological features of ulcerative diseases of the small bowel.

METHODS: Thirty-five patients (20 men and 15 women) with inflammatory ulcerative bowel diseases were studied by radiography (barium meal and/or double contrast study). Patient diseases included eleven cases of tuberculosis (TB), thirteen cases of Crohn's disease, seven cases of bowel Behcet disease, two cases of simple ulcers, and two cases of ischemic bowel disease. Diagnosis was established pathologically in 33 cases and by clinical observation after therapy in two cases.

RESULTS: The lesions were located in the ileum of 82% of TB cases, 77% of Crohn's disease cases, 71% of bowel Behcet disease cases, 50% of simple ulcer cases, and 100% of ischemic bowel disease cases. Ulceration was always present with variable appearances. Longitudinal ulcers, and fissures were noted in Crohn's disease only. There were five cases of large and deep ulcers, three of which were bowel Behcet disease. Superficial and irregular ulcers were present in ten TB cases, and , and transverse ulcers were identified in two TB cases.

CONCLUSION: The morphological appearances of the ulcer, surrounding mucosal alterations, and bowel deformation were the basis for the radiological diagnosis. Correct diagnosis was dependent on optimal X-ray examination techniques and proper interpretation of the morphological changes.

Key words: Small intestine; Gastrointestinal tuberculosis; Crohn's disease/radiography

© The Author(s) 1996. Published by Baishideng Publishing Group Inc. All rights reserved.

Lu Y, Duan JY, Gao Y. Radiological diagnosis of inflammatory ulcerative diseases of the small bowel. *World J Gastroenterol* 1996; 2(3): 144-145 Available from: URL: <http://www.wjgnet.com/1007-9327/full/v2/i3/144.htm> DOI: <http://dx.doi.org/10.3748/wjg.v2.i3.144>

INTRODUCTION

Intestinal ulcers are often found in cases of small intestine inflammatory disease. They are accompanied by a high mortality rate.

It is difficult to make differential diagnoses by radiographic examination^[1,2]. In this study, we reviewed 35 cases of small intestine disease, and analyzed the radiographic characteristics of the disease. Serial changes in radiographic examination were observed.

MATERIALS AND METHODS

We performed radiography (barium meal and/or double contrast study) in 35 patients (20 men and 15 women). All patients were diagnosed with small intestine inflammation with an intestinal ulcer. Diagnosis was established by pathology in 33 cases and by clinical observation after therapy in two cases. The age range of the patients was 14 years to 78 years. Most patients had gastrointestinal symptoms such as abdominal pain, diarrhea, and bloody stool. The inflammatory ulcerative bowel diseases included eleven cases of tuberculosis (TB), thirteen cases of Crohn's disease, seven cases of bowel Behcet disease, two cases of simple ulcers, and two cases of ischemic bowel disease.

RESULT

The lesions were located in the ileum of 82% of TB cases, of 77% of Crohn's disease cases, of 71% of bowel Behcet disease cases, of 50% of simple ulcer cases, and of 100% of ischemic bowel disease cases. Ulceration was always present with variable appearances. Longitudinal ulcers and fissures were noted in Crohn's disease only. There were 5 cases of large and deep ulcers, three of which occurred in bowel Behcet disease. Superficial and irregular ulcers were present in ten TB cases, and transverse ulcers were observed in two TB cases (Figures 1 and 2).

DISCUSSION

Ulceration is present in the majority of small bowel inflammatory diseases including TB, Crohn's disease, bowel Behcet disease, simple ulcers, and ischemic bowel disease. The morphological appearances of the ulcer, surrounding mucosal alterations and bowel deformation were the basis for radiological diagnosis^[3-9]. TB was located in the terminal ileum. Ulcerations had variable appearances, but no longitudinal ulcers and fissures were noted. In Crohn's disease, the above characteristics were noted. In addition, cobblestone and fistulas

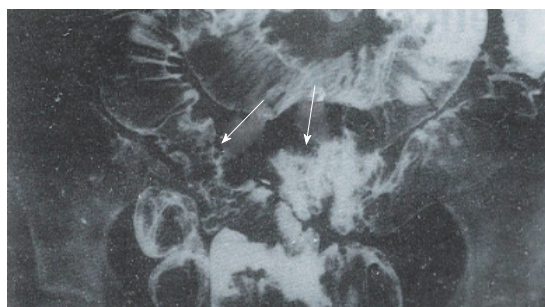


Figure 1 The mucosa is irregular and superficial ulcers (arrows) were present in several segments of the terminal ileum of TB cases.

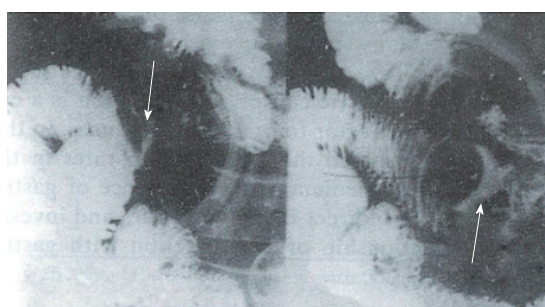


Figure 2 After compression, a transverse ulcer (arrow) is observed in a TB case.

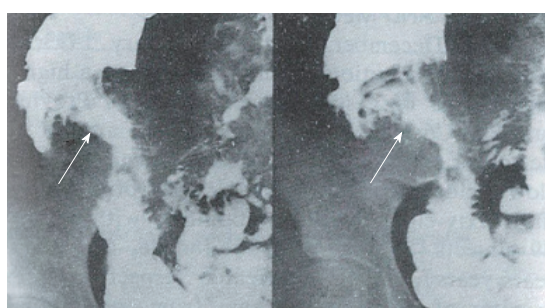


Figure 3 Triangular ulcers measuring 4 cm² in size at the terminal ileum (arrow) were present Crohn's disease cases. The surrounding mucosal pattern exhibited a cobblestone appearance.

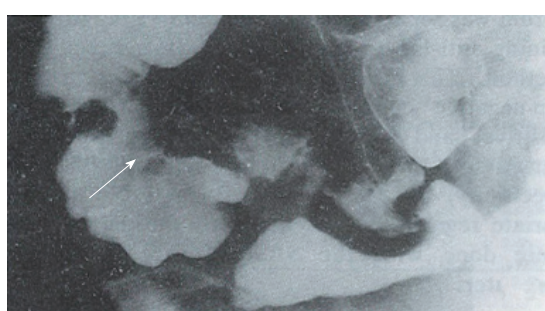


Figure 4 A round ulcer (arrow), with surrounding mild mucosal edema in the ileocecal region was present in a Crohn's disease case.

occurred frequently (Figures 3 and 4). The radiographic findings of bowel Behcet disease and simple ulcer were similar. However, the ulcers in bowel Behcet disease tended to be larger and deeper with surrounding mucosal edema (Figures 5 and 6). All patients had mucocutaneous ocular symptoms. Ulcers in ischemic bowel disease had no characteristics (Figure 7). Correct diagnosis was dependent on optimal X-ray examination techniques and proper interpretation of the morphological changes. Enteroclysis, a controlled infusion method offering a double contrast and highly detailed examination of the small bowel, is relatively easy to perform. Despite the introduction of enteroclysis, the peroral small bowel examination remains the predominant radiographic method of imaging the small intestine. This

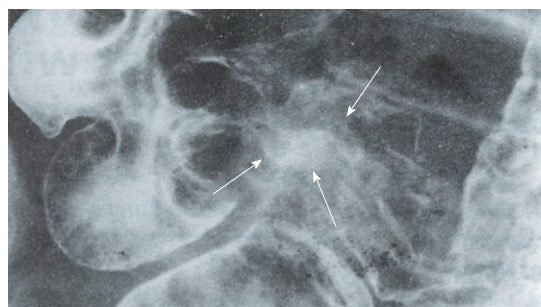


Figure 5 A large and deep irregular ulcer (4 × 3 cm² in size) at the terminal ileum near the ileocecal valve (double arrow) was present in a bowel Behcet disease case. The surrounding mucosal edema (arrow) is shown.

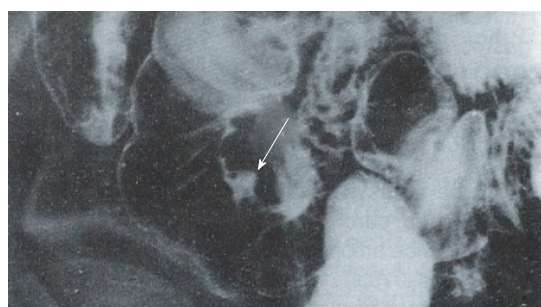


Figure 6 A small ulcer (0.3 × 0.4 cm² in size) at the ileum (arrow) was present in a bowel Behcet disease case. The surrounding mucosal edema (arrow) is shown.

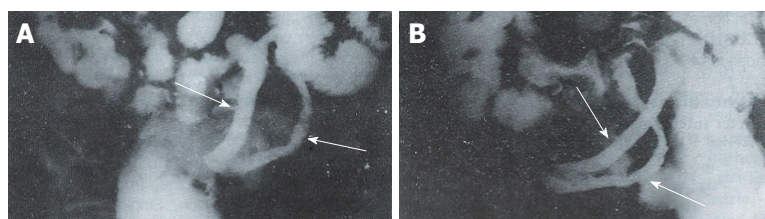


Figure 7 A and B: Several long, segmented, contracted, narrow, and rigid loops of the bowel in the ileum (arrow), with superficial ulcers were present in ischemic bowel disease. No mucosal abnormalities were observed.

report emphasizes the technical factors needed to produce excellent peroral small bowel examinations.

REFERENCES

- 1 Feczko PJ, Holpert RD. Radiology of inflammatory bowel disease. *Radiol Clin North Am* 1987; **25**: 1-20
- 2 Xie JX. Diagnosis and Differential Diagnosis of inflammatory ulcerative diseases of the small bowel. *Zhonghua Fangshexue Zazhi* 1994; **28**: 128-130
- 3 Vaidya MG, Sodhi JS. Gastrointestinal tract tuberculosis: a study of 102 cases including 55 hemicolectomies. *Clin Radiol* 1978; **29**: 189-195 [PMID: 639458 DOI: 10.1016/S0009-9260(78)80230-X]
- 4 Yao T, Okada M, Fuchigami T, Iida M, Takenaka K, Date H, Fujita K. The relationship between the radiological and clinical features in patients with Crohn's disease. *Clin Radiol* 1989; **40**: 389-392 [PMID: 2758748 DOI: 10.1016/S0009-9260(89)80131-X]
- 5 Marshak RH. Granulomatous disease of the intestinal tract (Crohn's disease). *Radiology* 1975; **114**: 3-22 [PMID: 1108108 DOI: 10.1148/114.1.3]
- 6 Nolan DJ, Piris J. Crohn's disease of the small intestine: a comparative study of the radiological and pathological appearances. *Clin Radiol* 1980; **31**: 591-596 [PMID: 7471637 DOI: 10.1016/S0009-9260(80)80064-X]
- 7 Nolan DJ, Goursoyannis NC. Crohn's disease of the small intestine: a review of the radiological appearances in 100 consecutive patients examined by a barium infusion technique. *Clin Radiol* 1980; **31**: 597-603 [PMID: 7471638 DOI: 10.1016/S0009-9260(80)80065-1]
- 8 Iida M, Kobayashi H, Matsumoto T, Okada M, Fuchigami T, Niizeki H, Yao T, Fujishima M. Intestinal Behcet disease: serial changes at radiography. *Radiology* 1993; **188**: 65-69 [PMID: 8511319 DOI: 10.1148/radiology.188.1.8511319]
- 9 Scholz FJ. Ischemic bowel disease. *Radiol Clin North Am* 1993; **31**: 1197-1218 [PMID: 8210346]

S- Editor: Ma JY L- Editor: Filipodia E- Editor: Li RF

An epidemiologic study of *Helicobacter pylori* infection in three areas with high, moderate or low incidences of gastric carcinoma

Wan-Dai Zhang, Yan Yu, Guo-Long Liu, Hai-Tao Yang, Dian-Yuan Zhou

Wan-Dai Zhang, Hai-Tao Yang, Dian-Yuan Zhou, Department of Gastroenterology, Nanfang Hospital, First Military Medical University, Guangzhou 510515, Guangdong Province, China

Yan Yu, Bangbu Medical College

Guo-Long Liu, Department of Oncology, Nanfang Hospital

Wan-Dai Zhang, male, born on August 18, 1930 in Shenyang City of Liaoning Province, graduated from Changchun Medical University. He is the director of the Gastroenterologic Association of Guangdong Province. He has 38 papers and three books on gastroenterology published.

Author contributions: All authors contributed equally to the work.

Original title: *China National Journal of New Gastroenterology* (1995-1997) renamed *World Journal of Gastroenterology* (1998-).

Correspondence to: Dr. Wan-Dai Zhang, Professor, Department of Gastroenterology, Nanfang Hospital, First Military Medical University, Guangzhou 510515, Guangdong Province, China
Telephone: +86-20-57705577-3095

Received: September 11, 1995
Revised: July 25, 1996
Accepted: August 14, 1996
Published online: September 15, 1996

Abstract

AIM: To study the relationship between the *Helicobacter pylori* (Hp) infection rate and the incidence and mortality of gastric cancer.

METHODS: The Hp infection rates of the natural population in three areas were detected by measuring the specific IgG antibody to Hp using the indirect ELISA method.

RESULTS: The Hp positive rates were 59.4%, 55.9% and 34.5% in the areas with high, moderate and low incidences of gastric carcinoma, respectively. The differences in incidence among the areas were significant ($\chi^2 = 25.029$, $P < 0.05$). The Hp infection rate was the highest in the high incidence area of gastric cancer in people younger than 40 years. The Hp infection rate was 50% in children younger than 5 years in the high incidence area. The Hp infection rates were not different among the three areas in the people older than 40 years. The average levels of anti-Hp IgG in the high, moderate and low incidence areas were 2.3 ± 0.49 , 2.04 ± 0.47 and 1.84 ± 0.46 , respectively. Multivariate regression analysis showed that the Hp infection was related to bad hygienic habits, low income, frequent use of antibiotics, and mental depression. Univariate analysis showed that Hp infection might also be associated with raising animals in the home.

CONCLUSION: Gastric cancer is closely related to the incidence of Hp infection.

Key words: Stomach neoplasms/etiology; *Helicobacter* infections/epidemiology

© The Author(s) 1996. Published by Baishideng Publishing Group Inc. All rights reserved.

Zhang WD, Wu Y, Liu GL, Yang HT, Zhou DY. An epidemiologic study of *Helicobacter pylori* infection in three areas with high, moderate or low incidences of gastric carcinoma. *World J Gastroenterol* 1996; 2(3): 146-148 Available from: URL: <http://www.wjgnet.com/1007-9327/full/v2/i3/146.htm> DOI: <http://dx.doi.org/10.3748/wjg.v2.i3.148>

INTRODUCTION

Gastric carcinoma is the most common malignant tumor in China. However, the cause of the disease remains unclear. Many studies have proved that environmental factors may play a very important role in the pathogenesis of gastric cancer. Hp infection is an environmental risk factor for gastric carcinoma. In this study, we determined the Hp infection rates in areas with high, moderate or low incidences of gastric cancer using an indirect ELISA method. We then investigated the relationship of the Hp infection with the gastric cancer incidence.

MATERIALS AND METHODS

From December 1992 to February 1993, we collected samples from people in Changle County, a high incidence area of gastric cancer of Fujian Province, Huaiyuan County, a moderate incidence area of gastric cancer of Anhui Province, and Conghua County, a low incidence area of gastric cancer of Guangzhou City. A total of 639 subjects from 68 families in the high incidence area, 64 families in the moderate incidence area, and 63 families in the low incidence area participated. There were 358 males and 281 females, with ages ranging from 1 year old to 65 years old. Two milliliters of blood was drawn from each subject. Serum was separated and stored at -20°C until the samples were processed for the anti-Hp IgG antibody by an indirect ELISA method. If the ratio of the OD of the subject to the OD of the Hp-negative control was ≥ 2.0 , then the sample was considered Hp-positive. If the ratio of the OD of the subject to the OD of the Hp-negative control was < 2.0 , then the sample was considered Hp-negative. The sensitivity of this method was 93.9%, and the specificity was 86.8%. Statistical analysis and multivariate regression analysis of all the data obtained were done with the SAS software on an AST-486 computer.

RESULTS

The overall positive rate of the anti-Hp IgG antibody was 50.5% (329/639) in these subjects. The Hp infection rates of the populations in the high, moderate and low incidence areas are shown in Table 1. The Hp infection rate in the high incidence area

Table 1 *Helicobacter pylori* infection rates of subjects from areas with low, moderate, and high incidence rates of gastric cancer

Age (yr)	Low (Conghua County)		Moderate (Huaiyuan County)		High (Changle County)	
	<i>n</i>	Positive rate (%)	<i>n</i>	Positive rate (%)	<i>n</i>	Positive rate (%)
1-4	13	15.4	14	35.7	14	50.0
5-9	43	30.2	17	41.2	42	54.8
10-19	32	37.5	23	43.5	32	53.1
20-29	27	33.3	66	63.6	44	72.7
30-39	30	33.3	34	64.7	40	67.5
40-49	23	43.5	28	53.6	19	47.4
50 +	29	41.4	31	58.7	38	55.3
Total	197	34.5	213	55.9 ^a	229	59.4 ^a

$\chi^2 = 25.029$, ^a $P < 0.05$, compared with the area of low incidence rate (Conghua County)

Table 2 Anti-*Helicobacter pylori* IgG levels in subjects from areas with low, moderate, and high incidence rates of gastric cancer

	<i>n</i>	(S/N)
Low (Conghua County)	197	1.84 ± 0.46 ^b
Moderate (Huaiyuan County)	213	2.04 ± 0.47 ^b
High (Changle County)	229	2.30 ± 0.49

^b $P < 0.01$, compared with the area of high incidence rate (Changle County)

Table 4 Univariate analysis of *Helicobacter pylori* related factors

N (Xi)	Variable	χ^2 M-H	P value
X11	Eating red pepper	10.53	0.001
X25	Frequent use of antibiotics	6.39	0.011
X29	Raising animals in the home	3.86	0.049
X32	Abdominal symptoms	5.82	0.016
X39	Low income	9.99	0.002
X51	Mental depression	5.26	0.022

was higher than that in the moderate incidence area, and much higher than that in the low incidence area in people younger than 40 years. Also, the Hp infection rate in children under 5 years of age in the high incidence area was 50%, which was significantly higher than those in the other two areas ($P < 0.05$). However, the Hp infection rates were not different among the three areas in the subjects older than 40 years. The Anti-Hp IgG level in the subjects of the high incidence area was significantly higher than that of the other two areas ($P < 0.01$) (Table 2). A Mantel-Haenszel analysis showed that X1, X25, X29, X32, X39 and X51 were highly associated with an Hp infection (Table 3). Multivariate regression analysis and logistic regression analysis showed that X3, X11, X18, X25, X39 and X51 were risk factors for an Hp infection (Table 4).

DISCUSSION

Gastric cancer is the most common malignant tumor in China. The average yearly mortality from gastric cancer between 1975 and 1978 was 15.41 people out of 1000000 people. Interestingly, mortality rates varied by geographic location^[1]. Changle County is located on the southeast coast and has the highest incidence and mortality rates from gastric carcinoma (120.47 people out of 1000000 people) in China. Conghua County of Guangzhou City has a low incidence rate of gastric carcinoma in China, with a mortality rate of one person out of 100000. Huaiyuan County of Anhui Province has a moderate incidence of gastric cancer. The mortality rate of gastric cancer approaches the average level in China^[2-4].

In the present study, each family was taken as an observation unit for determining the Hp infection rates in Changle (high incidence), Huaiyuan (moderate incidence) and Conghua (low incidence) counties. The overall Hp infection rate was 50.55%. The Hp infection rate and anti-Hp IgG antibody levels in the subjects of the high incidence area were higher than those of the other two areas, especially in children younger than 5 years. However, the Hp infection rates were not different among the three areas in subjects older than 40 years.

Many studies have shown that atrophic gastritis incidence is

Table 3 Multivariate regression analysis of *Helicobacter pylori* related variables

N (Xi)	Variable	<i>r</i>	<i>F</i>	P value
X3	Drinking natural water	0.052	4.34	0.038
X11	Eating red pepper	0.079	8.57	0.003
X18	Poor dietary habits	-0.110	11.98	0.001
X25	Frequent use of antibiotics	-0.110	12.79	0.000
X39	Low income	0.087	21.14	0.000
X51	Mental depression	-0.108	4.23	0.040

associated with an Hp infection. The Hp infection rate was 60% to 90% in patients with atrophic gastritis and 92% in patients with active atrophic gastritis in China^[5]. In other countries the Hp infection rate was 43.5% to 89.5% in patients with atrophic gastritis^[6]. Atrophic gastritis is considered to be a risk factor for gastric cancer. The incidence of gastric cancer in high incidence areas is seven times higher than in low incidence areas of gastric cancer, and atrophic gastritis is usually more severe in high incidence areas of gastric cancer^[7]. Notably, the majority of atrophic gastritis cases and Hp infections affect the gastric antrum. Anti-Hp IgG antibody levels were related to the number of Hp and the reaction of the gastric mucosa to Hp^[8]. The Hp infection rates and anti-Hp IgG levels were higher, and the average age of the infected patients were younger in the high incidence areas of gastric cancer than in the low incidence areas^[9,10]. This data suggests that gastric cancer might be associated with an Hp infection, and thus an Hp infection may be one of the risk factors for gastric cancer.

Multivariate regression analysis showed that drinking natural water, poor dietary habits, low income and mental depression were all risk factors for an Hp infection. Ling *et al*^[8] proved that Hp can live in natural river water for approximately 10 days, indicating that Hp infection may be transmitted by water. Inhabitants of Changle County (high incidence area) usually drink natural water. The nitrate and nitrosamine levels are higher there than the nitrate and nitrosamine in water of other areas. Hp infection or long time exposure to high levels of nitrate and nitrosamine may destroy gastric mucosa and result in gastric cancer. It is hypothesized that an Hp infection and high levels of nitrate and nitrosamine in the drinking water may be the cause of the high incidence rate of gastric cancer in Changle County.

Graham *et al*^[11] observed that the Hp infection rate was 70% in black people and 34% in white people in the United States. They also found that the Hp infection rate was higher in low-income families, which coincides with our results. Univariate analysis showed that an Hp infection was also associated with raising animals in the home. Some studies have shown that both humans and animals can be infected with Hp. Experimental Hp infection of the stomachs of newborn pigs, newborn dogs, and nude mice has been successful^[12]. In addition, Euler isolated an Hp-like organism from the monkey, suggesting that humans and animals may transmit Hp to one another.

In summary, we observed an association between gastric cancer and Hp infections. Hp infection rates were higher and the age of the infected patents were younger in the high incidence area compared to the rates and ages in the low incidence area. The risk factors related to gastric cancer included low income, mental depression, and poor dietary habits. Our results also suggested that the gastric

cancer incidence and mortality have positive correlations with Hp infection. In other words, Hp infection may be a risk factor for gastric cancer.

REFERENCES

- 1 **Office for Prevention and Therapy of Tumors in the Ministry of Public Health.** Investigation on mortality of malignant tumors in China. Beijing: The People's Medical Publishing House 1980: 52-59
- 2 **Zhang WF, Zhang YC.** Gastric cancer. Shanghai: Shanghai Science and Technique Publishing House 1987: 16-17
- 3 **Tao SC, Xiu GW.** Gastric cancer. Beijing: The People's Medical Publishing House, 1980: 12-13
- 4 **Li YY, Hu PJ, Duo GG.** Hp epidemiologic investigation in China. *Zhonghua Yixue Zazhi* 1993; **73**: 168-175
- 5 **Jing SJ, Liu WZ.** Hp infection in China. *Zhongguo Yishi Zazhi* 1989; **9**: 393-397
- 6 **Correa P, Ruiz B.** Campylobacter pylori and gastric cancer. In: Rathbone BJ, Heatley RV, eds. Campylobacter pylori and gastroduodenal disease. Oxford. London: Blackwell Scientific 1989: 139-145
- 7 **Zhang LX, Sen HL, Jing ML.** Etiological survey on gastric in China. *Zhonghua Yixue Zazhi* 1982; **62**: 203-207
- 8 **Ling HZ, Zhang YC.** Geographical pathology of gastric cancer in China. *Zhonghua Yixue Zazhi* 1985; **14**: 1-5
- 9 **Parsonnet J, Friedman GD, Vandersteen DP, Chang Y, Vogelmann JH, Orentreich N, Sibley RK.** Helicobacter pylori infection and the risk of gastric carcinoma. *N Engl J Med* 1991; **325**: 1127-1131 [PMID: 1891020 DOI: 10.1056/NEJM199110173251603]
- 10 **Morris A, Ali MR, Brown P, Lane M, Patton K.** Campylobacter pylori infection in biopsy specimens of gastric antrum: laboratory diagnosis and estimation of sampling error. *J Clin Pathol* 1989; **42**: 727-732 [PMID: 2474579 DOI: 10.1136/jcp.42.7.727]
- 11 **Graham DY, Malaty HM, Evans DG, Evans DJ, Klein PD, Adam E.** Epidemiology of Helicobacter pylori in an asymptomatic population in the United States. Effect of age, race, and socioeconomic status. *Gastroenterology* 1991; **100**: 1495-1501 [PMID: 2019355]
- 12 **Han SY, Wang FC, Zhang LJ.** Epidemiologic investigation on gastritis, gastric ulcer and Hp infection in China. *Zhonghua Liuxingbingxue Zazhi* 1992; **13**: 150-158

S- Editor: Tao T L- Editor: Filipodia E- Editor: Li RF



Metal stent implantation for palliation of malignant biliary obstruction: A report of 57 cases

Bing Hu, Dai-Yun Zhou, Biao Gong, Feng-Mei Zhang, Shu-Zhi Wang, Hong-Yan Chang, Meng-Chao Wu

Bing Hu, Dai-Yun Zhou, Biao Gong, Feng-Mei Zhang, Shu-Zhi Wang, Hong-Yan Chang, Meng-Chao Wu, Department of Biliary Surgery and Endoscopic Office, Orient Hepatobiliary Surgery Hospital, Second Military Medical University, Shanghai 200433, China

Bing Hu, Attending Surgeon and Endoscopist, having 11 papers and two books published.

Author contributions: All authors contributed equally to the work.

Reported at the International Workshop and Symposium on Therapeutic Endoscopy and Gastroenterology, Shenyang, 17th July, 1995

Original title: *China National Journal of New Gastroenterology* (1995-1997) renamed *World Journal of Gastroenterology* (1998-).

Correspondence to: Dr. Bing Hu, Department of Biliary Surgery and Endoscopic Office, Orient Hepatobiliary Surgery Hospital, Second Military Medical University, Shanghai 200433, China
Telephone: +86-21-65564166-72856
Fax: +86-21-65564166-72896

Received: June 7, 1996
Revised: July 10, 1996
Accepted: August 12, 1996
Published online: September 15, 1996

Abstract

AIM: To report the first experience in China in the treatment of malignant biliary obstruction with expandable metal stent, which allows the insertion of an endoprosthesis as large as 1 cm in diameter.

METHODS: Between April 1994 and May 1996, we implanted expandable metal stents in 57 patients with incurable malignant biliary obstruction. Fifty-four patients underwent endoscopic procedure, and the other three patients received percutaneous transhepatic placement.

RESULTS: Insertion of the stent following guide wire positioning was successful in 95% of the patients. Two patients developed cholangitis after stent insertion and were successfully treated with conservative treatment. The jaundice was eliminated completely in 21 cases and markedly decreased in 23 cases within 2 wk after stent placement. However, nine patients had late cholangitis due to stent failure after a median interval of 147 d. Twenty-three cases underwent nasobiliary transient drainage, and three underwent plastic stent transient drainage prior to metal stent insertion. The advantages of transient drainage were drainage pre-assessment and infection control.

CONCLUSION: Our results show that an expandable metal stent is suitable for the unresectable malignant choledochal stenosis. It can eliminate jaundice and improve the patient's quality of life. To get the highest benefit, however, the indication should be strictly selected.

To get long-term patency, the proximal and distal end of the stent preceding the tumor should be no shorter than 2 cm. In the case of hilar cancer, Bismuth classification is helpful for the selection of the drainage site.

Key words: Biliary tract obstruction/surgery; Biliary tract, neoplasms/surgery; Stents

© The Author(s) 1996. Published by Baishideng Publishing Group Inc. All rights reserved.

Hu B, Zhou DY, Gong B, Zhang FM, Wang SZ, Cheng HY, Wu MC. Metal stent implantation for palliation of malignant biliary obstruction: A report of 57 cases. *World J Gastroenterol* 1996; 2(3): 149-151 Available from: URL: <http://www.wjgnet.com/1007-9327/full/v2/i3/149.htm> DOI: <http://dx.doi.org/10.3748/wjg.v2.i3.149>

INTRODUCTION

Endoscopic biliary drainage with polyethylene endoprosthesis has become a well-established palliative treatment for patients with inoperable, malignant, and obstructive jaundice. The main drawback of this method is rapid incrustation or occlusion as a result of bacterial biofilm formation on the stent, and biliary sludge^[1]. Drainage occlusion of the commonly used 7-12 Fr gauge plastic prosthesis occurs in 20% to 30% of cases within the first three mo and in up to 60% of cases within 6 mo^[2]. Though larger stents may perform better, stents over 14 Fr have not been used in the biliary tract up to now because the maximum diameter of the stent depends upon the diameter of the working channel of the endoscope. The development of expandable metal stents allows the insertion of an endoprosthesis as large as 1 cm in diameter. Such an endoprosthesis, previously employed for vascular and urethral stricture, recently became available for biliary use.

In this paper, we report our first experience in China in the treatment of 57 patients with malignant bile duct stenosis using metal stents during the period from April 1994 to May 1996.

MATERIALS AND METHODS

Fifty-seven patients (40 male and 17 female) with a median age of 56.1 years (range: 25 years to 85 years) were treated with a total of 60 expandable stents. In all patients, the malignant diseases led to invasive or compressive occlusion of the hepatocholedochal duct (Table 1). None were operable due to advanced stage, metastasis, post-operative recurrence of the disease, old age, or accompanying disease.

Two types (several kinds) of metal stents, self-expandable stents (Wallstent, Instent and Angiomed) and balloon-mounted stents (Strecker) were used.

General diagnostic endoscopic retrograde cholangiopancreatography was first made using a side-view duodenoscope (TJF-30,

Table 1 Causes of bile duct obstruction in 57 patients

Cause of bile duct obstruction	Location of stenosis			No. of patients
	P	M	D	
Cholangiocarcinoma	30	3	1	34
Gallbladder carcinoma	3	1	0	4
Hepatocellular carcinoma	7	0	0	7
Pancreatic carcinoma	1	0	6	7
Ampullary tumor	0	0	2	2
Metastasis	3	0	0	3
Total	44	4	9	57

P: Proximal part of the common bile duct; M: Middle part of the common bile duct; D: Distal part of the common bile duct.

Table 2 Relation between the Bismuth classification and drainage sites in patients with hilar malignancy

Type	No. of patients	Drainage site				
		H	L	R	RA	RP
I	8	2	3	2	0	1
II	3	0	1	1	0	1
IIIa	5	0	2	0	1	2
IIIb	4	0	0	0	0	4
IV	24	0	6	2	4	12
Total	44	2	12	5	5	20

H: Common hepatic duct; L: Left hepatic duct; R: Right hepatic duct; RA: Right anterior intrahepatic duct; RP: Right posterior intrahepatic duct.

4.2 mm working channel, or JF-1T30, 3.2 mm working channel). When biliary stenosis was found, a 4 m long, 0.035 inch standard guide was inserted into papilla passing the strictured segment. No papillotomy was performed, but a simple dilation was made with a 10 Fr or 8.5 Fr Teflon dilator (Wilson-Cook) instead. Afterward, the delivery catheter with the constrained stent was inserted over the guide wire. The stent was released under continuous fluoroscopic and endoscopic control. If we were uncertain of the drainage effect in the patients with extensive stenosis or severe infection, a transient nasobiliary drainage was performed first. After a satisfactory drainage was achieved, or the bile duct inflammation was successfully controlled, another endoscopic procedure for the metal stent implantation was given.

In three patients, endoscopic transpapillary implantation was impossible because of previous Billroth II gastrectomy, cannulation failure of the ampulla of Vater, or duodenal stricture. Percutaneous transhepatic route was therefore chosen. One week after an ordinary percutaneous transhepatic biliary drainage (PTBD), the drainage tract was dilated to 10 Fr. A passage through biliary stenosis was made using a guide wire, and then the metallic stent was delivered into the biliary tree and released under fluoroscopy.

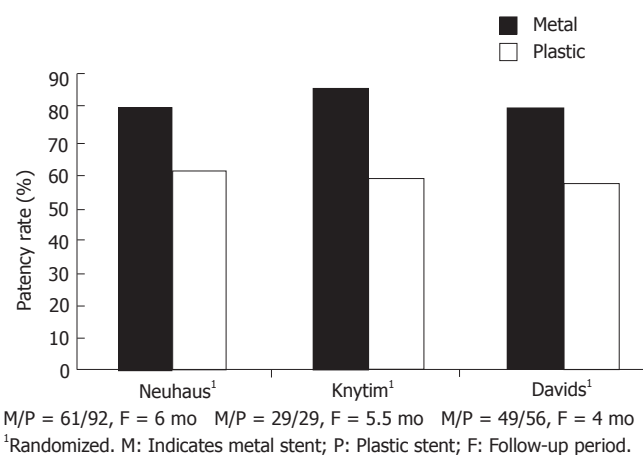
All patients were followed up as long as possible. Their general condition, laboratory findings, as well as recurrence of jaundice and fever were recorded.

RESULTS

Fifty-seven patients were implanted with a total of 60 metal stents. The success rate for metal endoprosthesis insertion was 95%. In three cases, there were technical problems during implantation of the first stent. In one of the patients, a Strecker stent failed to cannulate into papilla because its distal end had already been released. In another patient, a Wallstent could not be placed due to the breakage of its outer membrane. In the final patient, a Wallstent was released by mistake inside the working channel of the duodenoscope. However, in all three cases, another stent was successfully implanted the second time.

A transient rise in cholestasis parameters and fever indicating cholangitis as an early complication were seen in two (3.5%) patients. They were rapidly and effectively treated with antibiotics. No other complications related to stent insertion were found.

During the first two weeks after the placement of the stent, cholestasis parameters returned to normal in 21 cases, decreased significantly in 23 cases, and were unchanged or even elevated in two cases. Follow-up was unavailable for the remaining nine

**Figure 1** Overview of current comparative or randomized studies of patency rate on metal stents versus conventional plastic stents.

patients. However, during the long-term follow-up, nine patients had late cholangitis due to stent failure after a median interval of 146.7 d. The causes of stent failure were distal tumor overgrowth in four patients after a median interval of 127.5 d, tumor ingrowth through the meshes of the stent in four cases after a median of 150 d, and biliary sludge obstruction in one case after 210 d. The cholangitis was treated with a 9 Fr polyethylene stent through the metal stent in four patients, with a nasobiliary drainage in one patient, PTBD in one patient, and biliary lavage and balloon pull-through in one patient.

During the follow-up, four patients died due to non-stent related causes (renal failure in two cases 12 d and 210 d, respectively post stent insertion, esophageal variceal bleeding in one patient at 51 d post stent insertion, and ileus bleeding in one patient at 63 d post stent insertion). Two patients died of stent failure and cholangitis 90 d and 153 d after endoprosthesis, respectively. To our knowledge, eight patients with a successful stent insertion have been alive for more than 6 mo after stent implantation. The patient with the longest survival (over 18 mo) has been free from jaundice as of this publication.

DISCUSSION

Expandable intraluminal stents were initially developed to prevent early reocclusion or delayed restenosis after percutaneous transluminal coronary angioplasty (PTCA). The first biliary expandable stent was inserted in an animal study in 1985^[3]. The expandable diameters of the metal stents of up to 7-10 mm, the reduced surface area for bacterial attachment, and the capacity of being epithelialized by biliary mucosal cells are the major advantages in preventing bacterial colonization and biofilm formation. Figure 1 shows the results of current comparative or randomized studies by several specialists on wire mesh endoprotheses versus conventional plastic prostheses^[4-6]. Hoepffner *et al.*^[2] reported a long term study on Wallstent therapy for 118 malignant choledochal stenosis patients, and found the survival rate at 6 mo, 12 mo, and 24 mo was 40%, 20% and 10% respectively, with the longest survival of 1295 d, which was similar to that after palliation bypass surgery in a previous report.

There were 44 (77.2%) patients with malignant biliary obstruction due to proximal bile duct stenosis in our study. It is attributable to the high incidence of hilar tumor (Klatskin's tumor) and extraordinarily low resection rates of the cancer. According to the Bismuth classification^[7], our patients were classified into type I (8 cases, 18.2%), type II (3 cases, 6.8%), type III_a (5 cases, 11.4%), type III_b (4 cases, 9.1%) and type IV (24 cases, 54.5%). The relationship between the typing and drainage sites is shown in Table 2. Generally, type I patients can get satisfactory drainage, followed by type II and type III. Type IV patients can only achieve poor drainage. We emphasize the importance of total revelation of intrahepatic duct, upon which it is possible to select a suitable site for drainage. Normally, the wider the range of the intrahepatic tree, the better the drainage. If the drained region can reach a little more than half a liver, it is still hopeful to eliminate jaundice completely.

Table 3 Common complications of metal biliary stenting^[2,9]

	Huibregtse <i>et al</i> , 1992 (103 cases)	Hoepffner <i>et al</i> , 1994 (118 cases)	Our group, 1996 (57 cases)
Early cholangitis	2	5	2
Late cholangitis	18 (125 d) ¹	17 (148 d)	9 (147 d)
Tumor ingrowth	10	4 (150 d)	4 (150 d)
Tumor overgrowth	4	5	4 (128 d)
Sludge clogging	5 (175 d)	N/A	1 (210 d)

¹Numbers in parentheses are median days

Sharp angles should be avoided when selecting a drainage site in order to get full expansion of the stent.

The length of the stent should also be determined carefully. In our group, there were four patients with late stent failure due to tumor overgrowth after a median interval of 127.5 d. Therefore, we recommend that the two ends of the stent preceding the tumor should not be shorter than 2 cm after full expansion in order to get long-term stenting.

We also attach importance to the use of transient nasobiliary drainage prior to the stenting. Because the metal stent is very expensive, we should be more prudent in choosing cases. Nasobiliary drainage is a simple and cheap way to know the quantity of the drain, and is very effective in controlling bile duct infection. It also gives the surgeon time to discuss if the patient has any opportunity to undergo a radical operation. In our group, 23 patients had undergone nasobiliary drainage, and three patients had undergone plastic stent drainage for a mean period of 15 d before metal endoprosthesis insertion. When the bile fluid was less than 300 mL per day and the cholestasis parameters decreased significantly, another endoscopic procedure for metal stent implantation can be performed.

Though expandable metal stents provide a longer median period of patency over conventional plastic prosthesis, they are not without problems. Tumor ingrowth through the metal mesh, or overgrowth at the ends of the stents may occur several weeks to several mo later, causing occlusion of bile flow (Table 3). Many stent occlusions can be successfully treated by implantation of a second metal stent or a conventional plastic one through the metal stent. Some endoscopists also reported the method of coagulation using a unipolar electrohydraulic probe or bipolar electrohydrothermal probe^[2,8]. In recent studies, a "coating" stent or "electrolytic" stent may solve the above-mentioned disadvantages of metal stents^[10,11].

The indications of metal stent implantation remain controversial. Though some doctors have tried to use metal stents to treat benign biliary stricture, most specialists are reluctant to use this unremovable stent in patients with benign disease because the recurrent ulceration caused by sharp filaments of the metal stent

can give rise to resticture proximal to the stent. The high cost of this treatment is also under discussion. Although several authors have argued that when the costs of retreatment due to plastic stent failure are included, the metal stents are cost-effective, considering the limited life span of these patients with terminal malignancies, the price of the metal stent is still a concern. "Is the expanse worth the expense?" is an interesting question raised by Cotton^[12]. In our opinion, metal stent implantation is the treatment of choice for palliating jaundice in patients (1) with inoperable pancreatobiliary malignancies, (2) with adequate biliary tree to drainage, (3) without major organic exhausting, (4) who may survive for more than 3 mo, and (5) whose financial condition allows.

REFERENCES

- 1 Sung JJ, Chung SC. Endoscopic stenting for palliation of malignant biliary obstruction. A review of progress in the last 15 years. *Dig Dis Sci* 1995; **40**: 1167-1173 [PMID: 7540126 DOI: 10.1007/BF02065519]
- 2 Hoepffner N, Foerster EC, Högemann B, Domschke W. Long-term experience in Wallstent therapy for malignant choledochal stenosis. *Endoscopy* 1994; **26**: 597-602 [PMID: 8001486 DOI: 10.1055/s-2007-1009046]
- 3 Carrasco CH, Wallace S, Charnsangavej C, Richli W, Wright KC, Fanning T, Gianturco C. Expandable biliary endoprosthesis: an experimental study. *AJR Am J Roentgenol* 1985; **145**: 1279-1281 [PMID: 3877438 DOI: 10.2214/ajr.145.6.1279]
- 4 Neuhaus H, Hagenmüller F, Classen M. Self expanding metal stents versus conventional plastic endoprostheses for malignant biliary obstruction. *Gastrointest Endosc* 1991; **37**: 253-260
- 5 Knyrim K, Wagner HJ, Pausch J, Vakil N. A prospective, randomized, controlled trial of metal stents for malignant obstruction of the common bile duct. *Endoscopy* 1993; **25**: 207-212 [PMID: 8519239 DOI: 10.1055/s-2007-1010294]
- 6 Davids PH, Groen AK, Rauws EA, Tytgat GN, Huibregtse K. Randomised trial of self-expanding metal stents versus polyethylene stents for distal malignant biliary obstruction. *Lancet* 1992; **340**: 1488-1492 [PMID: 1281903]
- 7 Bismuth H, Castaing D, Traynor O. Resection or palliation: priority of surgery in the treatment of hilar cancer. *World J Surg* 1988; **12**: 39-47 [PMID: 2449769 DOI: 10.1007/BF01658484]
- 8 Dertinger S, Ell C, Fleig WE, Hochberger J, Kam M, Gurza L, et al. Long-term results using self-expanding metal stents for malignant biliary obstruction. *Gastroenterology* 1992; **102**: 310-311
- 9 Huibregtse K, Carr-Locke DL, Cremer M, Domschke W, Fockens P, Foerster E, Hagenmüller F, Hatfield AR, Lefebvre JF, Liquori CL. Biliary stent occlusion--a problem solved with self-expanding metal stents? European Wallstent Study Group. *Endoscopy* 1992; **24**: 391-394 [PMID: 1505486 DOI: 10.1055/s-2007-1010505]
- 10 Bosco JJ, Muggia RA, Howell DA, Jones M. Gianturco-Rosch metal Z-stent for endoscopic treatment of malignant extrahepatic biliary obstruction. *Proceeding of World Congress of Gastroenterology* 1994: 2512-2516
- 11 Cwikiel W, Stridbeck H, Stenram U. Electrolytic stents to inhibit tumor growth. An experimental study in vitro and in rats. *Acta Radiol* 1993; **34**: 258-262 [PMID: 8489839 DOI: 10.1177/028418519303400311]
- 12 Cotton PB. Metallic mesh stents--is the expanse worth the expense? *Endoscopy* 1992; **24**: 421-423 [PMID: 1505490 DOI: 10.1055/s-2007-1010511]

S- Editor: Tao T L- Editor: Filipodia E- Editor: Li RF

Ultrastructural observation of *Helicobacter pylori* to the gastric epithelia in chronic gastritis and peptic ulcers

Shan-Min Yang, Bing-Zhen Lin, Ying Fang, Yun Zheng

Shan-Min Yang, Bing-Zhen Lin, Ying Fang, Yun Zheng, Department of Cell Biology, Cancer Research Center, Xiamen 361005, Fujian Province, China

Author contributions: All authors contributed equally to the work.

Supported by Science Foundation of Xiamen. No.95801.

Original title: *China National Journal of New Gastroenterology* (1995-1997) renamed *World Journal of Gastroenterology* (1998-).

Correspondence to: Dr. Shan-Min Yang, Department of Cell Biology, Cancer Research Center, Xiamen 361005 Fujian Province, China
Telephone: +86-529-2017309

Received: April 4, 1996
Revised: July 25, 1996
Accepted: August 16, 1996
Published online: September 15, 1996

Abstract

AIM: The relationship between *Helicobacter pylori* (Hp) and gastric epithelia in chronic gastritis and in peptic ulcers was studied by transmission electron microscopy (TEM).

METHODS: Seventy-five patients were screened for Hp. Gastric antral biopsy specimens were fixed in glutaraldehyde and treated with tannic acid before OsO₄ staining. Samples were routinely processed for TEM studies (at least four semi-thin sections oriented for ultrathin sections in each sample).

RESULTS: The bacilli were detected by TEM within the gastric mucosa in 53 of 55 patients infected with Hp. Ultrathin sections revealed clear glycocalyx by which the bacillus was connected to the epithelium. As the bacilli colonized, the adjacent mucous cells degenerated. They were characterized by erosion of the juxtaluminal cytoplasm, vacuolation or blebbing, and desquamation of the cell membrane. The bacilli located in the lumen attracted neutrophils, which migrated into intercellular space of the epithelia or into the lumen to begin phagocytosis of Hp.

CONCLUSION: The sensitivity and specificity of TEM diagnosis is 96% and 95%, respectively. Tannic acid is suitable for the preservation of the glycocalyx of a cell. The colonized bacilli, usually with the wide periplasm, contributed to the degeneration of epithelia, including mucous neck cells. If Hp infection persists, the degeneration and regeneration of mucous neck cells occurs alternatively. Ultimately the generative stem cells were damaged, and as a result chronic atrophic gastritis could occur.

Key words: Gastritis; Peptic ulcer; *Helicobacter pylori*

© The Author(s) 1996. Published by Baishideng Publishing Group Inc. All

rights reserved.

Yang SM, Lin BZ, Fang Y, Zheng Y. Ultrastructural observation of *Helicobacter pylori* to the gastric epithelia in chronic gastritis and peptic ulcers. *World J Gastroenterol* 1996; 2(3): 152-154 Available from: URL: <http://www.wjgnet.com/1007-9327/full/v2/i3/152.htm> DOI: <http://dx.doi.org/10.3748/wjg.v2.i3.152>

INTRODUCTION

Ultrastructural studies have demonstrated a loss of apical microvilli and depletion of mucin granules in *Helicobacter pylori* (Hp) infected cells^[1,2]. Further investigation of Hp adherence, cell penetration, and immune response of the gastric epithelia is needed to delineate the relationship between the bacilli and the epithelia or the monocytes.

MATERIALS AND METHODS

Biopsies of the gastric antrum (four biopsies), the body (one biopsy), and serum from 75 patients with chronic gastritis or peptic ulcers were individually tested for Hp by culture, histopathology, cytology of smear, Hp rapid analytical chemistry urease kit (Hp-RACU), Hp enzyme linked immunosorbent analysis kit (Hp-EIA), and Hp polymerase chain reaction kit (Hp-PCR) (Cancer Research Center, Xiamen University). Positivity in more than three methods was considered the standard for detection of Hp infection. One of antral biopsies was also examined by a JEM 100CX/II transmission electron microscope (TEM). Biopsies were prefixed in 2.5% glutaraldehyde, treated for 4 h in 1% tannic acid (except for ten samples), then post-fixed and stained in a 1% osmium tetroxide and a 1% potassium ferricyanide mixture. Ultrathin sections (90 nm) were selected from the oriented semi-thin sections (at least four blocks/sample), and were examined by TEM for the relationship between the bacilli and the gastric epithelia.

RESULTS

Hp appeared dense and opaque under the microscope. An electron-lucent zone in the mucin pool usually surrounded curved or spiral bodies. They were also located near the microvilli of epithelial cells, typically in the gastric neck region or adjacent to a depression in the plasma membrane that resulted from a lost microvillus (Figure 1) or apocrine secretion. Hp bacilli were found disrupting the cellular junction of rolled microvilli and fragmented cells, and were found to be insinuated deep in between the epithelial cells (Figure 2). Hp infection was confirmed in 55 (30 chronic gastritis and 25 peptic ulcer) patients out of 75 patients. Curved or spiral organisms were detected in 53 patients (with one false positive) by TEM in the gastric mucosa (96%). Specificity of TEM was 95%, with 19 true negative and one false negative. After tannic acid staining, the glycocalyx was observed at the surface of the organisms, especially on the tip of the microvilli (Figure 3).

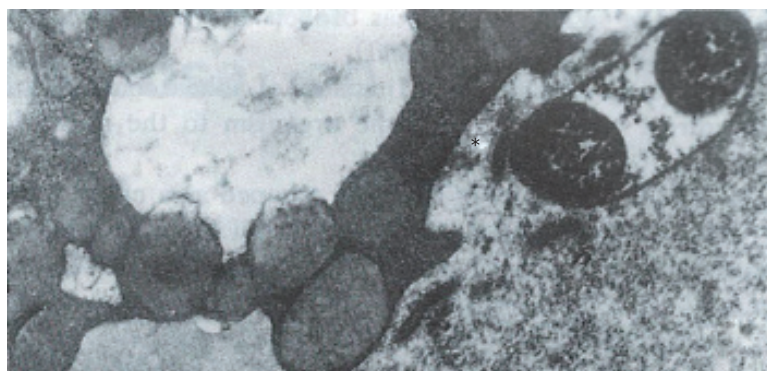


Figure 1 The bacillus abuts upon the depression of the plasma membrane (*) of the vacuolated cell. (× 21000)

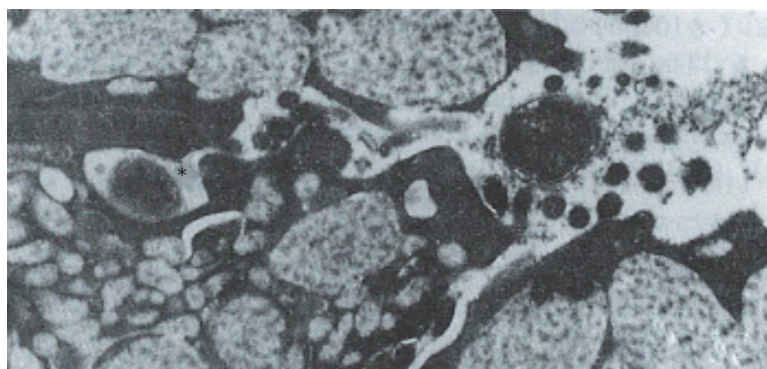


Figure 2 The bacilli (*) penetrating deep in between the mucous cells. The tight junction was broken and the intercellular space was dilated. (× 21000)

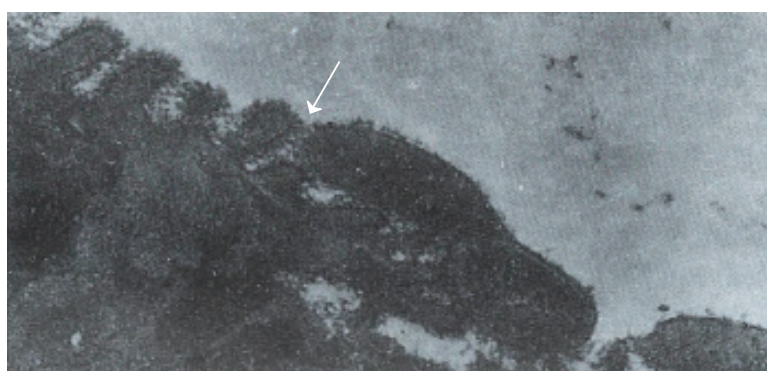


Figure 3 The bacillus shows the first step of adherence initiated by the direct contact of the organism to the microvilli glycocalyx. (× 28500)

Where the bacilli colonized, the adjacent mucous cells degenerated and were characterized by vacuolation (Figure 4), accumulation of lysosomes, and the appearance of mucous apocrine or blebs displaying a myeline figure. The bacilli located in the lumen attracted polymorphonuclear leukocytes (PMNL) that migrated into the intercellular space of the epithelia (Figure 5), or into the lumen to exert the effect of Hp phagocytosis (Figure 6).

DISCUSSION

In order to preserve delicate structures typically destroyed by osmium tetroxide, we fixed biopsies in a tannic acid solution. We found that some fragile glycocalyx on the bacilli and the epithelia remained intact (Figure 3). Based on our observation, where the bacilli colonized, mitotic figures and vacuolation of adjacent epithelial cells were present. A similar observation was noted by Caselli *et al*^[3]. The bacilli firmly attached to the epithelium or hiding in the niche of injured cells may have released cytotoxins or vacuolotoxin to impair the cells^[4]. As the organisms colonized, ammonia was released in order for the bacilli to escape the microbicidal effect for a long period of time.

Hp can be cleared by neutrophils from the site of infection most effectively through the opsonophagocytotic process *in vivo* and *in vitro*. Caselli *et al*^[5] demonstrated the specific IgG antibody-promoted complement-dependent phagocytosis and killing of Hp by

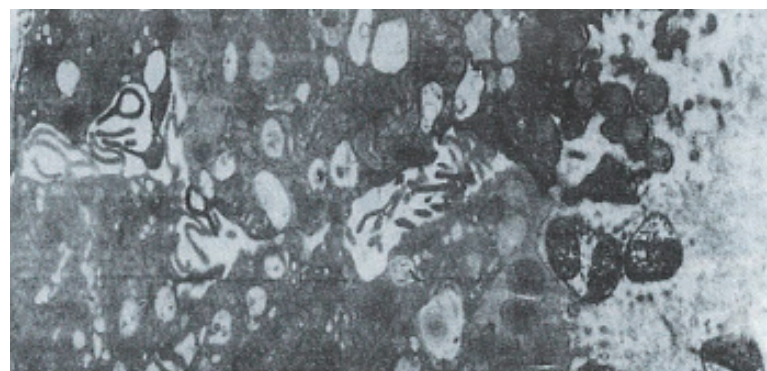


Figure 4 A great number of bacteria grouped in a colony shown with periplasmic pools (s). The bacilli abutting upon the depression of the plasma membrane of mucous neck cells lost microvilli and vacuolated. (× 8700)



Figure 5 Neutrophils (*) penetrated into the epithelia and migrated to the bacilli located in the apical region of mucous neck cells. (× 10800)

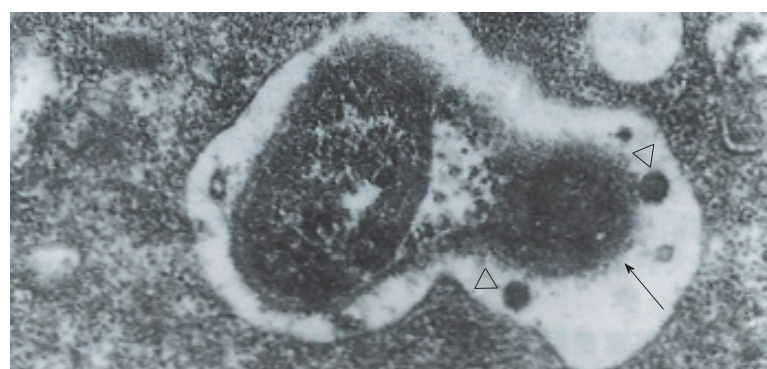


Figure 6 The bacillus is phagocytized by neutrophils located in the lumen. In the phagosome, two lysosomes approach the bacillus, of which the cell wall was lysed and discontinuous. (× 43500)

PMNL *in vitro*. Until now, the evidence of Hp phagocytosis by PMNL in antrum *in vivo* was scant. It is known that a certain protein or chemotactic factor of Hp^[6] can attract neutrophils to migrate into the epithelia or the gland and begin phagocytosis. Degranulation of proteolytic enzymes from neutrophils may also contribute to gastric mucosa damage, especially in the cells of the generative mucous neck region. As a result of persistent Hp infection, the degeneration and regeneration of the mucous neck region alternatively occurs and gives rise to atrophic gastritis. Regeneration of the stem cells of the mucous neck region would ultimately promote gene instability, which accounts for genetic mutation in neoplastic transformation in gastric stem cells.

REFERENCES

- 1 Kazi JL, Sinniah R, Zaman V, Ng ML, Jafarey NA, Alam SM, Zuberi SJ, Kazi AM. Ultrastructural study of *Helicobacter pylori*-associated gastritis. *J Pathol* 1990; **161**: 65-70 [PMID: 2370600 DOI: 10.1002/path.1711610111]
- 2 Hopwood D, Milne G, Penston J. Leakiness of gastric superficial and foveolar cells. A quantitative electron microscopic study using tannic acid. *J Pathol* 1991; **165**: 119-124 [PMID: 1744797 DOI: 10.1002/path.1711650206]
- 3 Caselli M, Aleotti A, Boldrini P, Ruina M, Alvisi V. Ultrastructural patterns of *Helicobacter pylori*. *Gut* 1993; **34**: 1507-1509 [PMID: 8244133 DOI: 10.1136/gut.34.11.1507]
- 4 Cover TL, Cao P, Lind CD, Tham KT, Blaser MJ. Correlation between vacuolating cytotoxin production by *Helicobacter pylori* isolates in vitro and in

- 5 vivo. *Infect Immun* 1993; **61**: 5008-5012 [PMID: 8225576]
Caselli M, Figura N, Trevisani L, Pazzi P, Guglielmetti P, Bovolenta MR, Stabellini G. Patterns of physical modes of contact between *Campylobacter pylori* and gastric epithelium: implications about the bacterial pathogenicity. *Am J Gastroenterol* 1989; **84**: 511-513 [PMID: 2719007]
- 6 **Kozol R**, McCurdy B, Czanko R. A neutrophil chemotactic factor present in *H. pylori* but absent in *H. mustelae*. *Dig Dis Sci* 1993; **38**: 137-141 [PMID: 8420746 DOI: 10.1007/BF01296786]

S- Editor: Yang ZD L- Editor: Filipodia E- Editor: Li RF

Quantitative ultrastructure analysis of neuroendocrine cells of gastric mucosa in normal and pathological conditions

Ji-Yao Yu, T Adda

Ji-Yao Yu, Department of Pathology, Navy General Hospital, Beijing 100037, China

T Adda, Parma University, Italy

Author contributions: All authors contributed equally to the work.

Original title: *China National Journal of New Gastroenterology* (1995-1997) renamed *World Journal of Gastroenterology* (1998-).

Correspondence to: Dr. Ji-Yao Yu, Department of Pathology, Navy General Hospital, Beijing 100037, China
Telephone: +86-10-68581865

Received: June 20, 1996
Revised: July 1, 1996
Accepted: August 16, 1996
Published online: September 15, 1996

Abstract

AIM: To study the quantitative ultrastructure of neuroendocrine cells of the gastric mucosa in normal and pathological conditions, including the duodenal ulcer (DU) and Zollinger-Ellison syndrome (ZES).

METHODS: The neuroendocrine cells of the gastric mucosa of eight normal subjects, six patients with DU, and five patients with ZES were quantitatively investigated with by electron microscopy and ultrastructure image analysis.

RESULTS: The volume density of neuroendocrine (NE) cells in the DU was 1.3% and 0.8% (*vs* 1.6% and 0.9%, $P < 0.05$) in gastric antrum and corpus, respectively. In the antrum, G cells were 65% ($P < 0.05$), D cells decreased in cell density (3% *vs* 9.5%) and in number per unit area ($P < 0.01$). In the corpus, the cell density of enterochromaffin-like (ECL) cells increased (49% *vs* 30%, $P < 0.05$); D cells and enterochromaffin (EC) cells decreased (2%, $P < 0.01$ and 4%, $P < 0.05$, respectively), and the number of D cells per unit area markedly decreased. In ZES, D cells in the corpus decreased in cell density (4% *vs* 22%, $P < 0.01$), and P cells also decreased (11% *vs* 24%, $P < 0.05$). The density of ECL cells increased (65% *vs* 30%, $P < 0.01$).

CONCLUSION: In DU and ZES, both the number and type of NE cells presented some changes. Increased gastrin in DU and ZES patients may be caused by the decrease of D cells and somatostatin secretion.

Key words: Gastric mucosa/pathology; Neuroendocrine cells; Duodenal ulcer; Zollinger-Ellison syndrome

© The Author(s) 1996. Published by Baishideng Publishing Group Inc. All rights reserved.

Yu JY, Adda T. Quantitative ultrastructure analysis of neuroendocrine cells of gastric mucosa in normal and pathological conditions. *World J Gastroenterol* 1996; 2(3): 155-157 Available from: URL: <http://www.wjgnet.com/1007-9327/full/v2/i3/155.htm> DOI: <http://dx.doi.org/10.3748/wjg.v2.i3.155>

INTRODUCTION

Quantitation has increasingly become a fundamental supplement of investigations on gastric endocrine cells^[1]. In humans, up to six cell types [enterochromaffin-like (ECL), enterochromaffin (EC), D, P, D1 and X] in oxyntic mucosa and four endocrine cell types (G, D, P and EC)^[2] in antrum mucosa have been identified. However, the secretory product of some cell types is either unknown or requires non-conventional tissue processing, thus preventing the use of immunohistochemistry. We have developed an ultrastructural morphometric procedure for quantitative assessment of endocrine cells of human gastric mucosa in normal and pathological conditions.

MATERIALS AND METHODS

The material was obtained from eight healthy volunteers equally divided by sex, aged 19 years to 34 years, on whom the study of normal gastric endocrine cells was performed. Endoscopic biopsies were performed in the central area of the posterior wall of the gastric corpus and antrum on six patients with duodenal ulcer (DU) aged 31 years to 57 years, and five patients with Zollinger-Ellison syndrome (ZES) aged 36 years to 62 years. The samples were fixed in a glutaraldehyde-paraformaldehyde mixture and cut with a razor blade to obtain slices of mucosa sections perpendicular to the gastric surface. These fragments were post fixed in osmium tetroxide, dehydrated in acetone and embedded in Araldite. Four to five blocks from different biopsy specimens including the whole thickness of the mucosa were selected at random. The blocks were trimmed to examine the entire thickness of the mucosa. Thin sections were collected with formvar-coated Robertson multiple slot grids, stained and examined with the electron microscope. Measurements were made under low power ($\times 760$) electron micrographs mounted to cover the entire thickness of the mucosa between two bars of the grid, and under high power ($\times 13700$) electron micrographs to cover all endocrine cell profiles in the same area. By using an ultrastructural quantitative analysis (GmbH German Str), the relative volumes of the epithelial component and the lamina propria were estimated with low power micrographs whereas morphometric analysis of endocrine cells was performed with high power micrographs.

RESULTS

The volume densities of different endocrine cells depended on the amount of the measured lamina propria, which was 26% in our estimation in normal subjects, but 33% in the patients with ZES ($p < 0.01$) and 32% in the patients with DU ($p < 0.05$). Such

Table 1 Quantitative ultrastructure analysis of neuroendocrine cells of gastric mucosa in normal subjects

Cell type	Volume fraction (%)	Profiles/unit area (n/m ²)	Cytoplasm composition (%)	Granule constituents (%)
Antrum				
NE	1.6 ± 0.5			
G	65.0 ± 2.0	2.4 ± 0.8	75.0 ± 3.0	16.0 ± 9.0
D	9.5 ± 0.6	0.3 ± 0.8	81.0 ± 4.0	35.0 ± 6.0
EC	8.6 ± 2.9	0.3 ± 0.7	76.0 ± 12.0	18.0 ± 7.0
Remaining cells	16.9 ± 3.2	0.6 ± 0.6	77.0 ± 8.0	3.8 ± 2.9
Corpus				
NE	0.9 ± 0.4			
ECL	30.0 ± 9.0	1.6 ± 0.7	70.0 ± 2.0	8.0 ± 2.0
EC	7.0 ± 5.0	0.3 ± 0.2	72.0 ± 13.0	16.0 ± 8.0
D	22.0 ± 4.0	1.5 ± 0.8	81.0 ± 7.0	31.0 ± 5.0
P	24.0 ± 7.0	0.8 ± 0.3	72.0 ± 7.0	6.0 ± 2.0
Remaining cells	17.6 ± 8.0	0.9 ± 0.5	68.0 ± 19.0	3.2 ± 2.6

Table 2 Quantitative ultrastructure analysis of neuroendocrine cells of the corpus mucosa in Zollinger-Ellison syndrome patients

Cell type	Volume fraction (%)	Profiles/unit area (n/m ²)	Cytoplasm composition (%)	Granule constituents (%)
Antrum				
NE	3.2 ± 1.1			
ECL	65.0 ± 15.0 ^d	5.2 ± 2.4 ^c	82.0 ± 2.0 ^d	5.0 ± 2.0 ^c
EC	5.0 ± 2.0	0.7 ± 0.5	80.0 ± 13.0	6.0 ± 9.0 ^a
D	4.0 ± 4.0 ^d	0.6 ± 0.4	75.0 ± 14.0	18.0 ± 5.0 ^d
P	11.0 ± 8.0 ^a	1.1 ± 0.4	76.0 ± 7.0	3.0 ± 0.5 ^b
Remaining cells	10.0 ± 3.0	2.8 ± 1.5	78.0 ± 9.0	1.6 ± 0.8

^a*P* < 0.05; ^b*P* < 0.01; ^c*P* < 0.05; ^d*P* < 0.01

Table 3 Quantitative ultrastructure analysis of neuroendocrine cells of gastric mucosa in duodenal ulcer patients

Cell type	Volume fraction (%)	Profiles/unit area (n/m ²)	Cytoplasm composition (%)	Granule constituents (%)
Antrum				
NE	1.3 ± 0.2			
G	46.0 ± 2.0	1.8 ± 0.7	71.0 ± 3.0	16.0 ± 9.0
D	3.0 ± 1.6 ^a	0.1 ± 0.8 ^b	87.0 ± 4.0 ^a	28.0 ± 12.0
EC	16.0 ± 6.5	0.6 ± 0.7 ^b	77.0 ± 12.0	12.0 ± 5.0
Remaining cells	35.0 ± 13.0	1.2 ± 1.5	81.0 ± 8.0	3.8 ± 2.9
Corpus				
NE	0.8 ± 0.3			
ECL	49.0 ± 16.0 ^a	1.7 ± 1.0	70.0 ± 5.0	5.0 ± 2.0 ^a
EC	4.0 ± 2.0	0.3 ± 0.2	72.0 ± 24.0	8.0 ± 8.0
D	2.0 ± 4.0 ^a	0.3 ± 0.3 ^c	93.0 ± 6.0 ^a	33.0 ± 4.0
P	25.0 ± 4.0	1.7 ± 1.0	67.0 ± 5.0	3.0 ± 1.0
Remaining cells	20.0 ± 12.0	1.9 ± 1.5	81.0 ± 9.0	3.2 ± 2.8

^a*P* < 0.05; ^b*P* < 0.01; ^c*P* < 0.05

differences, which were statistically significant, were related to inflammatory changes in the upper region of the lamina propria occurring in pathological conditions. For this reason, the epithelial compartment alone has to be kept as the reference volume for endocrine cell densities in comparative studies. Ultrastructural characteristics^[3] of secretory granules in different types of gastric endocrine cells including G, D, P, EC and ECL cells are shown in Figures 1-5.

Table 1 shows the quantitative ultrastructural data of the mucosa in the antrum and corpus from normal male subjects. The volume density of endocrine cells in corpus mucosa in patients with ZES was 3.2% of the mucosal epithelial component, a 168% increase (*p* < 0.01) over the value found in normal subjects (Table 2). This result is evidence for a net increase in the total volume of endocrine cells of corpus mucosa augmented in ZES. In all the cases, the ECL cells composed more than 50% of the whole endocrine cell mass. As shown in Table 2, the mean volume fraction of this cell type was 65%, a 119% increase over the normal value. In contrast, other cell types of endocrine cells showed a mean volume fraction lower than that found in normal subjects, a difference statistically significant in the case of D and P cells.

In this series of DU patients (Table 3), the mean volume density

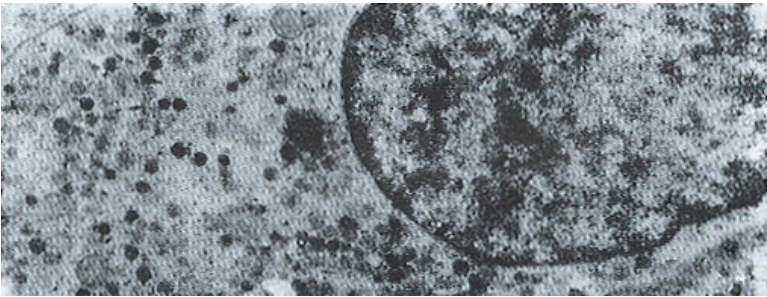


Figure 1 G cell of the antrum containing both vesicular and compact granules with a floccular content.

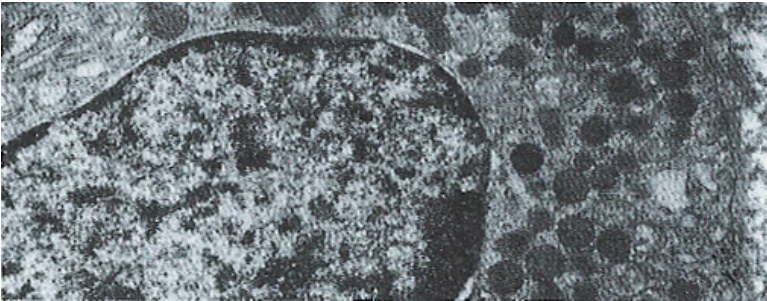


Figure 2 D cell granules are usually rounded, homogeneous, of low electron density and with closely applied membranes.

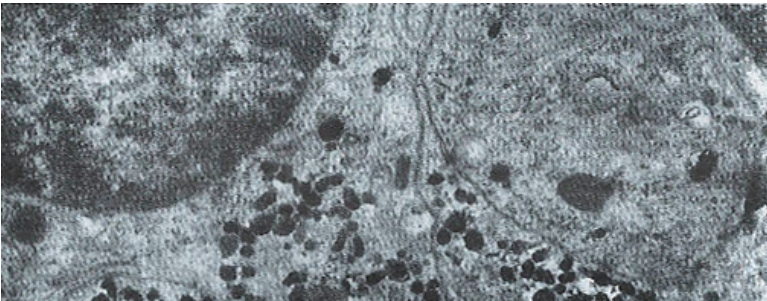


Figure 3 EC cell granules appear to be pleomorphic, such as being oblong, ovoid, round, etc., with high density.

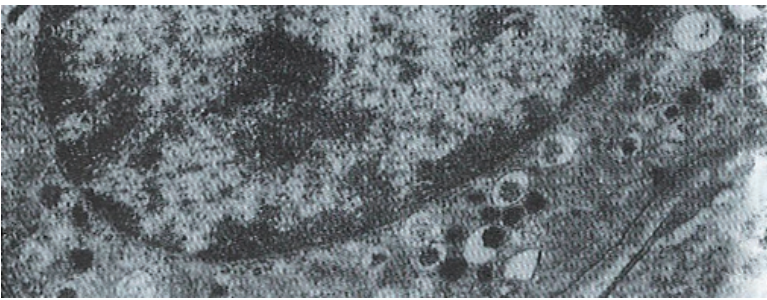


Figure 4 ECL cells show the characteristic of vesicular-type granules and thin haloed granules with an irregular argyrophilic core eccentrically located in wide space.

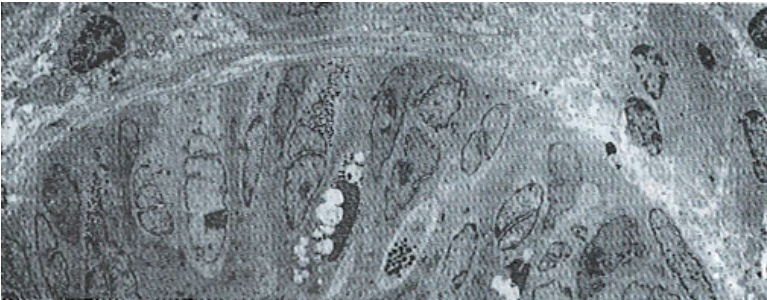


Figure 5 Electron micrograph of contiguous gastric glands shows cross sections belonging to different endocrine cells.

of the whole endocrine cell population was 1.6% and 0.8% in the gastric antrum and corpus, respectively, which did not differ significantly from that of healthy subjects. In the antrum, D cells decreased in cell density and in number per unit area, as well as in

the corpus. The mean volume fraction of ECL cells was found to be increased 49%.

DISCUSSION

From the morphometric point of view, absolute counts of cells, usually restricted to nucleated sections, have commonly been used. The frames of reference for these counts, however, include visual fields, unit length of mucosa, unit area of tissue section, unit area of mucosa surface, gland crypt, nucleus-containing gland cells, and whole antrum or whole stomach. Such heterogeneity makes comparisons between different studies difficult, and occasionally opposite results would be achieved. Direct counts of endocrine cells from pelleted cell suspensions of gastric mucosa have also been proposed^[4]. With this background in our laboratory, we have developed an ultrastructural morphometric procedure for quantitative assessment of endocrine cells of human gastric mucosa in normal and pathological conditions. In ECL cells of ZES patients, the number of cell profiles per unit area, the cross section area and the cytoplasmic values were tested. These data supported the previous observations that both hyperplasia and hypertrophy occurred in the oxyntic endocrine cells in the pathological condition. Secretory granules were not restricted to ECL cells, but were shared by the other cell types, which were significant in the case of P, D, and EC cells^[5]. On the basis of experimental evidence obtained from the rat, reduction of the granule volume density in corpus endocrine cells could be regarded as a sign of gastrin induction increase in functional activity, which was associated with activation of the specific enzyme, histidine decarboxylase^[6]. Therefore, our studies supported a similar result about the functional activity of gastrin in humans involving cell types that were not influenced by the stimulus of gastrin.

In this series of DU patients, the mean volume density of the endocrine cells of gastric mucosa did not differ significantly from that of normal subjects. In contrast, the mean volume fraction of ECL cells was increased. The volume fraction of D cells markedly decreased. Although age influences cannot be ruled out, such changes are possibly relevant to the pathophysiology of the DU disease^[7]. In this regard, it is pertinent to note that the gastric

mucosa of DU patients releases significantly lower amounts of somatostatin^[8]. Our results, therefore, provide a cellular basis for this functional deficiency and suggest a reduced paracrine control of gastric secretion in this pathological condition.

From the above discussions, it can be concluded that ultrastructural morphometry is a useful tool for investigating endocrine cells of human gastric mucosa. Indeed, it allows identification of all cell types composing the gastric endocrine cell population. Recently developed stereological procedures, such as the selector or the nucleator, may efficiently supplement the data provided here with unbiased estimates of absolute structural quantities, including cell volume, thus opening new dimensions to the ultrastructural morphometry of gastric endocrine cells.

REFERENCES

- 1 D'Adda T, Bertelé A, Pilato FP, Bordi C. Quantitative electron microscopy of endocrine cells in oxyntic mucosa of normal human stomach. *Cell Tissue Res* 1989; **255**: 41-48 [PMID: 2736608 DOI: 10.1007/BF00229064]
- 2 Solcia E, Capella C, Vassallo G, Buffa R. Endocrine cells of the gastric mucosa. *Int Rev Cytol* 1975; **42**: 223-286 [PMID: 53215 DOI: 10.1016/S0074-7696(08)60982-1]
- 3 Bordi C, Ferrari C, D'Adda T, Pilato F, Carfagna G, Bertelé A, Missale G. Ultrastructural characterization of fundic endocrine cell hyperplasia associated with atrophic gastritis and hypergastrinaemia. *Virchows Arch A Pathol Anat Histopathol* 1986; **409**: 335-347 [PMID: 3088827 DOI: 10.1007/BF00708251]
- 4 Moore C, Saik RP. Total counts of antral gastrin cells: a simple direct method. *Stain Technol* 1985; **60**: 137-144 [PMID: 3895584 DOI: 10.3109/10520298509113904]
- 5 Kobayashi S, Fujita T, Sasagawa T. Electron microscope studies on the endocrine cells of the human gastric fundus. *Arch Histol Jpn* 1971; **32**: 429-444 [PMID: 5101964 DOI: 10.1679/aohc1950.32.429]
- 6 Alumets J, El Munshid HA, Håkanson R, Liedberg G, Oscarson J, Rehfeld JF, Sundler F. Effect of antrum exclusion on endocrine cells of rat stomach. *J Physiol* 1979; **286**: 145-155 [PMID: 439021 DOI: 10.1113/jphysiol.1979.sp012610]
- 7 Green DM, Bishop AE, Rindi G, Lee FI, Daly MJ, Domin J, Bloom SR, Polak JM. Enterochromaffin-like cell populations in human fundic mucosa: quantitative studies of their variations with age, sex, and plasma gastrin levels. *J Pathol* 1989; **157**: 235-241 [PMID: 2926564 DOI: 10.1002/path.1711570310]
- 8 Ligumsky M, Wengrower D, Karmeli F, Rachmilewitz D. Somatostatin release by human gastric mucosa. Studies in peptic ulcer disease and pernicious anemia. *Scand J Gastroenterol* 1988; **23**: 687-690 [PMID: 2902682]

S- Editor: Cao LB L- Editor: Filipodia E- Editor: Li RF

Comparative study on the effects of hepatic arterial embolization with *Bletilla striata* or Gelfoam in treatment of primary hepatic carcinoma

Gan-Sheng Feng, B Kramann, Chuan-Sheng Zheng, Ru-Ming Zhou, Bo Liang, Yan-Fang Zhang

Gan-Sheng Feng, B Kramann, Chuan-Sheng Zheng, Ru-Ming Zhou, Bo Liang, Yan-Fang Zhang, Department of Radiology; Union Hospital of Tongji Medical University, Wuhan 430022, China

Gan-Sheng Feng, Professor of Radiology, Director of the Department of Radiology. Has previously published 36 papers and six books.

Author contributions: All authors contributed equally to the work.

Supported by the National Natural Science Foundation of China, No. 93019512.

Original title: *China National Journal of New Gastroenterology* (1995-1997) renamed *World Journal of Gastroenterology* (1998-).

Correspondence to: Dr. Gan-Sheng Feng, Professor, Department of Radiology, Union Hospital of Tongji Medical University, Wuhan 430022, China
Telephone: +86-27-5807711-598

Received: July 19, 1996
Revised: August 6, 1996
Accepted: August 27, 1996
Published online: September 15, 1996

Abstract

AIM: To study the safety and efficacy of hepatic arterial embolization (HAE) with *Bletilla striata* powders containing traditional Chinese herbs in the treatment of primary hepatic carcinoma (PHC).

METHODS: From May 1990 to September 1993, 106 patients with PHC were treated by HAE with different types of *Bletilla striata* powders ($n = 56$) or Gelfoam powders ($n = 50$) under clearly specified conditions. We analyzed the effects and complications associated with these two types of treatment.

RESULTS: The *Bletilla striata* powders produced extensive and permanent proximal embolization of the hepatic artery, and stimulated the formation of collateral circulation. Treatment could be stopped for as long as 6-12 mo, and there was obvious evidence of tumor necrosis and shrinkage. The patient survival rates at 1, 2, and 3 years were 81.9%, 44.9%, and 33.6%, respectively, and the mean survival time without a serious complication was 19.8 mo. Patients in the *Bletilla striata* group displayed better clinical effects from their treatment when compared with patients in the Gelfoam group.

CONCLUSION: *Bletilla striata* powders are superior to Gelfoam powders when used for angioembolus in patients with hepatic carcinoma.

Key words: Liver neoplasms/therapy; Embolization; Therapeutic *Bletilla striata*

© The Author(s) 1996. Published by Baishideng Publishing Group Inc. All rights reserved.

Feng GS, Kramann B, Zheng CS, Zhou RM, Liang B, Zhang YF. Comparative study on the effects of hepatic arterial embolization with *Bletilla striata* or gelfoam in treatment of primary hepatic carcinoma. *World J Gastroenterol* 1996; 2(3): 158-160 Available from: URL: <http://www.wjgnet.com/1007-9327/full/v2/i3/158.htm> DOI: <http://dx.doi.org/10.3748/wjg.v2.i3.158>

INTRODUCTION

From May 1990 to September 1993, 106 patients with primary hepatic carcinoma (PHC) were treated by hepatic arterial embolization (HAE). We objectively compared the effects of permanent HAE produced with *Bletilla striata* with the effects of temporary HAE produced with Gelfoam.

MATERIALS AND METHODS

This study enrolled 166 patients (93 males and 13 females; mean age = 46 years) who were clinically diagnosed as PHC. The patients were randomly assigned to a *Bletilla striata* group (BS group) and a Gelfoam group (GF group). The general medical conditions of the patients and their respective methods of treatment are shown in Table 1. Both groups of patients received hepatic arterial chemotherapy with Adriamycin (ADM; 50 mg) and carboplatin (CAP; 500 mg). A peripheral angioembolus was created by administering an emulsion consisting of 40% Lipiodol (LP) and 10 mg mitomycin C (MMC). The femoral artery was percutaneously punctured using Seldinger's method, and a catheter was inserted into the segmental or lobar artery of the hepatic tumor. Following transcatheter intra-arterial infusion of the chemotherapeutic agents and the LP-MMC emulsion, 2-3 mL of mixed *Bletilla striata* powders (300 mg) and 5 mL of 76% meglumine diatrizoate composita were slowly infused to produce proximal HAE. If the normal hepatic segmental and lobar arteries were not available for catheterization, proximal HAE was performed using Gelfoam powder.

RESULTS

Vascular recanalization and revascularization of the tumor

At three mo after HAE, 92% of patients in the Gelfoam group showed recanalization of the embolized artery and formation of collateral circulation (Figures 1 and 2). In contrast, none of the patients in the *Bletilla striata* group showed recanalization, even at 3 yr after embolization. Collateral circulation was rarely formed, and when it did, it required > 6 mo to develop. Additionally, there was no collateral blood supply to the tumor in ~ 50% of the patients at one year after their embolization procedure (Figures 3 and 4).

Changes in tumor size and pathohistological characteristics

In the *Bletilla striata* group, 36.2%, 55.8%, and 71.4% of patients showed signs of tumor shrinkage at 3, 6, and 12 mo, respectively, after embolization. The corresponding rates in the Gelfoam group were 25.0%, 46.4%, and 64.3%, respectively. In the *Bletilla striata*

Table 1 General conditions and methods of treatment		
Subjects	GF group	BS group
Number	50	56
Clinical stage; cases (%)		
I	3 (6.0)	4 (7.1)
II	42 (84.0)	46 (82.2)
III	5 (10.0)	6 (10.7)
Pathologic type; cases (%)		
Massive	38 (76.0)	43 (76.8)
Multinodular	12 (24.0)	13 (23.2)
Proximal angioembolus	GF powders	BS powders
Total number of treatments	203	151
Mean number of treatments	4.06	2.7
Mean intermission between treatments (mo)	3-6	6-12

Table 2 Survival rates and survival times for patients in the two groups (Life-table method: U-test)						
Group	n	Survival rates (%)				Mean survival time (mo)
		6 m	12 m	24 m	36 m	
BS	56	92.9	81.9	44.9	33.6	19.8
GF	50	80.0 ^a	48.9 ^b	31.1 ^c	16.0 ^d	15.7

^a*P* > 0.05; ^{b,d}*P* < 0.01; ^c*P* < 0.05.

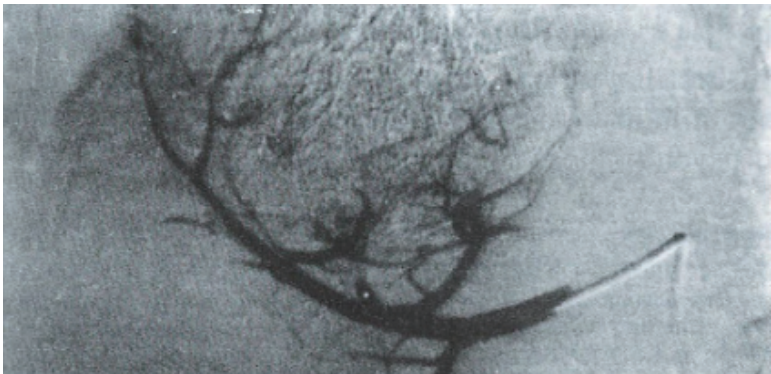


Figure 1 PHC treated by HAE with Lp MMC and GF powders.

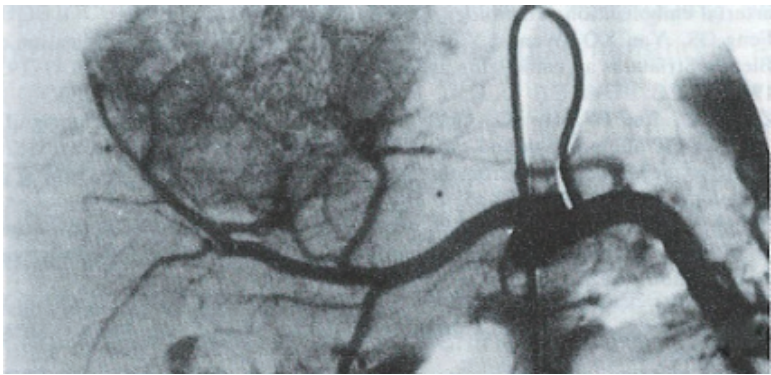


Figure 2 Three months after HAE, angiography of this patient showed tumor staining and slight shrinkage.

group, tumor necrosis was most obvious at 3 mo; at which time, the hepatic tumor tissue had sunken due to obvious fibrosis and lipiodol retention in the sites (Figures 5 and 6). In some patients, the tumor became calcified one year later.

Specimens obtained during second surgical resections showed no surviving tumor cells in 2 of 3 cases in the *Bletilla striata* group, while 2 cases in the Gelfoam group had surviving tumor cells.

Syndrome after HAE and changes in hepatic function

After HAE, hepatic pain, fever, and damage to hepatic function were all more severe in the *Blatilla striata* group when compared to the Gelfoam group. In both groups, pain lasted for 2-5 d and fever for 3-20 d, and the differences between groups were not statistically significant.

Survival rate and time

The survival rates and survival times in the two groups of patients

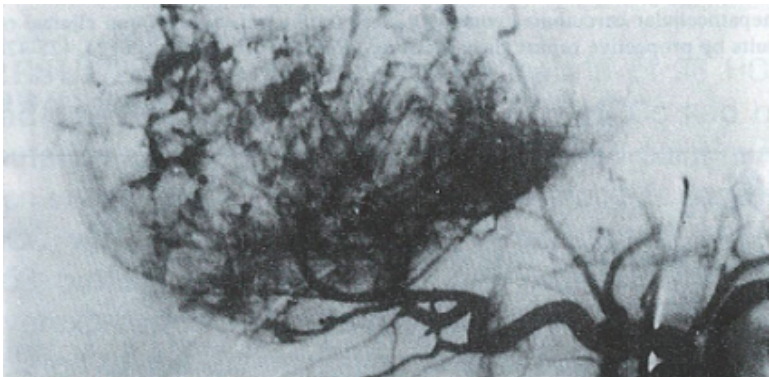


Figure 3 The right lobar massive PHC treated by HAE with Lp-MMC and BS powders.

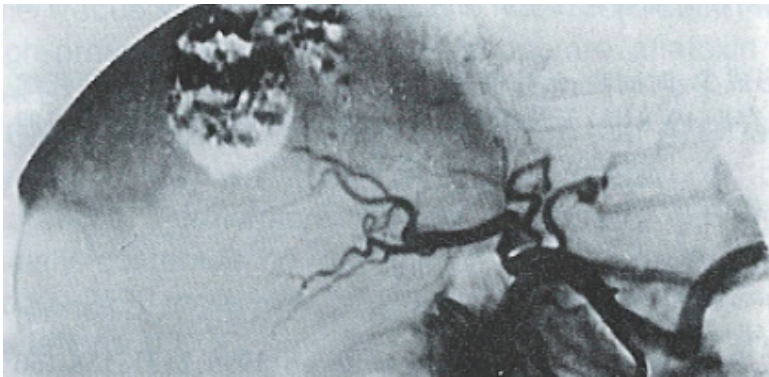


Figure 4 Ten months after HAE, angiography of this patient showed obvious tumor shrinkage, and no tumor vessels or collateral circulation.



Figure 5 Prior to HAE with Lp MMC and BS powders, a CT scan of the massive PHC showed local low density in the right hepatic lobe.

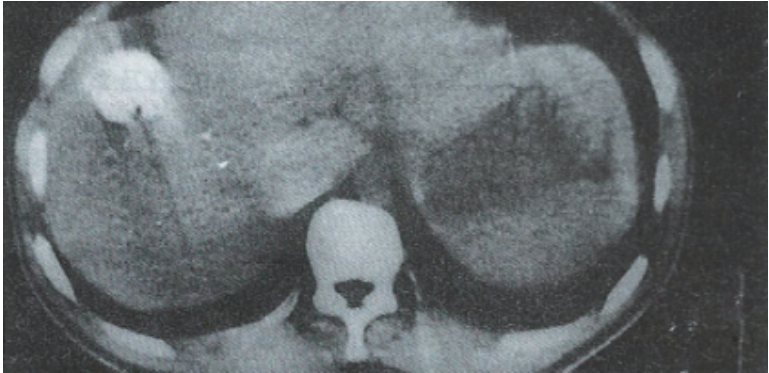


Figure 6 Nine months after HAE, a CT scan of this patient showed obvious tumor shrinkage and Lipiodol retention in the tumor area.

are shown in Table 2.

DISCUSSION

The use of HAE in treatment of PHC has attracted a great deal of attention as a novel methodology^[1,2]. *Bletilla striata* powders display the following characteristics when used in treatment of PHC: (1) They produce permanent proximal embolization of the hepatic artery. Besides mechanically blocking blood vessels, they

also induce extensive coagulation^[3]. Embolization occurs several seconds after the powder's application, and a vascular cast appears. (2) *Bletilla striata* powders can be custom produced at an appropriate concentration for use in combination with a contrast medium, and to meet the requirements of a particular embolization procedure. *Bletilla striata* powders not only embolize the main trunk of an artery, but also block tumor vessel beds that are not completely filled with Lipiodol. As a result, they effectively prevent the establishment of collateral circulation. However, this viewpoint is not consistent with some research conclusions which state that extensive embolization of a hepatic carcinoma artery may induce the formation of collateral circulation^[4,5]. The reason that tumors become revascularized and develop collateral circulation after HAE with Gelfoam powders may be that Lipiodol and Gelfoam powders only block small tumor vessels and blood supply arteries respectively, while mid-sized vessels that are not embolized allow the tumor to establish collateral circulation with surrounding hepatic segmental or lobar arteries. As a result, HAE with Gelfoam does not produce complete necrosis of the tumor, and these patients need to be re-embolized after a short time period^[6]. (3) Both the retention and elimination times of Lipiodol in the tumor area were better in the *Bletilla striata* group when compared with those parameters in the Gelfoam group. This may be because the arterial blood flow washes out the intratumor Lipiodol as intra-arterial Gelfoam powders are being absorbed^[7]. And (4) When performing HAE with *Bletilla striata* powders, the catheter must be inserted into the peripheral branch of the hepatic artery to avoid penetrating the normal hepatic parenchyma. If this is not possible, Gelfoam powders must be used when creating a proximal

angioembolus. Additionally, any backflow of the angioembolus must be avoided in order to prevent a misembolization.

In view of the characteristics of *Bletilla striata*, we believe that a permanent HAE produced with *Bletilla striata* powders in treatment of PHC not only produces a better clinical effect, but also reduces the economic burden and psychological pressure experienced by patients.

REFERENCES

- 1 Gou JY, Huang ZC, Yan D, Hu GD. Intraarterial infusion chemotherapy and embolization with mixture of lipiodol and anticancer drug in the treatment of hepatic carcinoma. *J of Clinical Radiology* 1987; **6**: 281-283
- 2 Matsui O, Kadoya M, Yoshikawa J, Gabata T, Arai K, Demachi H, Miyayama S, Takashima T, Unoura M, Kogayashi K. Small hepatocellular carcinoma: treatment with subsegmental transcatheter arterial embolization. *Radiology* 1993; **188**: 79-83 [PMID: 8390073 DOI: 10.1148/radiology.188.1.8390073]
- 3 Fen GS. [Animal experiment and clinical application of *Bletilla striata* as an embolizing agent]. *Zhonghua Fangshexue Zazhi* 1985; **19**: 193-196 [PMID: 2932309]
- 4 Zhao LZ, Luo PF, Hu JQ, Guan YH, Chen XM, Liang CH. The significance of CT angiography and radiography in guiding the interventional treatment for hepatocellular carcinoma and prediction of prognosis. *Zhonghua Fangshexue Zazhi* 1993; **27**: 450-453
- 5 Cheng YD, Qian XG, Zhang ZG, Jin JS, Shen BX. Analysis of survival time of hepatic carcinoma treated by intraarterial infusion chemotherapy and embolization. *Zhonghua Xiaohua Zazhi* 1991; **11**: 304-305
- 6 Koehler RE, Korobkin M, Lewis F. Arteriographic demonstration of collateral arterial supply to the liver after hepatic artery ligation. *Radiology* 1975; **117**: 49-54 [PMID: 1162072 DOI: 10.1148/117.1.49]
- 7 Von Huppert PE, Gei Bler F, Duda SH, Lewis F. Chemoembolization of hepatocellular carcinoma: computed tomography appearances and clinical results by prospective repeat therapy study. *Roentgenstr* 1994; **106**: 425-428

S- Editor: Yang ZD L- Editor: Filipodia E- Editor: Li RF

Overexpression and mutations of tumor suppressor gene *p53* in hepatocellular carcinoma

Dong Wang, Jing-Quan Shi

Dong Wang, Jing-Quan Shi, Department of Pathology, Third Military Medical College, Chongqing 630042, China

Dong Wang, MD, Associate Professor and Director of the Department of Clinical Pathology, Daping Hospital, having published 19 papers and one book.

This paper was presented at the 4th Congress, Asia Pacific Association of Societies of Pathologists, May 1995, Beijing.

Author contributions: All authors contributed equally to the work.

Original title: *China National Journal of New Gastroenterology* (1995-1997) renamed *World Journal of Gastroenterology* (1998-).

Correspondence to: Dong Wang, MD, Associate Professor, Director, Department of Pathology, Third Military Medical College, Chongqing 630042, China

Received: June 16, 1996

Revised: July 15, 1996

Accepted: August 13, 1996

Published online: September 15, 1996

Abstract

AIM: To examine the prevalence of *p53* mutations in cases of hepatocellular carcinoma (HCC) in the Chongqing area of China, and the relationship between *p53* mutations and the clinicopathological features of HCC, as well as its risk factors.

METHODS: The overexpression and point mutations of tumor suppressor gene *p53* in 38 cases of HCC were detected by a sensitive antigen retrieval fluid (ARF) immunohistochemical method, polymerase chain reaction (PCR) a2 restriction fragment length polymorphism (RFLP) analysis, and a single strand conformation polymorphism (SSCP) a2silver staining analysis.

RESULTS: The results showed that 16 of 38 HCCs were positive for P53 protein (42.1%). Seven HCCs (18.4%) had a *p53* mutation at codon 249, and 2 other HCCs had point a mutation within exon 7 but not at codon 249. Among 9 cases of HCC which showed genetic mutations, 8 cases (88.9%) were positive for p53 protein. Both *p53* overexpression and mutation were significantly related to the degree of HCC tissue differentiation and the presence or absence of metastases. The frequency of *p53* mutations was consistent with the high prevalence of HBV infection and moderate aflatoxin B1 (AFB1) exposure in the Chongqing area.

CONCLUSION: Our results suggest that AFB1 acts synergistically with HBV in the generation of *p53* mutations. Furthermore, dietary exposure to AFB1 may mainly contribute to the tumor specific mutation at codon 249, while HBV may account for other scattered mutations found in cases of HCC.

Key words: Liver neoplasms; Genes; Suppressor; Tumor protein *p53* point mutation

© The Author(s) 1996. Published by Baishideng Publishing Group Inc. All rights reserved.

Wang D, Shi JQ. Overexpression and mutations of tumor suppressor gene *p53* in hepatocellular carcinoma. *World J Gastroenterol* 1996; 2(3): 161-164 Available from: URL: <http://www.wjgnet.com/1007-9327/full/v2/i3/161.htm> DOI: <http://dx.doi.org/10.3748/wjg.v2.i3.161>

INTRODUCTION

Hepatocellular carcinoma (HCC) is one of the most common cancers in China. A striking correlation exists between the development of HCC and infection with the hepatitis B virus (HBV), as well as exposure to aflatoxin B1 (AFB1). However, the molecular mechanisms underlying these correlations are largely unknown. Tumor suppressor gene *p53*, located on the short arm of human chromosome 17 (17 p 13.1), is one of the most important and broad spectrum anti-oncogenes, and researchers have documented > 51 types of human tumors that have *p53* mutations. Since Bressac^[1] and Hsu *et al*^[2] first reported in 1991 that ~ 50% of resected HCCs in China and South Africa had *p53* mutations, increasing numbers of similar reports have been published by researchers in various areas of the world. It is very interesting that the presence of *p53* mutations in HCC appears to vary geographically^[3]. The city of Chongqing is located in southwestern China, an area with a high prevalence of HBV infections, and a moderate exposure to dietary AFB1. However, to date, there has been no report concerning the HCC incidence in that geographic region.

In this study, we used antigen retrieval fluid (ARF) immunohistochemistry, PCR, and PCR-SSCP silver staining methods to detect the gene overexpressions and mutations that existed in 38 cases of HCC. Our goal was to demonstrate the prevalence of *p53* mutations in cases of HCC in the Chongqing region of China, and investigate the relationship between the *p53* alterations and the clinicopathological features of HCC, as well as HCC risk factors.

MATERIALS AND METHODS

Tissue samples

Between 1992 and 1993, 38 samples of resected HCC tissue (one sample per case) were obtained from the Southwest Hospital affiliated with our college. Thirty-six of the samples were fresh tissue. The tissue specimens were fixed in 10% formalin and embedded in paraffin; after which, 5 µm thick sections were cut for use in our study. When based on their WHO classification, the tissue specimens represented the following types of HCC: trabecular (*n* = 15), pseudoglandular (*n* = 16), and compact (*n* = 7). Histological grading of the specimens based on Edmondson and Steiner's standard showed: grade I, 3 cases; grade, 7 cases; grade III, 15 cases; grade IV, 13 cases. The tumors could be divided into the following three groups depending on their diameter: 3 cases, ≤ 3 cm; 5 cases, 3 cm-5 cm; 30 cases, ≥ 5 cm. Fourteen cases had

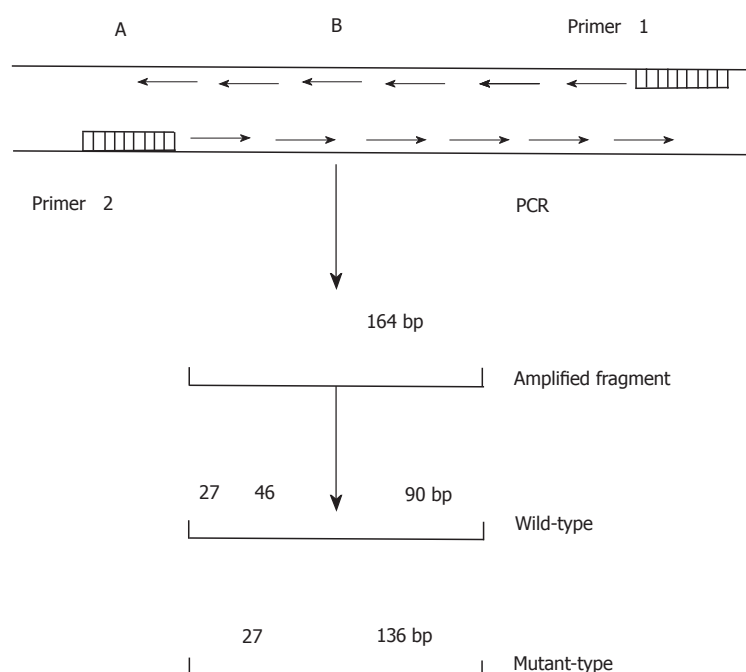


Figure 1 Schematic diagram of the p53 codon 249. A: control cleavage site of the restriction endonuclease, Hae III. B: Hae III cleavage site in codon 249.

intrahepatic metastases at the time of operation.

DNA extraction

High-molecular weight DNA was prepared from 36 fresh tissue samples, 2 paraffin-embedded blocks, and 2 samples of normal lymphocytes using promase K and phenol-chloroform methods as described in "Molecular Cloning: A laboratory Manual."

ARF-immunohistochemical staining

Monoclonal antibody Pab1801 donated by Dr. L. Crawford of ICRF, United Kingdom, and polyclonal antiserum CM-1, donated by Dr. D.P. Lane, Dundee, United Kingdom, were used to detect p53 protein expression. An ABC kit was purchased from the Dako Company (Demark). Immunohistochemical staining with enhancement was performed using the method described by Vendenberg *et al.*^[4,5].

Detection of mutated codon 249

The DNA sequence of p53 exon 7 was amplified by PCR (Figure 1) using primers with the following nucleotide sequences:

Primer 1: 5'CCCAAGGCGCACTGACCTCA3';

Primer 2: 5'GCTCCTGACCTGGAGTCTTC3'.

PCR was performed according to a standard protocol. Briefly, each PCR reaction was performed in a final volume of 40 μ L, which contained 1.8 μ L of target DNA, 28 μ L ddH₂O, 3.2 μ L of 2.5 mmol/L dNTP, 2 μ L of 20 pmol/L primers, and 4 μ L of 10 \times Taq DNA polymerase buffer. The samples and reagents were heated for 8 min at 93 $^{\circ}$ C to denature the DNA. Next, 1 μ L (2.2 U) of Taq DNA polymerase was added to each sample, which was then heated for 35 s at 94 $^{\circ}$ C for denaturation, followed by 40 s at 54 $^{\circ}$ C for annealing, and 60 s at 72 $^{\circ}$ C for extension. After a total of 35 rounds, each sample was maintained at 72 $^{\circ}$ C for 10 min. The final DNA product was purified with phenol/chloroform, precipitated with ethanol, dissolved with TE buffer, and then digested with Hae III for 12-24 h. The digests were separated by electrophoresis on an 8% polyacrylamide gel.

Single-strand conformation polymorphism-silver staining

A 5 μ L sample DNA was mixed with a loading solution containing 950 mM deionized formamide, 10 mmol/L EDTA, 0.05% bromophenol blue, and xylene cyanol. After denaturation at 85 $^{\circ}$ C for 5 min, 20 μ L of the mixture was applied to a 12% polyacrylamide gel (39:1 acrylamide:bisacrylamide ratio) containing 1 \times TBE buffer and 50 mL/L glycerol. The size of the gel was 10 cm \times 9 cm \times 0.1 cm (thickness). Electrophoresis was then performed for 4.5 h at 200 V using a buffer system containing 25 mM Tris and 192 mM glycine. The buffer temperature was

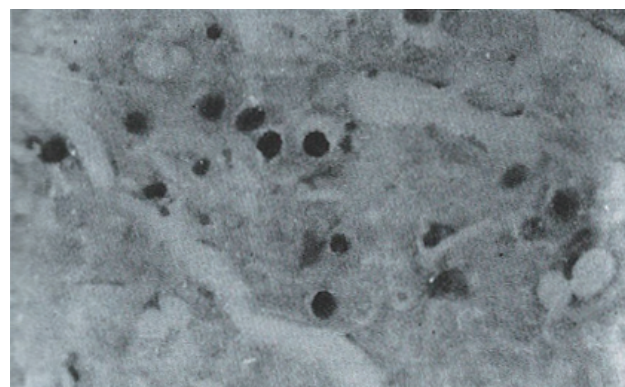


Figure 2 A well differentiated HCC with nuclear staining in carcinomatous cells in a single pattern. Some cells also show cytoplasmic staining. Immunohistochemistry with Pab1801. ABC, \times 400

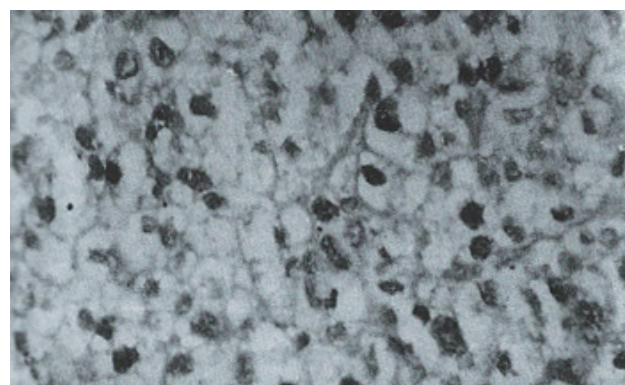


Figure 3 Moderately differentiated HCC with nuclear staining in carcinomatous cells in a diffuse pattern. Immunohistochemistry with CM-1; ABC, \times 400.

maintained in a range of 16 $^{\circ}$ C-23 $^{\circ}$ C.

After electrophoresis, the gel was fixed for 30 min in 100 mL of a mixture consisting of 100 mL/L ethanol and 50 mL/L acetic acid, and then washed twice in distilled water. The gel was stained in 1 mL/L AgNO₃ for 30 min, and then washed three times in distilled water. After washing, the gel was submerged in a mixture of 25 g/L Na₂CO₃ and 0.4 mL/L formalin, and then allowed to develop for 20 min-30 min until bands became visible. The reaction was stopped by transferring the stained gel into 100 mL/L acetic acid solution.

RESULTS

P53 Protein expression in HCC specimens

Sixteen of 38 HCC specimens were positive for P53 protein (42.1%), while the corresponding noncancerous tissues were all negative. The majority of malignant cells in all of the P53-positive specimens displayed a stained nucleus, and some also showed cytoplasmic staining. The distribution of p53-positive cells showed a single, focal or diffuse pattern (Figures 2 and 3).

Mutations of p53 exon 7

After digesting the PCR product with Hae III, seven (18.4%) of the 38 tissue samples were identified as mutant-types (136 bp and 27 bp fragments) (Figure 4). No mutations were found in 38 corresponding noncancerous tissue samples and 22 samples of normal lymphocytes. When the remaining 31 pairs of wild type HCC specimens were analyzed by PCR-SSCP-silver staining, two showed a mobility shift (Figure 5), indicating the presence of mutations in exon 7, rather than codon 249. Thus the mutation incidence in p53 exon 7 was 23.7% (9/38 samples). Among 9 mutant-type HCC specimens 8 specimens (88.9%) tested positive for P53 protein.

Correlation of p53 overexpression with the clinicopathological features of HCCs (Table 1).

Our results showed that overexpression of p53 was more frequent in cases of metastasized grade IV HCC. No significant relationship was found between p53 overexpression and either tumor size or histological classification.

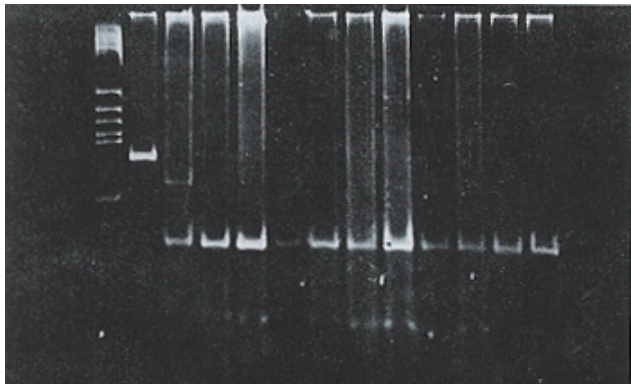


Figure 4 PCR analysis of p53 codon 249 in hepatocellular carcinoma. M: DNA size marker (PBR322 digest of Hae III); P: Product of PCR (164 bp); N: Surrounding noncancerous tissue; T: HCC tumor tissue; T1: Mutation of codon 249; L: Normal lymphocyte.

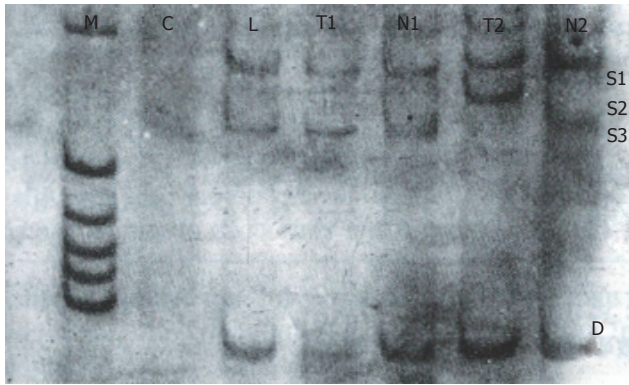


Figure 5 Analysis of p53 exon 7 by PCR-SSCP-silver staining in hepatocellular carcinoma. C: Negative control; L: Normal lymphocyte; N: Surrounding noncancerous tissue; T: HCC tumor tissue; T2: Mobility shift; S1 S3: Single strand DNA; D: Double strand DNA

Table 1 Correlations between p53 overexpression and clinicopathological features of Hepatocellular carcinoma				
Clinicopathological features	Number of cases	p53 expression (+)	p53 expression (-)	Significance
Tumor size (cm)				
< 3	3	1	2	a
3-5	5	2	3	
> 5	30	13	17	
Classification				
Trabecular	15	5	10	b
Pseudoglandular	16	8	8	
Compact	7	3	4	
Grade				
I	3	1	2	c
II	7	2	5	
III	15	5	10	
IV	13	8	5	
Metastasis				
Positive	14	10	4	d
Negative	24	6	8	

a and b: Significant; c and d: $P < 0.05$.

Correlation of p53 mutations with the clinicopathological features of HCCs (Table 2).
In this study, p53 mutations were found more frequently in HCCs having a large size, a grade IV classification, and which had metastasized.

DISCUSSION

P53 protein has a very short half life in normal cells, and is thus undetectable by standard immunocytochemical methods. In contrast, p53 gene mutations in tumor cells usually result in the stabilization and accumulation of p53 protein in the nuclei, at levels which can be detected by immunohistochemistry techniques. Therefore, p53 overexpression detected by immunohistochemistry strongly suggests the presence of a p53 gene mutation^[6]. Among the 9 mutant-type HCC specimens in this study, 8 specimens (88.9%) were positive for P53 protein, which confirms the above hypothesis. Because the location of a p53 point mutation can vary, DNA sequencing is essential to reveal this alteration of the gene. However, immunohistochemical techniques are more simple to perform, and especially useful when screening large numbers of specimens for the presence of mutations.

The presence of p53 mutations in HCC appears to vary with geographic location. In regions with a high risk for exposure to HBV and aflatoxins, (e.g., China^[2] and South Africa^[1]), p53 mutations have been reported in ~ 50% of HCC cases, and the majority of those mutations were found at codon 249. In Japan^[7], where HBV infections are relatively common, but dietary aflatoxin intake is low, p53 mutations have been reported in 29% of HCC cases. In countries where neither HBV nor dietary aflatoxin are prevalent (e.g., France^[8], Germany^[9], and Great Britain^[10]), mutated p53 is rarely found in HCCs, and there have been few or no mutations reported at codon 249 in the latter two countries^[3,11]. While the results of molecular epidemiological studies have suggested that HBV may act synergistically with aflatoxin in the generation of p53 mutations in HCC, its mechanism of action remains obscure.

Table 2 Correlations between p53 mutations and the clinicopathological features of Hepatocellular carcinoma				
Clinicopathological features	Number of cases	p53 expression (+)	p53 expression (-)	Significance
Tumor size (cm)				
< 5	8	0	8	b
> 5	30	9	21	
Classification				
Trabecular	15	4	11	b
Pseudoglandular	16	3	13	
Compact	7	2	7	
Grade				
I	3	0	3	c
II	7	1	6	
III	15	2	13	
IV	13	6	7	
Metastasis				
Positive	14	6	8	d
Negative	24	6	21	

b: Not significant; a, c and d: $P < 0.05$.

In this study, we divided p53 mutations into two groups: (1) a tumor-specific mutation at codon 249, and (2) various scattered mutations at codons other than codon 249. Among 38 cases of HCC, 7 cases (18.4%) were found to have specific mutations by PCR-RFLP analysis. This 18.4% mutation rate was much lower than the 50% rate reported in Qidong^[12], an area with a high exposure to aflatoxin, and much higher than the 2.2% rate reported in northern China^[13], an area with low exposure to aflatoxin. Meanwhile, immunohistochemistry and PCR-SSCP analyses identified 10 cases of HCC (26.3%) which showed scattered mutations. The overall frequency of p53 mutations in our geographic area was 44.7% (17/38 HCC cases), and these results are in agreement with the high prevalence of HBV and moderate exposure to aflatoxin in our area. We therefore conclude that HBV acts in conjunction with aflatoxin to generate p53 gene mutations in HCCs. Furthermore, dietary exposure to AFB1 may mainly contribute to the tumor-specific mutation, while HBV infection may account for other p53 gene mutations. As the most common tumor suppressor gene, p53 contributes to malignant transformation and the aggressiveness shown by several types of cancers. It was previously reported that p53 overexpression is correlated with the aggressiveness and metastasis of HCC^[14]. Because P53 protein is not abnormally expressed in peri-cancerous liver tissue, the p53 gene probably becomes mutated after the hepatocellular carcinogenesis process has already been initiated. Both p53 overexpression and p53 mutations were more frequent in poorly-differentiated HCCs and cases of metastasized HCC, suggesting that the number of p53 alterations had increased as the HCC progressed. These findings indicate that p53 mutations represent one of the most important genetic changes in the development of HCC, and can serve as a molecular marker for high grade and metastatic HCC.

ACKNOWLEDGEMENT

The authors thank Dr. Crawford L for his donation of monoclonal

antibody Pab1801, and Dr. Lane DP for his donation of polyclonal antiserum CM-1.

REFERENCES

- 1 Bressac B, Kew M, Wands J, Ozturk M. Selective G to T mutations of p53 gene in hepatocellular carcinoma from southern Africa. *Nature* 1991; **350**: 429-431 [PMID: 1672732 DOI: 10.1038/350429a0]
- 2 Hsu IC, Metcalf RA, Sun T, Welsh JA, Wang NJ, Harris CC. Mutational hot-spot in the p53 gene in human hepatocellular carcinomas. *Nature* 1991; **350**: 427-428 [PMID: 1849234 DOI: 10.1038/350427a0]
- 3 Unsal H, Yakicier C, Marçais C, Kew M, Volkmann M, Zentgraf H, Isselbacher KJ, Ozturk M. Genetic heterogeneity of hepatocellular carcinoma. *Proc Natl Acad Sci USA* 1994; **91**: 822-826 [PMID: 8290606 DOI: 10.1073/pnas.91.2.822]
- 4 van den Berg FM, Baas IO, Polak MM, Offerhaus GJ. Detection of p53 overexpression in routinely paraffin-embedded tissue of human carcinomas using a novel target unmasking fluid. *Am J Pathol* 1993; **142**: 381-385 [PMID: 8434637]
- 5 Wang D, Shi JQ. Antigen retrieval technique for immunohistochemical demonstration of p53 protein in paraffin sections. *Disan Junyi Daxue Xuebao* 1994; **16**: 52-54
- 6 Harris CC, Hollstein M. Clinical implications of the p53 tumor-suppressor gene. *N Engl J Med* 1993; **329**: 1318-1327 [PMID: 8413413 DOI: 10.1056/NEJM199310283291807]
- 7 Oda T, Tsuda H, Scarpa A, Sakamoto M, Hirohashi S. p53 gene mutation spectrum in hepatocellular carcinoma. *Cancer Res* 1992; **52**: 6358-6364 [PMID: 1330291]
- 8 Laurent-Puig P, Flejou JF, Fabre M, Bedossa P, Belghiti J, Gayral F, Franco D. Overexpression of p53: a rare event in a large series of white patients with hepatocellular carcinoma. *Hepatology* 1992; **16**: 1171-1175 [PMID: 1330867 DOI: 10.1002/hep.1840160511]
- 9 Kress S, Jahn UR, Buchmann A, Bannasch P, Schwarz M. p53 Mutations in human hepatocellular carcinomas from Germany. *Cancer Res* 1992; **52**: 3220-3223 [PMID: 1317262]
- 10 Challen C, Lunec J, Warren W, Collier J, Bassendine MF. Analysis of the p53 tumor-suppressor gene in hepatocellular carcinomas from Britain. *Hepatology* 1992; **16**: 1362-1366 [PMID: 1332921 DOI: 10.1002/hep.1840160610]
- 11 Wang D, Shi JQ. The progress of tumor suppressor gene in human hepatocellular carcinoma (Review). *Foreign Medical Sciences. Genetics* 1994; **17**: 240-244
- 12 Scorsone KA, Zhou YZ, Butel JS, Slagle BL. p53 mutations cluster at codon 249 in hepatitis B virus-positive hepatocellular carcinomas from China. *Cancer Res* 1992; **52**: 1635-1638 [PMID: 1311638]
- 13 Zhu MH, Wang WL. Study of allotype and suppressor gene p53 exon 7 in hepatocellular carcinoma. *Disi Junyi Daxue Xuebao* 1993; **14**: 241-246
- 14 Hsu HC, Tseng HJ, Lai PL, Lee PH, Peng SY. Expression of p53 gene in 184 unifocal hepatocellular carcinomas: association with tumor growth and invasiveness. *Cancer Res* 1993; **53**: 4691-4694 [PMID: 8402647]

S- Editor: Ma JY L- Editor: Filipodia E- Editor: Li RF

Clinical use of hepatic carcinoma associated membrane protein antigen (HAg18-1) for detection of primary hepatocellular carcinoma

Shi-Xian Hu, Gui-Ying Fang

Shi-Xian Hu, Gui-Ying Fang, Department of Pathology, Chinese PLA 165 Hospital, Hengyang 421002, Hunan Province, China

Shi-Xian Hu, Chief Physician, Director of the Department of Pathology, having published 38 papers and one book, *Pathology of Burns*. Born on March 17, 1935 in Lou Di City, Hunan Province, and graduated from the Chinese PLA Sixth Medical University (the Previous Zhong Zhen Medical College) in 1935.

Author contributions: All authors contributed equally to the work.

Original title: *China National Journal of New Gastroenterology* (1995-1997) renamed *World Journal of Gastroenterology* (1998-).

Correspondence to: Dr. Shi-Xian Hu, Chief Physician, Director, Department of Pathology, Chinese PLA 165 Hospital, Hengyang 421002, Hunan Province, China

Telephone: +86-734-8411452-83293

Received: July 2, 1996
Revised: July 29, 1996
Accepted: August 7, 1996
Published online: September 15, 1996

Abstract

AIM: To evaluate the sensitivity, specificity, and clinical value of hepatic carcinoma associated membrane protein antigen (HAg18a21) as a reagent in a serum quick enzyme linked immunosorbent assay (ELISA) for detection of primary hepatocellular carcinoma (PHCC).

METHODS: A serum quick enzyme linked immunosorbent assay (ELISA) which uses HAg18a21 as a reagent, was prepared from monoclonal antibodies against human hepatic carcinoma. We assayed blood serum obtained from 100 cases of primary hepatocellular carcinoma (PHCC), 5 cases of hepatic biliary carcinoma (HBC), 10 cases of metastatic hepatic carcinoma (MHC), 20 cases of hepatitis B (HB), 20 cases of liver cirrhosis (LC), 20 cases of malignant gastrointestinal tumors, and 20 cases of inflammatory gastrointestinal diseases (including ulcers). Alpha 2 fetoprotein (AFP) was concurrently detected for each case. Twenty samples of blood bank serum were tested as controls.

RESULTS: The respective positive rates for the HAg18a21 ELISA assay and AFP detection assay were 81% and 68% in PHCC, 20% and 40% in HBC, 19% and 20% in MHC, 10% and 20% in BH, 10% and 20% in LC, 10% and 15% in malignant gastrointestinal tumors, and 5% and 10% in inflammatory gastrointestinal diseases. Neither assay showed a positive result for any tested blood bank sample.

CONCLUSION: The HAg18a21 ELISA demonstrated high sensitivity and specificity in the detection of PHCC. HAg18a21 ELISA and AFP detection, if used together, may compliment each other in the diagnosis of PHCC.

Key words: Liver neoplasms/diagnosis; Carcinoma; Hepatocellular

diagnosis; Antigens; Neoplasm

© **The Author(s) 1996.** Published by Baishideng Publishing Group Inc. All rights reserved.

Hu SX, Fang GY. Clinical use of hepatic carcinoma associated membrane protein antigen (HAg18-1) for detection of primary hepatocellular carcinoma. *World J Gastroenterol* 1996; 2(3): 165-166 Available from: URL: <http://www.wjgnet.com/1007-9327/full/v2/i3/165.htm> DOI: <http://dx.doi.org/10.3748/wjg.v2.i3.165>

INTRODUCTION

Hepatic carcinoma is the third leading cause of death in China, and accounts for 15.08% of all cancer-related deaths^[1]. Currently, hepatocellular carcinoma (PHCC) is primarily diagnosed by imaging studies and serological tests. While alpha-fetoprotein (AFP) is an internationally accepted specific biological marker for PHCC, and can be detected in 68.5%-76.5% of all cases^[2], serum AFP levels can vary with the degree of tumor differentiation and the size of the tumor mass^[3]. Also, AFP may be absent or present at only low concentrations in a certain proportion of PHCC cases, whereas cases of metastatic hepatic carcinoma and benign hepatic diseases may have elevated AFP levels^[4]. Therefore, there is an urgent need to identify more sensitive and specific markers of hepatic carcinoma.

MATERIALS AND METHODS

Source of materials

All 195 serum samples used in this study were collected from January 1990 to December 1993 from patients at the Chinese PLA 165th Hospital, The First Affiliated Hospital of Hengyang Medical University, Hengyang Municipal Central Hospital, and The 415th Hospital of the Ministry of Nuclear Industry. The samples were obtained from 100 patients with PHCC, 5 patients with HBC, 10 patients with MHC, 20 patients with HB, 20 patients with LC, 20 patients with gastrointestinal malignant tumors, and 20 patients with various inflammatory gastrointestinal diseases (including ulcers). Twenty samples of blood bank serum served as control samples.

Methods

HAg18-1 qualitative assays were performed using a HAg18-1 serum quick ELISA Kit (Chinese PLA Fourth Medical University and Zhengzhou Bo-sai Biological Reagent Laboratory, China), and methods described in the kit's instructions. Quantitative HAg18-1 assays were performed as follows: a known HAg18-1-positive sample (blue in color) was diluted with 1 mL of 0.5 N H₂SO₄ to terminate the reaction; after which, the sample's OD at 450 nm was measured using a STAT FAX 303 plus photometer system (Awareness Technology; Technology, Palm City, FL, United States). A positive assay sample was defined as one having an OD > 0.15.

Table 1 The results of HAg18-1 Eenzyme linked immunosorbent assays and alpha-fetoprotein radioimmunoassays

Disease	No. of cases	No. of positive cases		Positive rate (%)	
		HAg18-1	AFP	HAg18-1	AFP
PHCC	100	81	68	81	68
HBC	5	1	2	20	40
MHC	10	1	2	10	20
HB	20	2	4	10	20
LC	20	2	4	10	20
GI malignant tumor	20	2	3	10	15
GI inflammatory diseases	20	1	2	5	10
Bank blood ¹	20	0	0	0	0

¹Controls

AFP was detected with an AFP radioimmunoassay (RIA) Kit (Shanghai Biological Product Institute; Shanghai, China), using the procedure described in the instruction manual. AFP antibody was supplied by Fuzhou MaiXin Biological Technique Development Co. (China), and the “SP” method was adopted.

RESULTS

Relationship between HAg18- 1 serum assay results and AFP detection in 100 cases of PHCC (Table 1)

HAg18-1 serum assays and AFP detection assays both showed positive results for 61% (61/100) of all the cases. AFP detection assays showed positive results for 86.4% (70/81) of the HAg18-1 positive cases, and among the 19 HAg18-1 negative cases, 7 cases (36.8%) were AFP positive. The HAg18-1 serum assay showed positive results for 88.23% (62/68) of the AFP positive (> 400 ng/mL) cases, and among the 32 AFP negative cases (< 400 ng/mL), 24 cases (75%) were positive with the HAg18-1 serum assay. Four HAg18-1 serum assay positive cases (2 clinically diagnosed cases of HB and 2 cases of LC) had been followed up for 3 years. One of the LC cases was later proven to be PHCC by autopsy after death.

The AFP test showed 100% positive results when the “SP” method was used to test sections of paraffin-embedded liver tissue from all 100 patients with PHCC.

DISCUSSION

There are numerous biological markers for human hepatic carcinoma, and substantial advances have been made in both the theories and technology involved in this area of research. Several new techniques that were previously used only in experimental studies are now used in the clinic. In summary, four types of assays are now used to detect PHCC, and these involve detecting proteins, enzymes, hormones, and metabolites, respectively^[5]. Because these assays vary greatly in their sensitivity and specificity, there remains an urgent need to identify new a biological marker for hepatic carcinoma.

Practical value of the HAg18-1 assay

In this study, the HAg18-1 assay was able to detect 81% of the PHCC cases, which was markedly or slightly higher than the detection rates reported from studies conducted in Nanjing (65.9%)^[6], Xi’an (74%)^[4], Chengdu (79.63%)^[7], and Lanzhou (80%)^[8]. The assay showed a < 10% positive rate when used to detect other types of malignant tumors or inflammatory diseases. The reasons that HAg18-1 is present at certain concentrations in different diseases remain unclear. In our study, the HAg18-1

assay was 90% specific when used to detect PHCC. This result was comparable to the 89.52% specificity the same assay showed in a study conducted in Chengdu. In that study, HAg18-1 was shown to be a tumor-associated antigen (TAA) closely linked with hepatic carcinoma. In our study, the HAg18-1 assay displayed higher sensitivity for detecting PHCC, when compared with the AFP assay (68% detection rate). The HAg18-1 assay showed positive results in 75% (24/32) of the 32 PHCC cases with a serum AFP level < 400 ng/mL, suggesting that it may be especially useful for detecting PHCC cases which are AFP negative or in which the patient has a low serum AFP concentration. On the other hand, among the 19 PHCC cases that tested negative with the HAg18-1 assay, 36.8% (7/19) were detected by the AFP assay. These results indicate that the two assays are complementary to each other in their clinical use. Four HAg18-1 assay positive cases (2 clinically diagnosed HB cases and 2 LC cases) had been followed up for 3 years. Among them, one clinically diagnosed LC case was proven to be PHCC by autopsy after death. Therefore, it is reasonable to believe that the HAg18-1 assay might be helpful in the early diagnosis of PHCC. While the HAg18-1 assay showed positive results in a certain proportion of non-PHCC tumors and inflammatory diseases, these types of results occurred far less often than when using the AFP assay, and had little influence on the final diagnosis of PHCC.

In recent years, researchers have suggested that a combined detection protocol with multiple markers would be superior to detecting only a single marker in the diagnosis of PHCC, and especially when attempting to diagnose patients who are AFP negative or have a low serum AFP concentration. The serum quick enzyme-linked immunosorbent assay with HAg18-1 is easy to perform, provides consistent results, and requires no special instruments. It is a simple technique that is especially suitable for surveying high-risk populations, and can be used in general practice. If combined with AFP detection, it should greatly increase the PHCC detection rate, and thus has great potential for widespread clinical use.

REFERENCES

- 1 **Tumor Prevention and Treatment Research Office of the Ministry of Health.** Survey of deaths due to malignant tumors in Chinese population (in Chinese). 1st ed, Beijing: People s Health Press 1980: 116-118
- 2 **Huang ZQ, Gu ZY.** Progress in hepatic biliary duct and pancreatic surgery (in Chinese). 1st ed, Beijing: People s Army Medical Press 1989: 87-90
- 3 **Ebara M, Ohto M, Shinagawa T, Sugiura N, Kimura K, Matsutani S, Morita M, Saisho H, Tsuchiya Y, Okuda K.** Natural history of minute hepatocellular carcinoma smaller than three centimeters complicating cirrhosis. A study in 22 patients. *Gastroenterology* 1986; **90**: 289-298 [PMID: 2416627]
- 4 **Chinese PLA Fourth Medical University, Zheng-zhou Bo-sai Biological Reagents Laboratory.** Serological diagnosis of hepatocellular carcinoma by use of monoclonal antibody against hepatocellular carcinoma (in Chinese). Material for a national studying class 1990: 16
- 5 **Meng XY.** Progress in research on serological markers of primary hepatocellular carcinoma (in Chinese). In: Tang ZX, Yang BH. Progress in research on primary liver carcinoma (in Chinese). Shanghai: Shanghai Medical University Press 1990: 131
- 6 **Zhang AZ, Wang YG.** Serological diagnosis of hepatocellular carcinoma with HAg18-1 prepared by monoclonal antibody against hepatocellular carcinoma (in Chinese). In: Li CH, Shan ZX. Progress in research on tumor markers (in Chinese). First Ed. Beijing: People s Army Medical Press 1992: 120
- 7 **Chu RJ, Jiang M, Chen Y, Chen X, Zhou JH, Li XY, et al.** Preliminary use of HAg18-1 serum ELISA reagent prepared by monoclonal antibody against hepatocellular carcinoma in diagnosis of hepatic carcinoma (in Chinese). *Jiefangjun Yixue Zazhi* 1992; **17**: 13-16
- 8 **Zhang FX, Liang SD.** Diagnostic value of multiple tumor markers to AFP negative hepatocellular carcinoma (in Chinese). In: Li CH, Shen ZX. Progress in Research on Tumor Markers. First Ed, Beijing: People s Army Medical Press 1992: 90

S- Editor: Cao LB **L- Editor:** Filipodia **E- Editor:** Li RF



Magnetic resonance imaging of portal vein invasion in hepatocellular carcinoma: Results from 25 cases

Xi-Xu Zhu, Jun-Kun Chen, Guang-Ming Lu

Xi-Xu Zhu, Jun-Kun Chen, Guang-Ming Lu, Department of Radiology, General Hospital of Chinese PLA, Nanjing Commanding Area; 305 Zhongshan Donglu, 210002, Jiangsu Province, China

Xi-Xu Zhu, Attending Physician, Master of Medicine, having published 4 papers.

Author contributions: All authors contributed equally to the work.

Original title: *China National Journal of New Gastroenterology* (1995-1997) renamed *World Journal of Gastroenterology* (1998-).

Correspondence to: Dr. Xi-Xu Zhu, Department of Radiology, General Hospital of Chinese PLA, Nanjing Commanding Area; 305 Zhongshan Donglu, 210002, Jiangsu Province, China

Received: April 19, 1996
Revised: May 12, 1996
Accepted: June 21, 1996
Published online: September 15, 1996

Abstract

AIM: To pre-operatively assess tumor thromboses associated with hepatocellular carcinoma in the portal vein.

METHODS: Twenty-five patients diagnosed with a thrombus due to hepatocellular carcinoma were included in the study. MR imaging was performed with a 1.0T superconducting magnetic imaging system. Both T1 and T2 weighed images as well as FLASH sequences were obtained in the transverse plane, and additional FLASH images were obtained in the coronal plane.

RESULTS: Thromboses located in the portal vein had signal intensities similar to those of the main tumor. An intrinsic portal vein thrombus was found in 16 patients, and six thromboses were occlusive. Thromboses were found in the diffuse narrow portal branches of 3 patients. The portal venous thromboses displayed an area of signal intensity that replaced the normal flow void of the portal vein. The affected portal veins displayed a stumpy appearance, had irregular areas of stenosis, and showed formation of a vascular net.

CONCLUSION: MRI was more sensitive, specific, and noninvasive for detecting a portal tumor thrombus, and can be used jointly with spin echo (SE) and gradient echo (GRE) imaging techniques.

Key words: Magnetic resonance imaging; Liver neoplasms/diagnosis

© The Author(s) 1996. Published by Baishideng Publishing Group Inc. All rights reserved.

Zhu XX, Chen JK, Lu GM. Magnetic resonance imaging of portal vein invasion in hepatocellular carcinoma: Results from 25 cases. *World J Gastroenterol* 1996; 2(3): 167-170 Available from: URL: <http://www.wjgnet.com/1007-9327/full/>

v2/i3/167.htm DOI: <http://dx.doi.org/10.3748/wjg.v2.i3.167>

INTRODUCTION

Primary hepatocellular carcinoma (HCC) is pathologically characterized by its propensity to invade the portal venous system. A pre-operative assessment should be performed when a tumor thrombus is present in the main portal vein. If the results confirm that the tumor has invaded the portal branches of one lobe, resection may be indicated. MRI is the least invasive method by which the scanning plane can be easily changed to allow the use of angiography for examining the vascular structure. Here, we summarized the results of pre-operative MR assessments of portal venous thromboses that had been confirmed by sonography, enhanced CT or arterial portography in 25 patients with HCC.

MATERIALS AND METHODS

Materials

Twenty-five male patients (age range 33-64 years, mean age = 54 years) with HCC were enrolled in this study. The patients had tumors that ranged from 3 cm to 10 cm in diameter. Fifteen of the patients had been diagnosed as HCC by a histologic examination of tissue biopsy, and ten were diagnosed based on having a serum alpha fetoprotein (AFP) level that was persistently > 500 µg/L.

Methods

A Magnetom Impact 1.0T superconducting magnetic resonance system (Siemens; Munich, Germany) was used to obtain T1 and T2 weighed images with a TR of 500 ms and an echo time (TE) of 15 ms (TR/TE = 500.660/15). Additionally, long TR/short TE and long TR/TE (1800-2150/22-120) images, as well as spin echo (SE) images in the transverse plane were obtained by using a multisection imaging technique [10 mm section thickness; 200 × 256 matrix; 380 mm × 400 mm field of view (FOV)]. Gradient echo (GRE) sequences were obtained for all patients using the sequential section technique with the following parameters: TR of 100 ms, TE of 6 ms, flip angle of 30 degrees, an 8 mm section thickness, a 128 × 256 matrix, and a 400 mm × 400 mm field of view. Additional FLASH images were obtained in the coronal plane so as to observe possible tumor thromboses located in the main portal vein or its branches, as well as the inferior vena cava (IVC). All patients were asked to momentarily suspend their respiration during GRE measurements.

RESULTS

A thrombosis was diagnosed in 25 patients enrolled in one or more studies which used contrast material enhanced CT alone, $n = 5$; color sonography alone, $n = 9$; contrast material enhanced CT plus color sonography, $n = 6$; angiography alone, $n = 5$, respectively. Tumor thromboses displayed signal intensities similar to those of the



Figure 1 Patient with HCC. T1 weighed (500/15) MR images of the upper abdomen showed the portal tumor thrombus as a clot of iso-signal intensity (arrow).

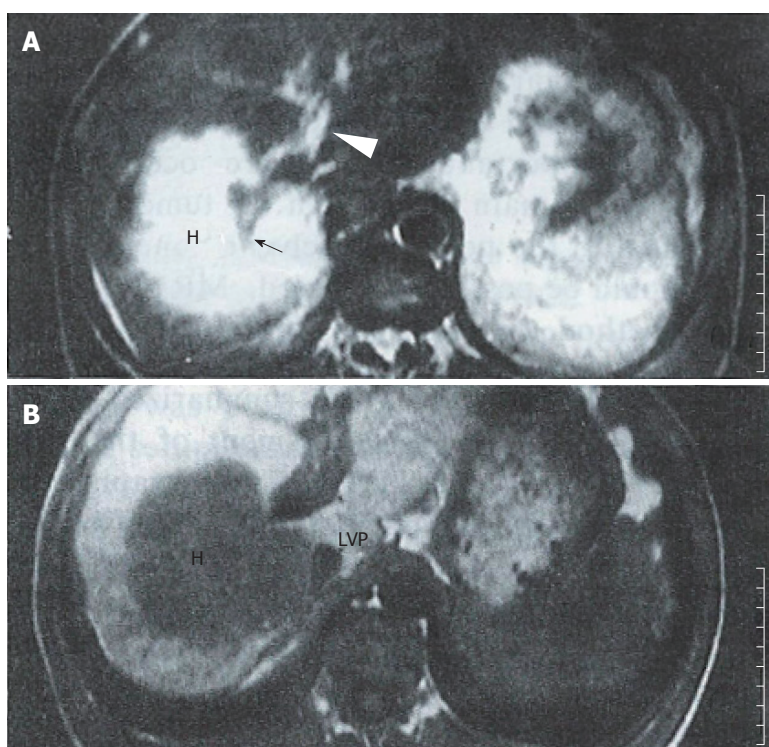


Figure 2 Patient with HCC enclosing the right branch. A: T2 weighed (2000/80) images showed the tumor (H) having a higher signal intensity than the parenchyma. The right branch of the portal vein in the tumor ended abruptly, and appeared as a stump (arrow). Some irregular hyperintensity was seen in the dilated main and left portal vein (arrowhead). B: FLASH (100/6) imaging showed main and left portal vein dilation with heterogeneous intensity more clearly than did SE imaging. The IVP was compressed by the tumor.

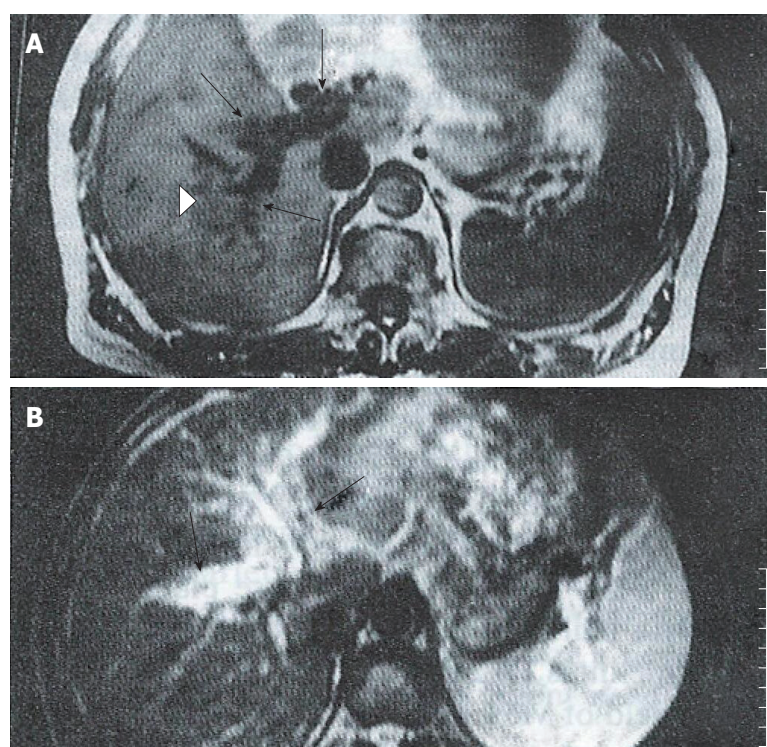


Figure 3 Patient with HCC. A: T1 weighed (500/15) images showed diffuse, irregular narrow right branches with numerous nodules (arrow); the distal portal vein was poorly delineated (arrowhead). Several small flowing voids representing collateral vessels were seen. B: T2 weighed (2000/80) MR images showed the left portal venous wall as slightly hyperintense, indicating invasion by the tumor (arrow).

main tumor masses. An intrinsic portal venous thrombus (PVT) was found in 16 patients, and appeared as an area of iso-signal intensity that replaced the normal flow void in the portal vein on SE images (Figure 1). On GRE images, the intrinsic thromboses appeared as areas of decreased signal intensity in bright blood vessels. In six cases with complete portal vein occlusion, the thrombus was located either laterally or in the surrounding portal branches. SE images showed a stumpy portal vein with dilated proximal branches; the main section of the portal vein and its peripheral branches could not be identified. On long TR images, the signal intensity was slightly higher than that of the hepatic parenchyma, and similar to that of the main tumor; additionally, occluded portal branches could be seen in the tumor (Figure 2). In the GRE images, the bright portal vein appeared to end abruptly due to poor contrast between the thrombus and adjacent stationary tissue. In 3 cases with diffuse narrow portal branches, T1 weighted images showed the portal branches had irregular stenoses with a flowing void area. T2 images showed some slight hyperintensity along the vascular wall caused by invasion of the tumor (Figure 3). Collateral vessels had developed in 3 cases. Numerous periportal collateral voids were seen on T1 weighed images. GRE images displayed features similar to those

shown on SE images, but with stronger signal intensities. GRE images conclusively demonstrated the presence of collateral vessels and showed more extensive collateralization than the standard SE images. Ten patients showed evidence of extrinsic compression of the main or proximal right or left portal vein or IVC by the tumor. The SE and GRE images showed similar findings; however, when compared with the SE images, the GRE images less clearly showed that the tumor was responsible for venous compression. This was due to poor contrast between the tumor and surrounding normal tissue on the GRE images.

DISCUSSION

Direct portography is the most accurate pre-operative method for assessing portal venous invasion by HCC^[1]. While arterial portography is the standard pre-operative method used in many hospitals, these examinations increase the risk of bleeding in patients with impaired clotting function. Noninvasive imaging of the portal venous system has been successfully accomplished with a variety of imaging techniques, including US, CT, and MRI. Color sonography has proved to be highly accurate in determining the presence, direction, and velocity of portal blood flow, but it

is operatively dependent^[2]. Although contrast-enhanced CT with dynamic scanning is highly sensitive for identifying a thrombus in the main portal vein or its large branches, the suboptimal opacity of portal vessels and allergic reactions limit the use of this technique.

Identification of a normal portal vein

The spin-echo (SE) technique provided anatomic information similar to that provided by CT, but did not require the IV injection of a liver contrast agent. Our standard assessment of the portal venous system (PVS) by use of SE imaging produced a typical signal void, "black blood" phenomenon, and the hepatic venous signal intensity was similar to that of the portal vein. While the portal and hepatic veins could be distinguished based on their direction, they were difficult to distinguish on the peripheral parenchyma without adding an additional plane. FLASH techniques^[3] generally offer two advantages that improve depiction of the hepatic vasculature: (1) high signal intensity within blood vessels due to flow enhancement; and (2) a reduction in motion artifacts, because the patients must hold their breath. The portal vein and its branches appeared to be clear when examined by FLASH with presaturation in additional coronal or sagittal planes. The high intensity signal produced by flowing blood clearly distinguished the intra-abdominal vasculature from the surrounding tissue. Additionally, the image acquisition time was significantly reduced when using GRE imaging rather than conventional SE imaging.

Appearance of PVT on MR images

Thrombus of the portal vein is usually clinically associated with hepatocellular carcinoma, and pathologically associated with its intra-hepatic metastasis. A tumor thrombus may extend into the portal trunk, even when a hepatocellular carcinoma is still small^[4]. There is a poor correlation between tumor size and the presence of a tumor thrombus in the portal vein. The MR findings of PVT were classified based on their location in the portal vein.

Intrinsic clot

An intra-luminal thrombus could be present at any location in the portal vein. On spin-echo MR images, a PVT usually appeared as an area with an abnormal signal within the lumen of the portal vein. Intrinsic PVTs appeared as an isointense signal that replaced the normal portal flow void on T1 weighed images (Figure 1). Additionally, intrinsic PVTs typically showed high signal intensities on T2 weighed images, and which were similar to that of the main tumor. Some spurious signals were difficult to distinguish from a thrombus on SE images; while, GRE images showed the portal vein as an area with a high signal and a reduced number of respiratory artifacts. A PVT usually appeared as an area having a diminished intravascular signal with an intensity similar to that shown by adjacent stationary soft tissue on GRE imaging. While GRE more clearly showed the PVT, it provided less anatomic resolution and live-lesion contrast.

Portal stump

Occlusion usually occurred at the base of the narrow portal vein. The stenosed portal vein was occluded by compression caused by the extrinsic tumor. This was also true for the tumor enclosed portal vein. In SE images, the portal vein or its branches were completely replaced by tumor tissue. T1 weighed images showed the branches as stumps, the flow void of the distal segment of the portal vein as being obliterated, and the proximal branches being dilated. A stumpy appearing portal vein could be seen in the tumor, which grew around the invaded branches (Figure 2). Secondary ischemic changes caused by the PVT in the HCC could be readily distinguished from the tumor. The use of MRI was advantageous in that it showed the patchy perfusion of the occluded vein. Dynamic MR imaging showed a fan-shaped area, and also high signal intensity areas with early and prolonged enhancement in segments that were affected by the portal vein thrombus^[5]. GRE images only showed a high signal portal stump, because the intensity of the thrombus was similar to that of the adjacent stationary tissues. Collateral veins and varices

were also visible.

Diffusely narrow portal vein

The portal vein was diffusely stenosed in one or more of its branches. Extensive stenosis is usually associated with cirrhosis. Sections of venous wall that had been penetrated by a growing tumor had an irregular appearance and displayed several small nodules. While the signal void of the portal vein was present, the small vessels were poorly delineated on the T1 weighed images. T2 weighted images showed hyperintense regions along portal branches which had been invaded by the tumor (Figure 3). The bright portal vein was poorly delineated on GRE images.

Cavernous changes

Collateral vessels developed and effectively replaced the obliterated portal vein. These vessels formed a major hepatportal venous conduit when the portal vein was severely stenosed or occluded. The collateral vessels usually appeared in the same area as the affected vessels, and a severely stenosed or occluded portal vein showed evidence of collateralization. Small dilated and expanded collateral veins near the edge of the portal vein showed numerous areas of periportal hypointensity on SE images. GRE images showed findings similar to those on SE images, but with hyperintensity. Collateral vessels and varices were seen clearly, and appeared to be more extensive on MR images.

Comparison of the different imaging sequences

SE images were slightly more specific. Motion or flow-related artifacts can sometimes produce a spurious signal in the portal vein that mimics the signal produced by a thrombus. This is due to the markedly variable signal intensity of flowing blood. Therefore, SE and GRE should be used in combination when attempting to diagnosis a thrombus. GRE images are more sensitive than SE images, because a thrombus is usually well differentiated from flowing blood. Also, GRE images can be obtained more rapidly due to the shorter examination time. The accuracy of a thrombosis diagnosis can be significantly improved by using a combination of SE and GRE imaging techniques^[6].

In our study, transverse plane images were obtained with both SE and GRE sequences for all patients, and additional coronal plane images were obtained with GRE sequences. The coronal plane provided wide coverage and was particularly useful when imaging tortuous vessels. Coronal GRE images acquired immediately after injection of Gd DTPA were similar to those acquired by X-ray angiography^[7]. MR angiography was used as a non-invasive method for displaying vasculature. The MIP algorithm provided extremely high levels of contrast between blood vessels and the surrounding tissues, and was particularly useful for displaying tortuous vessels. Johnson *et al.*^[8] showed that MR angiography was more sensitive than conventional angiography in detecting varices. However, the joint use of SE and GRE images still had some disadvantages. The major limitations are suboptimal spatial resolution and the production of artifacts. Also, the presence of a thrombus in small vessels can be extremely difficult to delineate by MR.

REFERENCES

- 1 Igawa S, Sakai K, Kinoshita H, Hirohashi K, Inoue T. Comparison of sonography, computed tomography, angiography, and percutaneous transhepatic portography in detection of portal tumor thrombus in hepatoma. *World J Surg* 1986; **10**: 876-883 [PMID: 3022490 DOI: 10.1007/BF01655264]
- 2 Ralls PW. Color Doppler sonography of the hepatic artery and portal venous system. *AJR Am J Roentgenol* 1990; **155**: 517-525 [PMID: 2117348 DOI: 10.2214/ajr.155.3.2117348]
- 3 Haase A, Frahm J, Mattaei D, Hanicke W, Merboldt KD. FLASH imaging. Rapid NMR imaging using low flip-angle pulse. *J Magn Reson* 1986; **67**: 258-266 [DOI: 10.1016/0022-2364(86)90433-6]
- 4 Imaeda T, Yamawaki Y, Hirota K, Suzuki M, Seki M, Doi H. Tumor thrombus in the branches of the distal portal vein: CT demonstration. *J Comput Assist Tomogr* 1989; **13**: 262-268 [PMID: 2538494 DOI: 10.1097/00004728-198903000-00015]
- 5 Mitani T, Nakamura H, Murakami T, Nishikawa M, Maeshima S, Nakaniishi K, Marukawa T, Harada K, Hori S, Kozuka T. Dynamic MR studies of hepatocellular carcinoma with portal vein tumor thrombosis. *Radiat Med* 1992; **10**: 232-234 [PMID: 1337618]
- 6 Arrivé L, Menu Y, Dessarts I, Dubray B, Vullierme MP, Vilgrain V, Najmark

D, Nahum H. Diagnosis of abdominal venous thrombosis by means of spin-echo and gradient-echo MR imaging: analysis with receiver operating characteristic curves. *Radiology* 1991; **181**: 661-668 [PMID: 1947078 DOI: 10.1148/radiology.181.3.1947078]

7 **Rodgers PM**, Ward J, Baudouin CJ, Ridgway JP, Robinson PJ. Dynamic contrast-enhanced MR imaging of the portal venous system: comparison with x-ray angiography. *Radiology* 1994; **191**: 741-745 [PMID: 8184055 DOI: 10.1148/radiology.191.3.8184055]

8 **Johnson CD**, Ehman RL, Rakela J, Ilstrup DM. MR angiography in portal hypertension: detection of varices and imaging techniques. *J Comput Assist Tomogr* 1991; **15**: 578-584 [PMID: 2061471 DOI: 10.1097/00004728-199107000-00010]

S- Editor: Yang RC L- Editor: Filipodia E- Editor: Li RF

Evaluation of the IL-2/IL-2R system in patients with liver cirrhosis or carcinoma

Xiao-Zhong Wang, Gu-Zhen Lin

Xiao-Zhong Wang, Gu-Zhen Lin, Department of Gastroenterology; Union Hospital of Fujian Medical University, Fuzhou 350001, Fujian Province, China

Author contributions: All authors contributed equally to the work.

Supported by the Fujian Provincial Health Bureau 91A047.

Original title: *China National Journal of New Gastroenterology* (1995-1997) renamed *World Journal of Gastroenterology* (1998-).

Correspondence to: Dr. Xiao-Zhong Wang, Department of Gastroenterology, Union Hospital of Fujian Medical University, Fuzhou 350001, Fujian Province, China
Telephone: +86-591-3357896-8482

Received: July 27, 1996
Revised: August 3, 1996
Accepted: August 21, 1996
Published online: September 15, 1996

Abstract

AIM: To evaluate the interleukin-2/interleukin-2 receptor (IL-2/IL-2R) system in patients with liver cirrhosis or carcinoma, and compare the immune function in those patients. The clinical significance of our results is also discussed.

METHODS: Fifty patients with liver cirrhosis (LC), 50 patients with hepatocellular carcinoma (HCC), and 30 normal control subjects were studied. Cellular expression of the interleukin-2 receptor (mIL-2R) was examined by immunofluorescence, and the serum levels of IL-2 and soluble interleukin-2 receptor (sIL-2R) were measured by ELISA.

RESULTS: The levels of IL-2 and mIL-2R expression in carcinoma patients were significantly lower than those in both patients with cirrhosis ($P < 0.01$) and control subjects ($P < 0.01$). The serum levels of IL-2 and the expression of mIL-2R in patients with cirrhosis were also lower than those in normal control subjects ($P < 0.05$). The serum levels of sIL-2R in carcinoma patients were significantly higher than those in both cirrhosis patients ($P < 0.05$) and control subjects ($P < 0.01$), and the sIL-2R levels in cirrhosis patients were higher than those in control subjects ($P < 0.05$).

CONCLUSION: Patients with liver cirrhosis or carcinoma both have decreased immune function; however, this decrease is more pronounced in carcinoma patients. Such similarities in immune disturbances may be an important factor affecting the development of carcinoma in a cirrhotic liver.

Key words: Liver cirrhosis; Liver neoplasms; Interleukin-2/analysis; Receptors interleukin/analysis

© The Author(s) 1996. Published by Baishideng Publishing Group Inc. All rights reserved.

Wang XZ, Lin GZ. Evaluation of the IL-2/IL-2R system in patients with liver cirrhosis or carcinoma. *World J Gastroenterol* 1996; 2(3): 171-172 Available from: URL: <http://www.wjgnet.com/1007-9327/full/v2/i3/171.htm> DOI: <http://dx.doi.org/10.3748/wjg.v2.i3.171>

INTRODUCTION

Both liver cirrhosis (LC) and hepatocellular carcinoma (HCC) are common diseases in China. HCC and LC are closely associated with each other in the majority of carcinoma patients (60%-80%), and 10%-30% of patients with cirrhosis will eventually develop HCC. While the various etiologies of HCC are complicated, LC appears to be a major risk factor for the eventual development of carcinoma. In the present study, we determined the serum levels of interleukin-2 (IL-2) and soluble interleukin-2 receptor (sIL-2R), as well as the expression of mIL-2R in patients with liver cirrhosis or carcinoma. The clinical significance of our findings is also discussed.

MATERIALS AND METHODS

Patients and controls

This study enrolled 50 patients with LC, 50 patients with HCC, and 30 normal control subjects. HCC and LC had been diagnosed either clinically or based on a histologic evaluation. None of the patients were taking any medication or had a history of immunotherapy. All of the LC cases were Child's grade B or C.

Assays for IL-2 and sIL-2R

Serum levels of IL-2 and sIL-2R were measured using commercially available ELISA kits. Both assays were performed on the same day and in a single batch to avoid variability. The assay methods are described in detail in a previous publication^[1]. Briefly, quadruplicate samples of peripheral blood mononuclear cells (PBMCs) which had been separated by density gradient centrifugation were cultured with phytohemagglutinin (PHA) for 72 h. Following culture, the cells were washed, placed in microtubes, and then incubated with fluorescein-labelled anti-IL-2R monoclonal antibodies. After incubation, the cells were washed 3 times with Hank's balanced salt solution, and then gently resuspended with a Pasteur pipette. One drop of liquid with cells was examined using a fluorescence microscope equipped with a barrier filter. The number of lymphocytes that displayed immunofluorescence staining for IL-2R was recorded, and expressed as a percentage of total cultured PBMCs.

Statistical analysis

The data were analyzed using the *t*-test, and results are expressed as the mean \pm SD

RESULTS

The serum levels of IL-2 and sIL-2R and the levels of mIL-2R

Table 1 Serum levels of IL-2 and sIL-2R, and expression of mIL-2R in patients with liver cirrhosis or hepatocellular carcinoma

	IL-2 (μ/mL)	sIL-2R (μ/mL)	mIL-2R (%)
LC	80.1 ± 15.2	264.2 ± 51.3	39.9 ± 7.2
HCC	42.5 ± 11.7	340.7 ± 63.9	33.1 ± 6.4

expression are shown in Table 1. The results showed that IL-2 levels and mIL-2R expression were both significantly lower in patients with HCC, when compared to those parameters in patients with LC ($P < 0.01$) as well as control subjects ($P < 0.01$). Furthermore, IL-2 levels and mIL-2R expression in LC patients were also lower when compared with those parameters in normal subjects (both P -values < 0.05). In contrast, the serum levels of sIL-2R in HCC patients were significantly higher when compared with those in both LC patients, ($P < 0.05$) and control subjects ($P < 0.01$), and the serum levels of sIL-2R in LC patients were also higher than those in control subjects ($P < 0.05$).

DISCUSSION

IL-2 secreted by activated T-lymphocytes interacts with specific membrane receptors (mIL-2R) to upregulate immune reactions in an autocrine manner^[2]. In addition to mIL-2R, both *in vivo* and *in vitro* studies have identified a soluble form of IL-2R (sIL-2R) in the supernatant fractions of activated mononuclear cells^[3]. This molecule apparently represents the Tac chain of the heterodimeric high affinity IL-2R complex found on the surface of activated T-lymphocytes. sIL-2R displays a lower binding affinity for supernatant IL-2 than it does for mIL-2R. The release of sIL-2R from activated T-lymphocytes may occur due to either proteolysis of mIL-2R or as the result of an alternative mRNA-related process^[4].

The decreased IL-2 levels and higher sIL-2R levels in the PBMCs of some individuals may result from several types of liver diseases, including acute and chronic viral hepatitis^[5]. High levels of sIL-2R in cases of acute or chronic HBV infection appear to be

directly related to the activity of liver diseases, and therefore may reflect the activation of effector cells which help kill the infected hepatocytes. One possible explanation for the reduced IL-2 activity might be that it reflects the compartmentalization of active cells in the liver, and the down-regulated or inhibited production of soluble factors by PBMCs. Similar to hepatitis patients, patients with LC or HCC also show reduced IL-2 activity and mIL-2R expression, accompanied by higher serum levels of sIL-2R. When considering the etiologic and morphologic characteristics of cirrhosis, LC appears to be the most important risk factor for HCC, and HBsAg positivity is one of several factors that increase the risk for HCC in patients with cirrhosis. Our results suggest that patients with LC or HCC have a similar type of immune dysfunction; however, HCC patients have a higher degree of the dysfunction. This similarity in immune disturbances may be an important factor affecting the progression of liver cirrhosis to liver cancer. Our results also indicate that an evaluation of the IL-2/IL-2R system can provide reliable information when selecting an immunotherapy or evaluating the effects of immunotherapy.

REFERENCES

1 **Lai KN**, Ho S, Leung JC, Tsao SY. Soluble interleukin-2 receptors in patients with nasopharyngeal carcinoma. *Cancer* 1991; **67**: 2180-2185 [PMID: 1848475 DOI: 10.1002/1097-0142(19910415)67:8<2180::AID-CNCR-2820670829>3.0.CO;2-T]

2 **Robb RJ**, Greene WC, Rusk CM. Low and high affinity cellular receptors for interleukin 2. Implications for the level of Tac antigen. *J Exp Med* 1984; **160**: 1126-1146 [PMID: 6090574 DOI: 10.1084/jem.160.4.1126]

3 **Rubin LA**, Kurman CC, Fritz ME, Biddison WE, Boutin B, Yarchoan R, Nelson DL. Soluble interleukin 2 receptors are released from activated human lymphoid cells in vitro. *J Immunol* 1985; **135**: 3172-3177 [PMID: 3930598]

4 **Robb RJ**, Kutny RM. Structure-function relationships for the IL 2-receptor system. IV. Analysis of the sequence and ligand-binding properties of soluble Tac protein. *J Immunol* 1987; **139**: 855-862 [PMID: 3036946]

5 **Alberti A**, Chemello L, Fattovich G, Pontisso P, Semenzato G, Colletta C, Vianante F, Pizzolo G. Serum levels of soluble interleukin-2 receptors in acute and chronic viral hepatitis. *Dig Dis Sci* 1989; **34**: 1559-1563 [PMID: 2507263 DOI: 10.1007/BF01537110]

S- Editor: Cao LB L- Editor: Filipodia E- Editor: Li RF

Assessment of natural and interleukin-2-induced production of interferon-gamma in patients with liver diseases

Shi-Bao Chen, Xiao-Hui Miao, Ping Du, Qing-Xuan Wu

Shi-Bao Chen, Xiao-Hui Miao, Department of Gastroenterology, Changzheng Hospital, Second Military Medical University, Shanghai 200003, China

Ping Du, Qing-Xuan Wu, Department of Microbiology, Second Military Medical University, Shanghai 200433, China

Shi-Bao Chen, Professor of Internal Medicine, advisor of postgraduate for doctorate, having 84 papers published

Author contributions: All authors contributed equally to the work.

Supported by National Science Foundation of China. No.89138970378.

Original title: *China National Journal of New Gastroenterology* (1995-1997) renamed *World Journal of Gastroenterology* (1998-).

Correspondence to: Dr. Shi-Bao Chen, Professor, Department of Gastroenterology, Changzheng Hospital, Second Military Medical University, Shanghai 200003, China
Telephone: +86-21-63275997-361

Received: July 8, 1996
Revised: August 9, 1996
Accepted: August 24, 1996
Published online: September 15, 1996

Abstract

AIM: To determine whether the production of lower interferon gamma (IFN λ) by lymphocytes in patients with liver diseases is due to defects of the lymphocytes themselves or to other cofactors, such as interleukin-2 (IL-2).

METHODS: Peripheral blood mononuclear cells (PBMCs) from patients with various liver diseases were cultured with or without phytohemagglutinin (PHA) and IL-2. The cells were harvested and counted, and the supernatants were tested for IFN λ by a sensitive and quantitative ABC-enzyme-linked immunosorbent assay (ELISA).

RESULTS: IFN λ was not found in serum samples from patients or normal individuals. However, IFN λ was detectable in supernatants of non-induced and induced PBMCs by ABC-ELISA. In non-induced PBMCs (group 1), the content of IFN λ in supernatants from control, chronic active hepatitis (CAH), chronic persistent hepatitis (CPH), and hepatocellular carcinoma (HCC) was 8.72/L, 5.03/L, 6.02/L, and 4.91/L, respectively. The production of IFN λ in liver disease was significantly decreased compared to control. In PBMCs stimulated with PHA (group 2), the content of IFN λ was 22.71/L, 17.12/L, 14.54/L, and 17.63/L, respectively. In PBMCs induced by IL-2 (group 3), the amount of IFN λ in supernatant from control (60.67/L) was much larger than those from CAH (21.70/L), CPH (24.00/L), and HCC (19.15/L) ($p < 0.01$). When comparing the amount of IFN λ in group 3 with that in group 1, we found that IFN λ production was enhanced by nearly 4-folds in liver diseases and by over 7-fold in control. In

contrast, the number of PBMCs, whether from liver diseases or from control, was increased by only approximately 3-fold.

CONCLUSION: The decreased production of IFN λ in liver diseases, including HCC, is mainly due to endogenous defects of lymphocytes but may also involve a decrease in stimulating cofactors, such as IL-2.

Key words: Liver disease; Interleukin-2; Interferon type II

© The Author(s) 1996. Published by Baishideng Publishing Group Inc. All rights reserved.

Chen SB, Miao XH, Du P, Wu QX. Assessment of natural and interleukin-2-induced production of interferon-gamma in patients with liver diseases. *World J Gastroenterol* 1996; 2(3): 173-175 Available from: URL: <http://www.wjgnet.com/1007-9327/full/v2/i3/173.htm> DOI: <http://dx.doi.org/10.3748/wjg.v2.i3.173>

INTRODUCTION

Abnormal immune function is an important mechanism of hepatitis B virus (HBV) infection-related liver diseases and hepatocellular carcinoma (HCC)^[1]. It was previously shown that disruption of cellular-mediated immune function, including defects in the production of lymphokines, is involved in HBV infection and HCC^[2,3]. Interferon-gamma (IFN γ), one of the most important cytokines with various activities, plays a key role in immunoregulation. It has been suggested that IFN γ production by lymphocytes is correlated with the cause, development, and prognosis of chronic liver diseases^[4]. However, it is not clear whether the decrease of IFN γ production is caused by defective secretion of IFN γ producing lymphocytes, by decreased levels of inducing cofactors, such as interleukin-2 (IL-2), or both. In the present study, we measured IL-2-induced IFN γ production in peripheral blood mononuclear cells (PBMCs) in order to evaluate the relationship between IFN γ production and liver diseases.

MATERIALS AND METHODS

Subjects

Twenty-one patients with chronic HBV infection (19 males and two females, 15-63 years old), including 12 cases of chronic persistent hepatitis (CPH) (three cases with cirrhosis) and nine cases of chronic active hepatitis (CAH), and nine patients with HCC (eight males and one female, 15-57 years old) were studied. The diagnoses were confirmed by clinical characteristics, laboratory analyses, and imaging examinations. Ten healthy blood donors served as controls.

Preparation of PBMCs

Five milliliters of venous blood were collected and heparinized. PBMCs were isolated from whole heparinized blood by centrifugation over Ficoll, washed three times with Roswell Park Memorial Institute

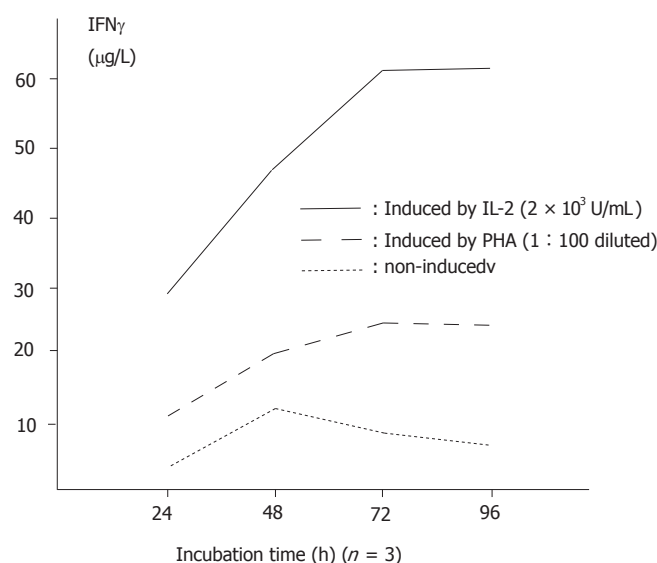


Figure 1 Interferon gamma (IFN γ) production by normal peripheral blood mononuclear cells (PBMCs) over time.

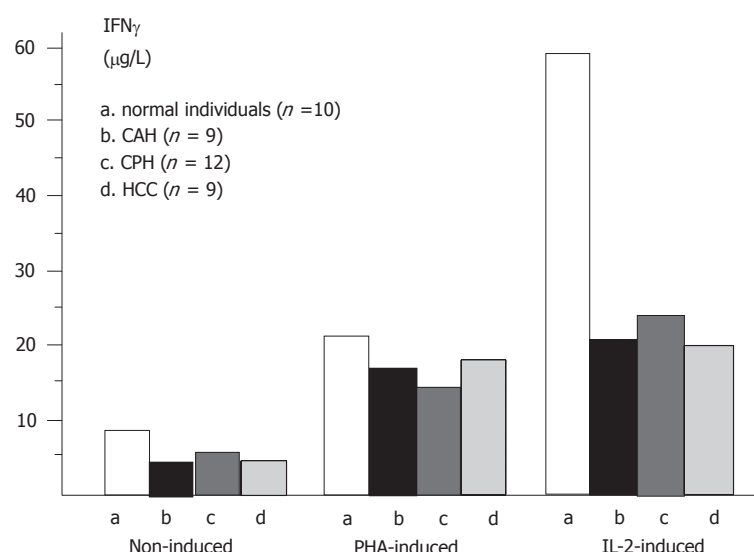


Figure 3 IFN γ production by PBMCs from patients with liver diseases and from normal individuals.

(RPMI)-1640 medium (Gibco, Carlsbad, CA, United States), and then suspended at 2×10^6 cells/mL in RPMI-1640 medium containing 10% fetal calf serum. The viability of cells was higher than 95% by the trypan blue exclusive test.

Induction of IFN γ from PBMCs

Each PBMC sample was placed in a 96-well plate (2×10^5 cells/100 μ L per well) in three groups. For each group, double wells were designed. In group 1, 100 μ L of medium was added and cultured without any inducers. In group 2, 100 μ L of 1:100 diluted phytohemagglutinin (PHA) (type M, Sigma, St Louis, MO, United States) was added. In group 3, 100 μ L of IL-2 (gift from the Department of Microbiology, SMMC) with the activity of 2×10^3 U/mL was added. The cells were incubated at 37 °C in 5% CO $_2$ for 72 h, and the culture supernatants were removed and tested for IFN γ . The cells were counted under a light microscope.

Detection of IFN γ

IFN γ in supernatants was detected by a quantitative ABC-enzyme linked immune sorbent assay (ELISA), as we previously described^[5].

Statistical analysis

Data were analyzed by Student's *t* test and *F* test.

RESULTS

IFN γ in serum samples

IFN γ was not detected in the sera of 21 patients with chronic HBV infection, the nine patients with HCC, or any of the controls.

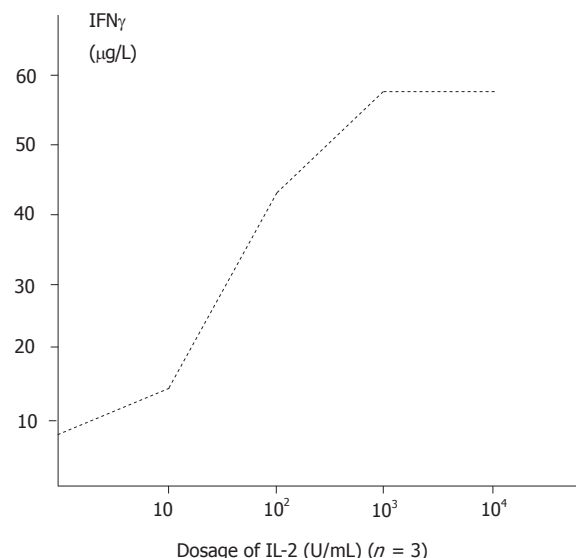


Figure 2 IFN γ production by normal PBMCs induced by various dosages of interleukin (IL)-2.

IFN γ production by PBMCs in normal individuals

The amount of IFN γ produced in non-induced supernatants was 8.72 ± 0.65 μ g/L ($n = 10$). Stimulation with PHA and IL-2 with increasing time durations and dosages significantly enhanced the production of IFN γ ($P < 0.01$). The relationships between course and effectiveness and between dosage and effectiveness are indicated in Figures 1 and 2.

Comparison of IFN γ production in various liver diseases

IFN γ production in either PHA-induced or non-induced PBMCs in liver diseases was significantly lower than that in normal individuals ($P < 0.01$). Although the production of IFN γ was the lowest in HCC patients, there was no significant difference in IFN γ production among various liver diseases ($P > 0.05$). The level of IFN γ was increased in the supernatants of IL-2 induced PBMCs from patients with CPH, CAH, and HCC, respectively, compared with non-induced PBMCs (Figure 3).

The number of IL-2 induced PBMCs

The number of IL-2 induced PBMCs was increased approximately 3 times compared to non-induced PBMCs in liver diseases and in control. When comparing the increase of IFN γ production (by 6.9 times in control, 4.3 times in CAH, 4.0 times in CPH and 3.9 times in HCC) with the increase in the number of PBMCs, we found that there was a difference between them.

DISCUSSION

Recently, the importance of cytokines in immunoregulation has been recognized, and the correlation between cytokines and body disorders is continuing to be elucidated^[6]. The dysfunction of cellular immunity is an important mechanism of HBV infection-related chronic liver diseases and is associated with persistent HBV infection^[7].

Some new therapies for HBV infection, such as the application of IFNs and lymphokine activated killer (LAK) cells, are partially effective for the clearance of HBV^[8]. More recently, cytokine gene transfer therapy for HBV infection and HCC has also been reported^[9]. All these therapies are based on findings that the production of cytokines is decreased in hepatitis B and that the replacement of cytokines is an effective way to maintain balance of the immune system. In this study, we found that IFN γ production by non-induced and lymphoblastized PBMCs from patients with various chronic liver diseases and HCC was significantly lower than that in normal individuals, with the lowest in patients with cirrhosis. These findings suggest that IFN γ producing cells, *i.e.*, T helper and natural killer (NK) cells, may be defective in the production of IFN γ . Among the factors that stimulate the production of IFN γ , IL-2 is the most important^[10]. In this study, when PBMCs were cultured with IL-2, the secretion of IFN γ was enhanced 3.9 (in HCC) to 6.8

(in control) fold, whereas the number of PBMCs was increased by only 3 times, suggesting that the enhancement of IFN γ production was related not only to the increase in PBMC number but also to the enhancement in the IFN γ producing ability of PBMCs. It was reported that LAK cell therapy was shortly effective for suppression of HBV duplication. These authors suggested that the increase in cytokine production of LAK cells was involved in the anti-HBV mechanism^[7]. Our results are consistent with these findings.

However, the inducing effects of IL-2 on IFN γ production are not the same in patients with liver diseases and normal controls. In patients with liver diseases, the amount of IFN γ produced by IL-2 induction in PBMCs was nearly 7 times greater than that in non-induced PBMCs; whereas in normal controls, the former is about 4 times greater than the latter. We conclude that the decreased production of IFN γ in patients with liver diseases is mainly due to endogenous defects of lymphocytes but may also be due to a decrease in some stimulating cofactors.

Notably, we failed to detect IFN γ directly from the sera of patients or normal individuals by a sensitive and quantitative ABC-ELISA established in our laboratory. Some other authors reported similar results by CPE. It may be concluded that the level of IFN γ secreted in serum is too small to be detected by the present methods. Moreover, the amount of IFN γ in serum may be influenced by many factors, such as the half-life of IFN γ , liver and renal function, and the time of collecting blood. Therefore, we recommend for future studies on cytokines, including IFN γ , the preparation of lymphocytes or PBMCs rather than serum.

REFERENCES

- 1 **Peters M**, Davis GL, Dooley TS. The interferon system in acute and chronic viral hepatitis. In: Popper H, Schaffner F, eds. Progress in liver disease. Vol . New York: Grune & Stratton 1986: 453-467
- 2 **Kato Y**, Nakagawa H, Kobayashi K, Hattori N, Hatano K. Interferon production by peripheral lymphocytes in HBsAg-positive liver diseases. *Hepatology* 1982; **2**: 789-790 [PMID: 6292067 DOI: 10.1002/hep.1840020607]
- 3 **Saibara T**, Maeda T, Miyazaki M, Onishi S, Yamamoto Y. Assessment of lymphokine-activated killer activity and gamma-interferon production in patients with small hepatocellular carcinomas. *Hepatology* 1993; **17**: 781-787 [PMID: 7684018 DOI: 10.1002/hep.1840170506]
- 4 **Fuji A**, Kakumu S, Ohtani Y, Murase K, Hirofuji H, Tahara H. Interferon-gamma production by peripheral blood mononuclear cells of patients with chronic liver disease. *Hepatology* 1987; **7**: 577-581 [PMID: 3106184 DOI: 10.1002/hep.1840070327]
- 5 **Miao XH**, Pan W, Wu QX, Du P, Chen SB, Qi ZT. An ABC-ELISA to detect human natural and recombinant interferon-gamma. *Zhonghua Weishengwuxue He Mianyixue Zazhi* 1994; **14**: 58-61
- 6 **Peters M**, Vierling J, Gershwin ME, Milich D, Chisari FV, Hoofnagle JH. Immunology and the liver. *Hepatology* 1991; **13**: 977-994 [PMID: 2030002 DOI: 10.1002/hep.1840130529]
- 7 **Dienstag JL**. Immunologic mechanisms in chronic viral hepatitis. In: Vyas GN, Dienstag JL, Hoofnagle JH, eds. Viral hepatitis and liver disease. New York, Grune & Stratton 1984: 135-166
- 8 **Bissett J**, Eisenberg M, Gregory P, Robinson WS, Merigan TC. Recombinant fibroblast interferon and immune interferon for treating chronic hepatitis B virus infection: patients' tolerance and the effect on viral markers. *J Infect Dis* 1988; **157**: 1076-1080 [PMID: 3129521 DOI: 10.1093/infdis/157.5.1076]
- 9 **Ledley FD**. Hepatic gene therapy: present and future. *Hepatology* 1993; **18**: 1263-1273 [PMID: 8225234 DOI: 10.1002/hep.1840180536]
- 10 **Farrar WL**, Johnson HM, Farrar JJ. Regulation of the production of immune interferon and cytotoxic T lymphocytes by interleukin 2. *J Immunol* 1981; **126**: 1120-1125 [PMID: 6161959]

S- Editor: Tao T L- Editor: Filipodia E- Editor: Li RF

Effects of acute hepatic damage on natriuresis and water excretion after acute normal saline loading in rats

Hong-Qun Liu, Chao-Ying Ren, Lian-Sun Jia, Xi-Xian Yao, Xi-Ling Ren

Hong-Qun Liu, Xi-Xian Yao, Department of Medicine, Second Affiliated Hospital, Hebei Medical University, Shijiazhuang 050000, Hebei Province, China

Lian-Sun Jia, Xi-Ling Ren, Department, Fourth Affiliated Hospital of Hebei Medical University, Shijiazhuang 050000, Hebei Province, China

Chao-Ying Ren, Department of Medicine, Hebei Provincial People's Hospital, Shijiazhuang 050000, Hebei Province, China

Hong-Qun Liu, Professor of Medicine, has 30 papers published, participated in six books

Author contributions: All authors contributed equally to the work.

Original title: *China National Journal of New Gastroenterology* (1995-1997) renamed *World Journal of Gastroenterology* (1998-).

Correspondence to: Dr. Hong-Qun Liu, Professor, Department of Medicine, Second Affiliated Hospital, Hebei Medical University, Shijiazhuang 050000, Hebei Province, China

Received: February 2, 1996

Revised: July 25, 1996

Accepted: August 14, 1996

Published online: September 15, 1996

Abstract

AIM: To investigate the relationship between liver functional impairment and sodium and water retention.

METHODS: An animal model of acute liver damage model was established by administering carbon tetrachloride (CCl₄) to male Sprague-Dawley rats. Twenty-four and 48 h after CCl₄ administration, the excretion of acute sodium and water load was measured. In controls, the excretion of acute sodium and water load was measured 24 h after administration of normal saline. In addition, the concentration of plasma caffeine was analyzed using high pressure liquid chromatography (HPLC). The half-life of plasma caffeine (Caf t_{1/2}) served as a quantitative index of hepatic function. Plasma alanine aminotransferase (ALT) was measured using the Reitman method. Hepatic tissue sections from the same site were used for water content measurement and pathological observation. The serum and urinary sodium levels were measured with flame photometry.

RESULTS: Twenty-four hours after CCl₄ administration, plasma ALT level ($n = 6$, $37.5 \pm 12.6 \rightarrow 189.4 \pm 34.4$ U, $P < 0.01$) and water content of hepatic tissue ($n = 6$, $70.0\% \pm 0.11\% \rightarrow 73.0\% \pm 1.0\%$, $P < 0.01$) were significantly increased, and Caf t_{1/2} was prolonged significantly ($94.9 \pm 18.9 \rightarrow 326.4 \pm 85.8$ min, $P < 0.01$) compared to saline treated control. Renal function, as assessed by excretion of acute salt and water load, was significantly decreased ($n = 6$, Na⁺: $92.4\% \pm 14.1\% \rightarrow 50.1\% \pm 13.1\%$, $P < 0.01$; H₂O: $86.3\% \pm 14.3\% \rightarrow 42.1\% \pm 8.8\%$, $P < 0.01$). The above indices had recovered

somewhat 48 h later but were still markedly different from those of control. In addition, the relationships between Caf t_{1/2} and ALT ($r = 0.752$, $P < 0.01$) and between Caf t_{1/2} and excretory rate of sodium ($r = 0.634$, $P < 0.05$) and water remained significant ($r = 0.612$, $P < 0.01$) at 48 h.

CONCLUSION: Caf t_{1/2} is a good index to assess the degree of hepatic damage. Hepatic dysfunction may contribute to impairments in renal excretion following acute sodium and water load.

Key words: Liver disease; Water-electrolyte imbalance; Kidney/ Metabolism

© The Author(s) 1996. Published by Baishideng Publishing Group Inc. All rights reserved.

Liu HQ, Ren CY, Jia LS, Yao XX, Ren XL. Effects of acute hepatic damage on natriuresis and water excretion after acute normal saline loading in rats. *World J Gastroenterol* 1996; 2(3): 176-178 Available from: URL: <http://www.wjgnet.com/1007-9327/full/v2/i3/176.htm> DOI: <http://dx.doi.org/10.3748/wjg.v2.i3.176>

INTRODUCTION

Most data to date have shown that there is a significant relationship between hepatic functional damage and sodium retention, but it remains unclear whether acute liver dysfunction results in sodium and water retention. To understand further the relationship between liver function per se and sodium retention, we investigated renal excretion following acute salt and water load in a rat model of acute hepatic damage.

MATERIALS AND METHODS

Acute hepatic damage model

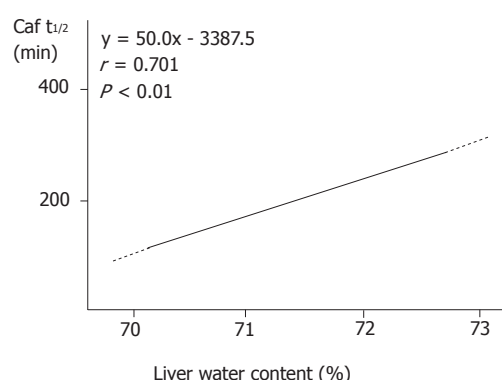
Eighteen male Sprague Dawley rats weighing 270-320 g were divided into three groups: control ($n = 6$), experimental group 1 ($n = 6$), and experimental group 2 ($n = 6$). Reduced salt chow (12.74 mmol/kg) and re-distilled water were available *ad libitum*. Three days later, carbon tetrachloride (CCl₄) (0.02 mL/100 g body wt) was administered intraperitoneally to experimental groups, and normal saline (0.02 mL/100 g body wt) was administered to the control group. Acute normal saline loading was conducted in experimental groups 2 and 3 24 and 48 h after CCl₄ administration, respectively, and 24 h after saline administration in the control.

Acute sodium and water loading experiment

Twelve hours after removing water and food, the animals received under urethane anesthesia normal saline (4 mL/100 g body wt) through the femoral vein. Urine was collected for 4 h and stored in an Eppendorf tube at -20 °C until analysis. One percent caffeine, 0.1 mL (1 mg/rat), was then administered to the femoral vein for

Table 1 Lesion indices of hepatic tissue and liver dysfunction after CCl₄ administration ($n = 6$, $\bar{x} \pm s$)

Group	Water content (%)	ALT (Reitman U)	Caf $t_{1/2}$ (min)
Control	70.1 \pm 1.1	37.5 \pm 12.6	94.8 \pm 18.9
CCl ₄ 24 h	73.0 \pm 1.0 ^b	189.4 \pm 34.4 ^b	326.4 \pm 85.8 ^b
CCl ₄ 48 h	72.0 \pm 0.8 ^b	126.1 \pm 59.1 ^a	169.5 \pm 37.9 ^b

^a $P < 0.05$; ^b $P < 0.01$ vs control. Liver water content (%)**Figure 1** Relationship between liver water content and liver function

3 h. Four milliliters of blood were taken from the inferior vena cava and anti-agglutinated with heparin. The plasma was separated to measure caffeine, ALT, and sodium. At this time, liver tissues were taken for pathologic examination and water content calculation.

Examination method

The plasma caffeine concentration was analyzed with high pressure liquid chromatography (HPLC). Plasma ALT was examined with Reitman method, and serum and urinary sodium levels were measured with flame photometry.

Calculation and statistics

The Caf $t_{1/2}$ was calculated using the following formula:

$$\text{Caf } t_{1/2} = \ln 2 \times (t / \ln (D / (\text{adv} \times \text{body wt}) \ln C_{\text{caf}}))$$

where D = the dosage of caffeine (1 mg in this experiment); t = time from caffeine injection to blood collection (180 min); C_{caf} = caffeine concentration when blood was taken (mg/L); adv = apparent distribution volume (0.64 mL/kg). Data for each parameter were compared between two groups with a t test and among the three groups with an F test. Regression analysis was used to correlate Caf $t_{1/2}$ and water content in hepatic tissue, sodium excretory rate, water excretory rate, and plasma ALT. P values less than 0.05 were considered to be statistically significant.

RESULTS

The changes of hepatic tissue

In the control group, the hepatic cells were arranged regularly, and the plates radiated from the central vein to the portal canals. Twenty four hours after CCl₄ administration, the hepatic tissue exhibited extensive necrosis, hepatocyte swelling, and vacuolization under light microscopy. In the 48 h group, hepatocyte necrosis, swelling, and vacuolization were still clearly seen but to a lesser extent than the 24 h group. Consistent with the histological changes in the hepatic tissue, water content was significantly higher in both experimental groups than the control group.

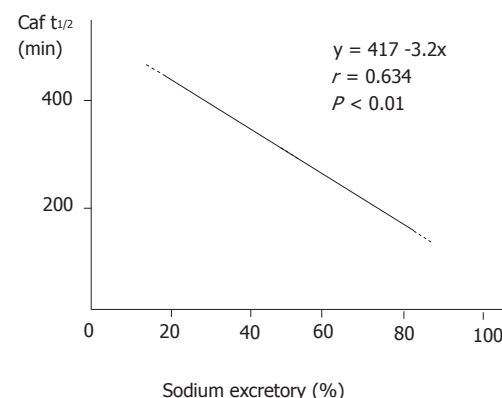
Liver function decline

Following structural damage to the liver tissue, the capability of the liver to metabolize caffeine was impaired. The Caf $t_{1/2}$ was prolonged significantly in the 24 h and 48 h groups compared to that in the control group (Table 1). Caf $t_{1/2}$ and water content in hepatic tissue were significantly correlated ($r = 0.701$, $P < 0.01$, Figure 1).

Consistent with our findings on water content in hepatic tissue and Caf $t_{1/2}$, plasma levels of ALT rose significantly in both experimental groups. There was a significant positive correlation between ALT levels and Caf $t_{1/2}$ ($r = 0.753$, $P < 0.01$).

Table 2 Serum Na⁺ and water salt excretory rate ($n = 6$, $\bar{x} \pm s$)

Group	serum Na ⁺ (mmol/L)	Na ⁺ excretory rate (%)	H ₂ O excretory rate (%)
Control	145.7 \pm 5.7	92.4 \pm 14.1	86.3 \pm 14.3
CCl ₄ 24 h	143.0 \pm 5.6	50.1 \pm 13.1 ^b	42.1 \pm 8.8 ^b
CCl ₄ 48 h	139.8 \pm 2.1	64.3 \pm 14.1 ^a	56.6 \pm 12.4 ^a

^a $P < 0.05$, ^b $P < 0.01$ vs control**Figure 2** Relationship between excretory rate of salt load and liver function

Relationship between liver dysfunction and sodium and water excretion

Following the impairment in liver function, the capability of the kidney to excrete acute water and sodium load declined significantly. Although this decline recovered somewhat in the 48 h group, it remained significantly different from that of the control (Table 2). The relationship between Caf $t_{1/2}$ and renal excretory rate of sodium (Figure 2) and water was significantly correlated ($r = -0.612$, $P < 0.01$). There was no significant difference among the three groups in serum sodium level ($F = 2.34$, $P > 0.05$, Table 2).

DISCUSSION

Recently, different models of hepatic damage^[1-3] have demonstrated that the decline in liver function is an important cause of salt and water retention. Caffeine is metabolized by hepatic cytochrome P-450, and the ability of the body to clear caffeine reflects metabolic function of the liver. Jost *et al*^[4] showed that the clearance rate of plasma caffeine is in significant agreement with the aminopyrine breath test ($r = 0.80$, $P < 0.01$), prothrombin time ($r = 0.59$, $P < 0.01$), indo cyanogreen test ($r = 0.51$, $P < 0.01$), and galactose clearance rate ($r = 0.46$, $P < 0.01$). Therefore, use of Caf $t_{1/2}$ to quantitate liver function is reliable; HPLC is an efficient and stable means to measure caffeine. Our results found that 24 and 48 h after CCl₄ administration, Caf $t_{1/2}$ was prolonged significantly. Changes in ALT levels and hepatic tissue water content paralleled Caf $t_{1/2}$. There was a significant relationship between Caf $t_{1/2}$ and ALT and between Caf $t_{1/2}$ and water content of hepatic tissue. These results illustrate that the decrease in liver function is linked to the degree of hepatic tissue damage. Thus, Caf $t_{1/2}$ may be considered a sensitive index that reflects the degree of acute hepatic tissue damage.

Importantly, following pathological damage of the liver, the plasma Caf $t_{1/2}$ was prolonged significantly and the ability of the kidney to excrete acute water and sodium load was declined significantly. Caf $t_{1/2}$ and renal excretory rate of sodium and water were negatively correlated. These results are consistent with the report by Wong *et al*^[5] and identify hepatic tissue damage and liver function decline as important contributors to salt and water retention.

REFERENCES

- Liu HQ, Liang KH, Tang WX, Zhang WY. Renal nerves effect on early sodium retention in bile duct ligated diseases in rats. *Zhonghua Xiaohua Zazhi* 1995; **15**: 15-17
- Liu HQ, Liang KH, Tang WX, Zhang WY. Impairment of hepatic function, increment of plasma atrial natriuretic peptide and sodium retention in experimental cirrhosis. *Tongji Yike Daxue Xuebao* 1993; **23**: 169-171

- 3 **Liu HQ**, Jia LS, Liang KH, Tang WX, Zhang WY. The changes of RAAS and sodium metabolism in the process of hepatic functional decline induced with 70% hepatectomy in rats. *Zhongguo Bingli Shengli Zazhi* 1996; **12**: 309-302
- 4 **Jost G**, Wahlländer A, von Mandach U, Preisig R. Overnight salivary caffeine clearance: a liver function test suitable for routine use. *Hepatology* 1987; **7**: 338-344 [PMID: 3557314 DOI: 10.1002/hep.1840070221]
- 5 **Wong F**, Massie D, Hsu P, Dudley F. Renal response to a saline load in well-compensated alcoholic cirrhosis. *Hepatology* 1994; **20**: 873-881 [PMID: 7927228 DOI: 10.1002/hep.1840200415]

S- Editor: Yang RC **L- Editor:** Filipodia **E- Editor:** Li RF

Effect of interferon in combination with ribavirin on the plus and minus strands of HCV RNA in patients with chronic hepatitis C

Yong-Wen He, Wei Liu, Ling-Lan Ren, Kai-Jin Xiong, Duan-De Luo

Yong-Wen He, Wei Liu, Ling-Lan Ren, Kai-Jin Xiong, Duan-De Luo, Department of Infectious Diseases, Union Hospital, Tong Ji Medical University, Wuhan 430022, Hubei Province, China

Yong-Wen He, Professor of Internal Medicine, having 23 papers published.

Author contributions: All authors contributed equally to the work.

Reported at the 5th National Congress of Infectious Diseases and Parasitosis, Beijing, China, May 1995.

Supported by the Science Foundation of the Education Committee of China (1990) 360.

Original title: *China National Journal of New Gastroenterology* (1995-1997) renamed *World Journal of Gastroenterology* (1998-).

Correspondence to: Dr. Yong-Wen He, Professor, Department of Infectious Diseases, Union Hospital, Tong Ji Medical University, Wuhan 430022, Hubei Province, China
Telephone: +86-27-5807711-512

Received: July 25, 1996
Revised: August 5, 1996
Accepted: August 24, 1996
Published online: September 15, 1996

Abstract

AIM: To probe the effect of interferon in combination with ribavirin on the plus and minus strands of hepatitis C virus RNA (HCV RNA).

METHODS: Twenty-three cases diagnosed as chronic hepatitis C (CHC), according to positive HCV RNA/anti-HCV, fluctuating levels of aminotransferase activities (< 1 year), and absence of other hepatitis virus marker, were studied. Among them, 13 patients received combined antiviral therapy (subcutaneous injection of 3 MU of interferon- α three times per week for 3 months and intravenous drip of 1 g of ribavirin per day during the first month of treatment with interferon), and 10 patients received single interferon therapy, as described above, as control. The plus and minus strands of HCV RNA in sera and peripheral blood mononuclear cells (PBMCs) of these patients were tested by nested reverse transcription-polymerase chain reaction (nested RT-PCR).

RESULTS: At the end of therapy, the abnormal alanine aminotransferase (ALT) levels decreased to normal range in nine (69.23%) cases in the combined antiviral group. Of them, five (55.56%) experienced post-therapy relapse, and four (44.44%) were complete responders. In the interferon group, ALT decreased to normal in six (60%) cases, of which, four (66.67%) had post-therapy relapse and two (33.33%) were complete responders. The differences between the two groups were not significant ($P < 0.05$). At the end of therapy, the positive rate of the plus strand in sera decreased from 92.30% to 38.46% ($P < 0.05$) and that of the minus strand in PBMCs

from 76.92% to 38.46% ($P < 0.05$) in the combined antiviral group. In the interferon only group, the former decreased from 100% to 50% ($P < 0.05$) and the latter, from 90% to 40% ($P < 0.05$). Again, no significant differences were found between groups ($P < 0.05$). Relapse occurred in patients whose plus strand HCV RNA in PBMCs remained after treatment.

CONCLUSION: Ribavirin did not enhance the antiviral effect of interferon when the plus and minus strands of HCV RNA were measured. The absence of HCV RNA in serum does not mean complete clearance of HCV, and its value for evaluating antiviral effects and prognosis is limited. Therefore, it is essential to measure the plus and minus strands of HCV RNA in sera and PBMCs simultaneously.

Key words: hepatitis C; RNA, viral; interferon-alpha; antiviral agents

© The Author(s) 1996. Published by Baishideng Publishing Group Inc. All rights reserved.

He YW, Liu W, Zen LL, Xiong KJ, Luo DD. Effect of interferon in combination with ribavirin on the plus and minus strands of HCV RNA in patients with chronic hepatitis C. *World J Gastroenterol* 1996; 2(3): 179-181 Available from: URL: <http://www.wjgnet.com/1007-9327/full/v2/i3/179.htm> DOI: <http://dx.doi.org/10.3748/wjg.v2.i3.179>

INTRODUCTION

Recently, interferon has been used to treat chronic hepatitis C (CHC). Abnormal alanine aminotransferase (ALT) levels become normal in 50%-70% of treated patients, and replication of hepatitis C virus (HCV) RNA in these patients is suppressed to various degrees^[1]. However, approximately 50% of CHC patients experienced post-therapy relapse after interferon withdrawal^[2]. Whether the therapeutic effect of combination of antiviral drugs is superior to monotherapy is rarely reported. In this study, we used interferon in combination with ribavirin to treat patients with CHC and investigated the effect of the combined antiviral therapy on the plus and minus strands of HCV RNA in sera and peripheral blood mononuclear cells (PBMCs) using nested reverse transcription polymerase chain reaction (RT-PCR) and serum ALT.

MATERIALS AND METHODS

Subjects

Twenty-three patients with CHC (29 to 55 years old, nine male and 14 female) were studied. All patients had positive HCV RNA/anti-HCV and fluctuating levels of aminotransferase activities (> 1 year) and did not have any hepatitis B virus (HBV) related markers, positive anti-hepatitis E virus (HEV), and anti-hepatitis A virus (HAV) immunoglobulin (Ig)M. Chronic active hepatitis (CAH) was confirmed in eight of the HCV patients by biopsy. Thirteen of

Table 1 The results of alanine aminotransferase (ALT) and hepatitis C virus (HCV) RNA before and after treatment

Cases	Type	Biopsy	Therapeutic effect	Before therapy			End of therapy			24 wk after therapy		
				HCV Serum	RNA P BMC	ALT U/L	HCV Serum	RNA P BMC	ALT U/L	HCV Serum	RNA P BMC	ALT U/L
1 IFN	CHC	NT	NR	+ (-)	+ (+)	230	+ (-)	+ (+)	77	+ (-)	+ (+)	112
2 IFN	CHC	NT	NR	+ (-)	+ (+)	146	+ (-)	+ (+)	68	+ (-)	+ (+)	57
3 IFN	CHC	CAH	NR	+ (-)	+ (+)	60	+ (-)	+ (+)	50	+ (-)	+ (+)	88
4 IFN	CHC	NT	NR	+ (-)	+ (+)	126	+ (-)	+ (-)	46	+ (-)	+ (+)	97
5 IFN	CHC	CAH	SR	+ (-)	+ (+)	175	- (-)	+ (-)	25	+ (-)	+ (+)	92
6 IFN	CHC	NT	SR	+ (-)	- (-)	108	- (-)	+ (-)	38	+ (-)	+ (-)	66
7 IFN	CHC	NT	SR	+ (-)	+ (+)	88	+ (-)	+ (-)	30	+ (-)	+ (+)	120
8 IFN	CHC	CAH	SR	+ (-)	+ (+)	105	- (-)	- (+)	40	+ (-)	+ (+)	68
9 IFN	CHC	NT	CR	+ (-)	+ (+)	200	- (-)	- (-)	28	- (-)	- (-)	27
10 IFN	CHC	CAH	CR	+ (-)	+ (+)	220	- (-)	- (-)	30	- (-)	- (-)	40
11 I+R	CHC	NT	NR	+ (-)	+ (+)	166	+ (-)	+ (+)	188	+ (-)	+ (+)	100
12 I+R	CHC	NT	NR	+ (-)	+ (+)	250	+ (-)	+ (+)	142	+ (-)	+ (+)	320
13 I+R	CHC	CAH	NR	+ (-)	+ (+)	98	+ (-)	+ (+)	66	+ (-)	+ (+)	146
14 I+R	CHC	CAH	NR	+ (-)	+ (+)	125	- (-)	- (+)	55	- (-)	- (+)	70
15 I+R	CHC	NT	SR	+ (-)	+ (+)	241	- (-)	+ (-)	26	- (-)	- (-)	67
16 I+R	CHC	NT	SR	+ (-)	+ (+)	225	+ (-)	- (+)	31	+ (-)	+ (-)	560
17 I+R	CHC	CAH	SR	+ (-)	- (-)	290	- (-)	+ (-)	20	+ (-)	+ (-)	50
18 I+R	CHC	NT	SR	+ (-)	+ (+)	90	+ (-)	+ (-)	34	+ (-)	+ (+)	60
19 I+R	CHC	NT	SR	+ (-)	+ (+)	110	- (-)	+ (-)	32	+ (-)	+ (+)	72
20 I+R	CHC	NT	CR	+ (-)	- (-)	450	- (-)	- (-)	16	- (-)	- (-)	34
21 I+R	CHC	NT	CR	+ (-)	+ (+)	140	- (-)	- (-)	36	- (-)	- (-)	40
22 I+R	CHC	NT	CR	+ (-)	+ (+)	204	- (-)	- (-)	30	- (-)	- (-)	28
23 I+R	CHC	CAH	CR	+ (-)	- (-)	200	- (-)	- (-)	28	- (-)	- (-)	28

IFN: Interferon; I + R: Interferon and ribavirin; NT: Not tested. Marks in parentheses are the results of minus strand.

them received the combined antiviral therapy, *i.e.*, interferon plus ribavirin (I + R group), which consisted of subcutaneous injection of 3 MU of interferon- α (α -2b interferon, Schering Corporation, Kenilworth, NJ, United States) three times per week for 3 mo and intravenous drip of 1 g of ribavirin (Wuhan Second Pharmaceutical Factory, Wuhan, China) per day during the first month of interferon therapy. The remaining 10 patients received single interferon therapy, as described, as control (IFN group). Serum ALT and plus and minus strands of HCV RNA in sera and PBMCs in all patients were detected before therapy, at the end of therapy, and 24 wk after therapy.

Primers

Primer sequences were selected from the highly conserved 5' noncoding region of the HCV RNA and were synthesized by the Institute of Immunology, Essen University, Germany. Two outer primers were sense: r-kf-10, 5'GGCGACACTCCACCATAGAT and antisense: r-kf-11c, 5'GGTGCACGGTCTACGAGACC. The inner sense primer was r-kf-15: 5'GGAGGATCCACTCCCCTGT, and the antisense primer was r-kf-16a: 5' GGAAAGCTTGAATTCACCCTATCAGGCAGT. The size of the expected amplification product was 295 bp.

Nested RT-PCR

PBMCs were separated by density gradient centrifugation on ficoll hypaque from 4 mL EDTA blood samples and then washed three times in 10 mL of 0.9% NaCl. The extraction of HCV RNA in sera and PBMCs and the synthesis of complementary DNA (cDNA) of the plus and minus strands of HCV RNA were performed, as described previously^[3]. Three microliters of cDNA were added to 25 μ L of PCR reaction mixture and amplified for 40 cycles. Next, 3 μ L of the first PCR products were added to 25 μ L of the second PCR reaction mixture, with inner primer instead of outer primers, and nested RT-PCR was performed in the same way as described above.

Judgement of antiviral effect

The patients were divided into three groups based on changes of HCV RNA and ALT levels before and after antiviral therapy. Patients whose sera ALT level and status of HCV RNA had not changed after antiviral therapy were named nonresponders (NR). Patients whose ALT level decreased to within the normal range, whose plus and/or minus strands of HCV RNA became negative at the end of the treatment, and who experienced post therapy relapse 24 wk after therapy were named short-term responders (SR). The third group consisted of complete responders (CR), who had sustained normal

ALT levels and had undetectable plus and/or minus strands not only at the end of therapy but also 24 wk after cessation of the therapy.

Statistics

Chi-square test was used to statistically analyze the percentages. $P < 0.05$ was considered significant.

RESULTS

Dynamics of ALT levels before and after antiviral therapy

A 295 bp fragment was found in the positive blood samples from the cases and the positive control serum but not in the negative control serum, which was an aliquot from the last wash of PBMCs and PCR reaction mixture without cDNA or primer.

The results (Table 1) showed that by the end of treatment, the increase in ALT levels in nine (69.23%) cases in the I+R group were restored to within the normal range, which took an average of 23.8 days. Of the nine cases, five (55.56%) were SR and four were CR. In the IFN group, the ALT level of six (60.00%) cases decreased to normal, taking an average of 29.6 days. Four (66.67%) of the six cases were SR and two (33.33%) were CR. There were no significant differences between the two groups ($P > 0.05$).

The effect of antiviral therapy on the plus and minus strands of HCV RNA

The minus strand of HCV RNA in sera was negative in all patients. At the end of therapy in the I+R group, the positive rate of the plus strand in sera (92.31%) decreased to 38.46% ($P < 0.05$) and that of the minus strand in PBMCs (76.92%) decreased to 38.46% ($P < 0.05$). In the IFN group, the former decreased from 100% to 50% ($P < 0.05$) and the latter from 90% to 40% ($P < 0.05$). Although the results indicated that antiviral therapy suppressed the reproduction of HCV, the differences between the two groups were not significant ($P > 0.05$). Regarding the percentage of HCV RNA turned negative at the end of the therapy in the I + R group (Table), we found that if the plus strand of HCV RNA in sera alone was tested, HCV RNA of seven (58.33%) cases turned negative; and if the plus and minus strands of HCV RNA in sera and PBMCs were simultaneously tested, HCV RNA of only four (30.77%) cases became negative. Regarding the relationship between HCV RNA and relapse, we found that if the plus strand of HCV RNA in sera alone was tested, HCV RNA of three out of five patients who had relapsed turned negative. When the plus and minus strands of HCV RNA in PBMCs were simultaneously detected, the plus strand of HCV RNA of four out of five and the minus strand of HCV RNA of one out of the five patients remained

positive. These data indicate that the plus strand of HCV RNA in the sera of the three cases turned negative and that HCV was actually not cleared. In contrast, the four cases whose plus and minus strands of HCV RNA in sera and PBMCs remained negative 24 wk after the treatment, no post-therapy relapse occurred.

DISCUSSION

It is now clear that when HCV is replicated, a minus strand of HCV RNA, *i.e.*, the replicative form of HCV RNA, can be detected^[4,5]. Here, we showed that interferon in combination with ribavirin made the replicative form of HCV RNA negative in more than 50% of patients with CHC, confirming that combined antiviral therapy suppressed the replication of HCV. About half of the responders, as defined as those in whom the plus strand of HCV RNA in sera became negative, had relapse after interruption of the treatment. In these patients, however, the plus strand in PBMCs remained positive during and after treatment. Importantly, in the cases that did not have relapse, the plus and minus strands of HCV RNA in sera and PBMCs were both negative, indicating that (1) the absence of HCV RNA in serum did not mean complete clearance of HCV, and its lack of detection was due primarily to the low serum concentration of HCV following antiviral therapy that suppressed the replication of HCV; and (2) HCV in extrahepatic sites, such as PBMCs, is difficult to eliminate, which might serve as a source of reinfection of the liver^[6] and might be one of the causes of relapse. It has been suggested that the value of the plus strand of HCV RNA in sera alone for evaluating the antiviral effect and prognosis is limited. Therefore, it is essential to measure the plus and minus strands of HCV RNA in sera and PBMCs simultaneously to identify complete clearance of HCV.

Falling serum ALT levels means a reduction of hepatocellular damage, which might be related to the ability of antiviral therapy to suppress the replication of HCV or to eliminate HCV. Thus, diminishing or eradicating the viral load of the liver may improve liver disease^[2].

Although the percentage of and average time for restoring ALT

levels to the normal range and the percentage of HCV RNA turned negative in the I + R group were slightly better than those in the IFN group, the differences were not statistically significant. The reasons for this lack of significance might be that (1) the course of treatment with ribavirin was too short or the dosage of ribavirin was too small; and (2) ribavirin could not enhance the antiviral effect of interferon.

ACKNOWLEDGEMENT

We thank Dr. Ferencik S of the Institute of Immunology, University Hospital of Essen, Federal Republic of Germany, for supplying us with primers and other reagents.

REFERENCES

- 1 **Diodati G**, Bonetti P, Noventa F, Casarin C, Rugge M, Scaccabarozzi S, Tagger A, Pollice L, Tremolada F, Davite C. Treatment of chronic hepatitis C with recombinant human interferon-alpha 2a: results of a randomized controlled clinical trial. *Hepatology* 1994; **19**: 1-5 [PMID: 7506223 DOI: 10.1002/hep.1840190102]
- 2 **Gil B**, Qian C, Riezu-Boj JI, Civeira MP, Prieto J. Hepatic and extrahepatic HCV RNA strands in chronic hepatitis C: different patterns of response to interferon treatment. *Hepatology* 1993; **18**: 1050-1054 [PMID: 8225209 DOI: 10.1002/hep.1840180506]
- 3 **He Y**, Liu W, Zeng L. [The effect of interferon in combination with ribavirin on the plus and minus strands of hepatitis C virus RNA in patients with hepatitis]. *Zhonghua Neike Zazhi* 1996; **35**: 32-35 [PMID: 9275644]
- 4 **Fong TL**, Shindo M, Feinstone SM, Hoofnagle JH, Di Bisceglie AM. Detection of replicative intermediates of hepatitis C viral RNA in liver and serum of patients with chronic hepatitis C. *J Clin Invest* 1991; **88**: 1058-1060 [PMID: 1653272 DOI: 10.1172/JCI115368]
- 5 **Bouffard P**, Hayashi PH, Acevedo R, Levy N, Zeldis JB. Hepatitis C virus is detected in a monocyte/macrophage subpopulation of peripheral blood mononuclear cells of infected patients. *J Infect Dis* 1992; **166**: 1276-1280 [PMID: 1385547 DOI: 10.1093/infdis/166.6.1276]
- 6 **Wang JT**, Sheu JC, Lin JT, Wang TH, Chen DS. Detection of replicative form of hepatitis C virus RNA in peripheral blood mononuclear cells. *J Infect Dis* 1992; **166**: 1167-1169 [PMID: 1328405 DOI: 10.1093/infdis/166.5.1167]

S- Editor: Tao T L- Editor: Filipodia E- Editor: Li RF

Recent advances in the application of cultured hepatocytes into bioartificial liver

Xiao-Ping Xu, Ji-Zhen Yang, Yi Gao

Xiao-Ping Xu, Ji-Zhen Yang, Yi Gao, Department of General Surgery, Zhu Jiang Hospital, First Military Medical College, Guangzhou 510282, Guangdong Province, China

Author contributions: All authors contributed equally to the work.

Original title: *China National Journal of New Gastroenterology* (1995-1997) renamed *World Journal of Gastroenterology* (1998-).

Correspondence to: Dr. Xiao-Ping Xu, Department of General Surgery, Zhu Jiang Hospital, First Military Medical College, Guangzhou 510282, Guangdong Province, China

Received: July 8, 1996

Revised: July 24, 1996

Accepted: August 16, 1996

Published online: September 15, 1996

Key words: Bioartificial/Liver; Liver/Cytology

© **The Author(s) 1996.** Published by Baishideng Publishing Group Inc. All rights reserved.

Xu XP, Yang JZ, Gao Y. Recent advances in the application of cultured hepatocytes into bioartificial liver. *World J Gastroenterol* 1996; 2(3): 182-184
Available from: URL: <http://www.wjgnet.com/1007-9327/full/v2/i3/182.htm>
DOI: <http://dx.doi.org/10.3748/wjg.v2.i3.182>

INTRODUCTION

Over the past 3 decades, various experimental liver support systems have been studied. Early artificial liver support systems included hemodialysis, extracorporeal liver perfusion, human cross circulation, charcoal hemoperfusion, hepatodialysis, fresh blood, and plasma exchange transfusion. These systems were developed to remove toxic substances from the blood. Clinical trials showed that these detoxification systems could promote the recovery of consciousness in patients with deep coma, although the survival of patients was not improved. Recently, advances in biotechnology and tissue engineering have brought into focus the importance of biological components for a hybrid artificial liver support system (HALSs). Biological components may include isolated enzymes, cellular components, slices of liver, or cultured hepatocytes. Hepatocyte systems have shown the greatest promise for HALSs. The advantages of hepatocyte systems may be summarized as follows: (1) supplying crucial liver specific metabolic functions; (2) being easily scaled up; (3) having immunoisolation from the host defenses by semipermeable membrane; and (4) being cryopreserved for later use. The disadvantage of hepatocyte systems is the problem of maintaining normal hepatocyte viability and function at high cell density necessary for clinical application. With the development of cell culturing technology and cell engineering technology, great progress has been made in the

research of using cultured hepatocytes as a bioreactor to provide hepatic support.

Current situation of cultured hepatocytes system research

Cultured hepatocytes must maintain good viability and function to be used in HALSs. However, when they are cultured on a plastic surface with standard cell-culture medium, they flatten and become agranular; tissue specific functions are lost in 3 to 5 d, followed by hepatocyte death within 1 to 2 wk^[1]. Therefore, the techniques of cell culture should be improved. The approaches include: (1) addition of growth factors and hormones to culture medium; (2) co-culturing of hepatocytes with nonparenchymal liver cells; (3) using biologic gel or matrix; and (4) cultivation of cells in hollow fiber.

Addition of growth factors and hormones to culture medium

It has been reported that hormones and growth factors, such as insulin, glucagon, dexamethasone, epithelial growth factor (EGF), and hepatocytes growth factor (HGF), may play an important role in modulating the differentiation and proliferation of cultured hepatocytes as well as maintaining tissue-specific functions.

According to Hamad's results, EGF can prolong the survival of cultured hepatocytes and stimulate hepatocyte proliferation^[2]. The DNA contents of hepatocytes were reported to be well preserved in media supplemented with insulin and EGF by Hamad^[2] and Dich *et al*^[3] respectively.

It has also been reported that glucagon is necessary for maintaining the synthesis of urea by cultured hepatocytes for about 2 wk. Moreover, Takahashi *et al*^[4] reported in 1993 that the growth and differentiation functions of hepatocytes cultured at different densities were modulated by EGF and insulin when hepatocytes were cultured at a low cell density of 2.5×10^4 cells/cm². Conversely, cellular functions were induced by hormones at a high cell density of 12.5×10^4 cells/cm², whereas the hepatocyte proliferation was suppressed.

Co-culture with nonparenchymal liver cells (NPC)

Co-culturing is a technique in which two more cell types are cultured together, resulting in cell behavior and physiological responses that would not occur if the cell types were cultured alone. It was first reported by Puck and Marcus in 1955 in studies with Hela cells. One of the most successful methods of co-culturing is using mito-mycin-C-treated "feeder layers" of another cell type (often fibroblasts), which are thought to supply the primary cells with nutrients or factors. Begue *et al*^[5] found that the cytochrome P-450 content in adult rat hepatocytes was maintained over a 10-d period when these cells were co-cultured with another rat liver epithelial cell type.

Use of biologic gel and cell engineering techniques

Hepatocytes are anchorage dependent. Currently, biologic gel, microcarriers, micro-encapsules, and Poly-N-P-Vinylbenzyl-D-

Lactamide (PVLA) are used to culture hepatocytes with high density and slight differentiation.

Immobilized hepatocytes in hydrogel or microencapsule

Miura *et al*^[6] demonstrated the long term maintenance of the capacity to synthesize urea, albumin, and glucose as well as the ability to detoxify hepatic toxins like phenols and fatty acids when isolated hepatocytes were encapsulated within calcium alginate gel. The encapsulating technique can avoid immunological hazards and maintain the cellular function of isolated hepatocytes. Micro-encapsulated hepatocytes are mainly used in hepatocytes transplantation, and HALSs produced using such cells would be large and, therefore, inconvenient for clinical use.

Microcarrier hepatocytes

Van Wezel reported the microcarrier technique in 1967. It has the advantage of increasing the adhesive area of culturing cells (the surface area of 1 g dextran is 0.6 m²), thus facilitating transplantation of large quantities of hepatocytes in very small volumes of microcarrier suspension. Being cultured on the collagen-covered microcarriers, hepatocytes can maintain long-term cellular function and growth. Kasai *et al*^[7] found that the metabolic activity of rat hepatocytes attached to collagen-coated multiporous cellulose microcarriers can be preserved for at least 1 week. Nezuil *et al*^[8] developed a HALSs using porcine hepatocytes attached to microcarriers and placed on the outer surface of hollow fibers. The HALSs was used to treat a 33-year-old male patient with alcohol induced cirrhosis. The patient's mental status greatly improved 2 h after initiation of HALSs treatment. Three weeks later, the patient's liver function improved gradually and steadily. He underwent orthotopic liver transplantation 6 months later.

PVLA hepatocytes

Recently, rapid progress has been made in research on using PVLA to culture hepatocytes. In hepatocytes cultured on the PVLA coated dishes, growth and functional activity was regulated by the simulated three-dimensional environment *in vivo*^[9]. Hepatocytes cultured on PVLA coated dishes are able to maintain a high level of differentiation functions and longevity because PVLA has the ligand, β -galactose for asialoglycoprotein receptors on hepatocytes^[10,11]. Kobayashi *et al*^[12] found that the regulation of differentiation function and proliferation of hepatocytes is low for cells cultured on dishes coated with high level PVLA (200 μ g/mL) and is high for those with low level PVLA (1 μ g/mL). Moreover, bile acid release was maintained at higher levels in hepatocytes attached on dishes coated with a high level of PVLA.

Toke *et al*^[13] found that the hepatocytes initially attached onto PVLA substratum and then migrated together to form multilayer aggregations by the stimulation of growth factors, such as EGF and insulin. They observed many orifices of tube-like structures on the surface of the multilayer aggregation by scanning electron microscopic analysis. Transmission electron microscopic analysis of the aggregation revealed the maintenance of endoplasmic reticulum and the appearance of bile canaliculi-like structure. This tissue-reconstruction of primary cultured rat hepatocytes exhibited long-term maintenance of specific cellular functions, such as the secretion of albumin and bile acid, and retained mitochondrial enzyme activity. These data showed that PVLA could potentiate the differentiation and proliferation of hepatocytes. However, hepatocytes cultured with high proliferation and high maintenance of differentiation function could not be achieved with the same coating concentration. Further refinement of the PVLA hepatocytes systems is expected to assist in the development of HALSs.

Hollow fiber hepatocytes

Hollow fiber hepatocyte bioreactors consists of two compartments: (1) an intraluminal compartment within the fibers and (2) an extraluminal compartment outside the fibers and within the rigid housing. Hepatocytes are cultured within the extraluminal compartment, and the patient's blood is circulated within the capillaries. Through pores in the walls of the hollow fiber, communication between the compartments occurs. Toxic substance

in the patient's blood permeates through the pores and is acted on by the hepatocytes attached on the hollow fibers.

Hollow fiber systems have several advantages, such as immunological separation between the patient and the support hepatocytes and providing a large membranous area for hepatocytes to attach. Recently, several versions of hollow fiber membrane based systems have been reported in the literature^[14-16]. Sussman *et al*^[15] cultured a CAS cell line on the fibers, and Nyberg *et al*^[16] proposed a novel hollow fiber based HALSs. The primary hepatocytes were entrapped in cylindrical gels inside the lumen of the hollow fibers.

Recent experimental studies with these devices have demonstrated their efficacy in animal models of acute liver failure. Rozga *et al*^[17] treated seven patients with acute liver failure with a HALSs based on hollow fiber bioreactor. These patients recovered gradually and underwent liver transplantation. However, randomized clinical trials are still needed to evaluate these forms of HALSs.

Problems and future aspects of the cultured hepatocytes systems

In the last 5 years, research on cultured hepatocytes in bioartificial liver has made rapid progress with the aid of recent advances in cryobiology and tissue culture. Isolated hepatocytes or differentiated cell lines can be cultured at a density of 10⁷/mL. However, for clinically applicable HALSs, the cell density needs to be increased to 10⁸/mL. Therefore, much effort should be made to obtain the effective HALSs.

As mentioned above, only hepatocytes have been used in HALSs to date. Nonparenchymal liver cells were confined to co-culturing. Some experts proposed that the ideal HALSs may be developed with co-cultured hepatocytes systems. Thus, further studies are needed to ascertain its feasibility.

The development of HALSs is still in its infancy. Some of the HALSs designs using cultured hepatocytes have satisfied the rigors of animal testing and now are being studied in phase I clinical trials. We expect that the randomized clinical trials will establish the value of bioartificial liver therapy for patients with hepatic failure.

REFERENCES

- 1 Reid LM, Jefferson DM. Culturing hepatocytes and other differentiated cells. *Hepatology* 1984; **4**: 548-559 [PMID: 6373552 DOI: 10.1002/hep.1840040332]
- 2 Hamad T. The functional evaluation of plated pig hepatocyte monolayers for hybrid artificial liver. *Acta Hepato Jpn* 1990; **31**: 669-677 [DOI: 10.2957/kanzo.31.669]
- 3 Dich J, Vind C, Grunnet N. Long-term culture of hepatocytes: effect of hormones on enzyme activities and metabolic capacity. *Hepatology* 1988; **8**: 39-45 [PMID: 3276589 DOI: 10.1002/hep.1840080109]
- 4 Takahashi M, Matsue H, Matsushita M, Nakajima Y, Uchino J. Isolation and culture of human hepatocytes from resected liver tissue as a bioreactor for a hybrid artificial liver. *Artif Organs* 1993; **17**: 653-659 [PMID: 8338442 DOI: 10.1111/j.1525-1594.1993.tb00610.x]
- 5 Begue JM, Guguen-Guillouzo C, Pasdeloup N, Guillouzo A. Prolonged maintenance of active cytochrome P-450 in adult rat hepatocytes co-cultured with another liver cell type. *Hepatology* 1984; **4**: 839-842 [PMID: 6434390 DOI: 10.1002/hep.1840040507]
- 6 Miura Y, Akimoto T, Fuke Y, Yamazaki S, Yagi K. In vitro maintenance of terminal-differentiated state in hepatocytes entrapped within calcium alginate. *Artif Organs* 1987; **11**: 361-365 [PMID: 3689172 DOI: 10.1111/j.1525-1594.1987.tb00946.x]
- 7 Kasai S, Sawa M, Nishida. Cellulosic micro-carriers for high-density culture of hepatocytes. *Transplant Proc* 1991; **24**: 2960-2961
- 8 Neuzil DF, Rozga J, Mosconi AD, Ro MS, Hakim R, Arnaout WS, Demetriou AA. Use of a novel bioartificial liver in a patient with acute liver insufficiency. *Surgery* 1993; **113**: 340-343 [PMID: 8441969]
- 9 Sato Y, Ochiya T, Yasuda Y, Matsubara K. A new three-dimensional culture system for hepatocytes using reticulated polyurethane. *Hepatology* 1994; **19**: 1023-1028 [PMID: 8138242]
- 10 Akaike T, Kobayashi A, Kobayashi Y, Matsumoto A. Separation of parenchymal liver cells using a lactose substituted styrene polymer substratum. *J Bioactive Compatible Polymers* 1989; **4**: 51-56 [DOI: 10.1177/088391158900400106]
- 11 Kobayashi A, Goto M, Sekine T, Masumoto A, Yamamoto N, Kobayashi K, Akaike T. Regulation of differentiation and proliferation of rat hepatocytes by lactose-carrying polystyrene. *Artif Organs* 1992; **16**: 564-567 [PMID: 1482325 DOI: 10.1111/j.1525-1594.1992.tb00553.x]
- 12 Kobayashi A, Tokei Y, Tobe S, Goto M, Sekine T, Matsumoto A. Induction of liver-tissue reconstruction in primary cultured rat hepatocytes by non-parenchymal liver cells. *Artif Organs* 1991; **15**: 296
- 13 Kobayashi A, Tokei Y, Tobe S, Goto M, Kobayashi K, Akaike T. Tissue-

- reconstruction of primary cultured rat hepatocytes on asialoglycoprotein model polymer for hybrid artificial liver. *Artif Organs* 1991; **15**: 324
- 14 **Takeshita K**, Ishibashi H, Suzuki M, Yamamoto T, Akaike T, Kodama M. High cell-density culture system of hepatocytes entrapped in a three-dimensional hollow fiber module with collagen gel. *Artif Organs* 1995; **19**: 191-193 [PMID: 7763200 DOI: 10.1111/j.1525-1594.1995.tb02310.x]
- 15 **Sussman NL**, Chong MG, Koussayer T, He DE, Shang TA, Whisennand HH, Kelly JH. Reversal of fulminant hepatic failure using an extracorporeal liver assist device. *Hepatology* 1992; **16**: 60-65 [PMID: 1618484 DOI: 10.1002/hep.1840160112]
- 16 **Nyberg SL**, Shatford RA, Peshwa MV, White JG, Cerra FB, Hu WS. Evaluation of a hepatocyte-entrapment hollow fiber bioreactor: a potential bioartificial liver. *Biotechnol Bioeng* 1993; **41**: 194-203 [PMID: 18609538 DOI: 10.1002/bit.260410205]
- 17 **Rozga J**, Podesta L, LePage E, Morsiani E, Moscioni AD, Hoffman A, Sher L, Villamil F, Woolf G, McGrath M. A bioartificial liver to treat severe acute liver failure. *Ann Surg* 1994; **219**: 538-544; discussion 544-546 [PMID: 8185403 DOI: 10.1097/00000658-199405000-00012]

S- Editor: A L- Editor: Filipodia E- Editor: Li RF



Combination assay for serum tumor markers in patients with hepatic carcinoma

Shuang-Luo Zhao, Xiu-Feng Pan, Su-Xiao Li, Dong-Gang Liu

Shuang-Luo Zhao, Xiu-Feng Pan, Su-Xiao Li, Department of Medicine, Hebei Provincial People's Hospital, Shijiazhuang 050071, Hebei Province, China

Dong-Gang Liu, Clinical Assay Center of Hebei Medical University, Shijiazhuang 050071, Hebei Province, China

Shuang-Luo Zhao, Associate Professor, engaged in digestive disease studies, has 33 papers published.

Author contributions: All authors contributed equally to the work.

Original title: *China National Journal of New Gastroenterology* (1995-1997) renamed *World Journal of Gastroenterology* (1998-).

Correspondence to: Dr. Shuang-Luo Zhao, Department of Medicine, Hebei Provincial People's Hospital, Shijiazhuang 050071, Hebei Province, China
Telephone: +86-0311-7046996

Received: December 20, 1995

Revised: May 25, 1996

Accepted: July 16, 1996

Published online: September 15, 1996

Key words: Liver neoplasms; Tumor markers; Biological

© **The Author(s) 1996.** Published by Baishideng Publishing Group Inc. All rights reserved.

Zhao SL, Pan XF, Li SX, Liu DG. Combination assay for serum tumor markers in patients with hepatic carcinoma. *World J Gastroenterol* 1996; 2(3): 185-186
Available from: URL: <http://www.wjgnet.com/1007-9327/full/v2/i3/185.htm>
DOI: <http://dx.doi.org/10.3748/wjg.v2.i3.185>

INTRODUCTION

In general, hepatic solid space occupying lesions (HSSOL) can be found by both ultrasonoscopy (US) and computed tomography (CT). If the customary alpha-fetoprotein (AFP) standard for diagnosis of primary hepatic carcinoma is used, those cancers with lower AFP concentration may go undiagnosed^[1]. On the other hand, using the standard AFP-positive ($\geq 20 \mu\text{g/L}$) + HSSOL to diagnose primary hepatocellular carcinoma (PHCC) may yield false positive results^[2, 3]. In order to elevate both the preoperative and differential diagnosis levels for hepatic carcinoma, we assayed the preoperative levels of serum AFP, carbohydrate antibody (CA) 19-9, and carcinoembryonic antigen (CEA) in patients with HSSOL.

SUBJECTS AND METHODS

Subjects

Four groups of patients (30 patients in each group) with benign HSSOL (BHSSOL group; including 17 cases of hepatic cyst, 10 of benign hepatic tumor, and three of hepatic tuberculosis), secondary hepatic carcinoma (SHC group; the cancer stemmed from the

stomach in 12 cases; the pancreas in eight cases; the colon in seven cases; the bile duct in two cases; and the uterus in one case), primary non-hepatocellular carcinoma (PNHCC group; including 29 cases of intrahepatic duct cell carcinoma and one case of mixed type cancer), and primary hepatocellular carcinoma (PHCC group) were verified by percutaneous transhepatic biopsy and/or hepatic postoperative pathology. All patients met the following criteria: (1) HSSOL was confirmed by US or CT. (2) The peripheral venous blood samples were collected before the operation. The concentrations of serum AFP, CA19-9, and CEA were assayed. Patients with serum AFP levels between $20 \mu\text{g/L}$ and $200 \mu\text{g/L}$ were reexamined by the same method 1 mo later. And (3) The main organs, including stomach, pancreas, biliary tree, colon, lung, kidney, uterus, etc. were examined by endoscopy, X-ray, or CT combined with biopsy to check for the existence of tumor lesions. In this series, 74 patients were male and 46 were female, and they were between 17 and 76 years old, with a mean age of 53.5.

Methods

CA19-9 radioimmunoassay (RIA) kit was purchased from Symtron (USA), and other kits were provided by the Institute of Chinese Atomy (China). Serum AFP, CA19-9, and CEA levels were measured according to the manufacturer's protocols.

Judging

Serum AFP $\geq 200 \mu\text{g/L}$ or between $20 \mu\text{g/L}$ and $200 \mu\text{g/L}$, which was enhanced or unchanged after 1 month, was defined as AFP positive. Antigen levels higher than the cutoff value (serum CA19-9 $\geq 37 \text{ KU/L}$ and CEA $\geq 15 \mu\text{g/L}$) or a single item two times higher than the cutoff value were considered positive.

Statistical analysis

Analysis of variance was used for the multivariant measurement data, and a *t* test was used to make comparisons between two groups.

RESULTS

Serum AFP

Using a cutoff value of $20 \mu\text{g/L}$, the sensitivity of AFP to PHCC was 100% (30/30 cases, Table 1), and the specificity was 85.7% (78/90 cases). With a cutoff of $200 \mu\text{g/L}$, the sensitivity was 76.7% (23/30 cases), and the specificity was 100% (90/90 cases).

Serum CA19-9

With a cutoff value of 37 KU/L for CA19-9, the sensitivity in detecting PNHCC was 93.3% (28/30 cases, Table 1), and the specificity was 65.6% (59/90 cases). In SHC, the sensitivity and specificity of CA19-9 were 90.0% (27/30 cases) and 63.3% (57/90 cases), respectively. At a cutoff value of 74 KU/L , the sensitivity and specificity of CA 19-9 were 43.3% (13/30 cases) and 77.8% (70/90 cases), respectively, in detecting PNHCC, and 13.3% (18/30 cases)

Table 1 Comparison serum alpha-fetoprotein, carbohydrate antibody19-9 and carcinoembryonic antigen in patients with hepatic solid space occupying lesions ($\bar{x} \pm s$)

Grouping	n	AFP (μg/L)	CA19-9 (KU/L)	CEA (μg/L)
1 BHSSOL	30	11.07 ± 4.30	28.43 ± 15.76	10.49 ± 6.93
2 SHC	30	15.23 ± 13.13	231.20 ± 196.64	27.08 ± 13.35
3 PNHCC	30	14.03 ± 8.13	169.67 ± 140.08	19.27 ± 8.67
4 PHCC	30	320.65 ± 180.12	23.73 ± 12.91	10.73 ± 3.94

Notes: The comparison of AFP levels between group 4 and groups 1, 2, and 3: $P < 0.01$; among groups 1, 2, and 3: $P > 0.05$. CA 19-9 levels in groups 2 and 3 were higher than those in groups 1 and 4: $P < 0.01$; between group 2 and 3 and between group 1 and 4: $P > 0.05$. CEA levels in groups 2 and 3 were higher than those in groups 1 and 4 ($P < 0.01$); between group 2 and 3 and between group 1 and 4: $P > 0.05$. AFP, alpha-fetoprotein; BHSSOL, benign HSSOL; CA19-9, carbohydrate antibody 19-9; CEA, carcinoembryonic antigen; HSSOL, hepatic solid space occupying lesion; PHCC, primary hepatocellular carcinoma; PNHCC, primary non-hepatocellular carcinoma; SHC, secondary hepatic carcinoma

Table 2 Serum alpha-fetoprotein and carbohydrate antibody19-9 + carcinoembryonic antigen in patients with hepatic solid space occupying lesions

Grouping	No. of cases	AFP		CA19-9 + CEA	
		Positive	Negative	Positive	Negative
BHSSOL	30	0	30	0	30
SHC	30	3	27	30	0
PNHCC	30				
Biliary cell cancer	29	0	29	29	0
Mixed cancer	1	1	0	1	0
PNCC	30	30	0	0	30

and 81.1% (73/90 cases), respectively, in detecting SHC.

Serum CEA

At a cutoff of 15 μg/L, the sensitivity of CEA in detecting PNHCC was 73.3% (22/30 cases, Table 1), and the specificity was 63.3% (58/90 cases). In SHC, the sensitivity and specificity were 80.0% (24/30 cases) and 66.7% (53/90 cases), respectively. At a cutoff of 30 μg/L, the sensitivity and specificity of CEA were 16.7% (5/30 cases) and 84.4% (76/90 cases), respectively, in detecting PNHCC; and 13.3% (18/30 cases) and 83.3% (75/90 cases), respectively, in detecting SHC.

Combined assay

The results from the combined assay are shown in Table 2. With US, X-ray, CT, and endoscopy in combination with biopsy, 29 cases (96.7%) of extrahepatic primary cancer nests were clinically discovered in the SHC group; and four cases (13.3%) of extrahepatic transition cancer nests were discovered in the PNHCC group. The difference between the two groups was significant ($P < 0.05$, Table 2).

DISCUSSION

There are four types of HSSOL, namely, PHCC, PNHCC, SHC, and BHSSOL. We found that serum AFP level was much higher in PHCC than in the other three types ($P < 0.01$, Table 1), while there was no statistically significant difference among the other three groups ($P > 0.05$). By raising the cutoff value of AFP, the specificity for detecting cancer was improved, but the sensitivity was reduced. Using the standard in our study (serum AFP ≥ 200 μg/L or between 20 μg/L and 200 μg/L, which was elevated 1 mo later), specificity and sensitivity for diagnosing PHCC were the highest. Therefore, we recommend that this standard be adopted as the diagnosis standard of PHCC. Assaying serum AFP level helps to differentiate PNHCC and SHC from BHSSOL and PHCC. Serum CA19-9 levels were much higher in the SHC and PNHCC groups than in PHCC and BHSSOL groups ($P < 0.01$). CA19-9 is a gastrointestinal tumor marker, and its content is the highest in tumor epithelial cells of the digestive tract^[4,5]. Since PNHCC is an abdominal adenocarcinoma, the serum CA19-9 level in PNHCC is elevated, which is normal in PHCC and BHSSOL. Therefore, these diseases can be differentiated by assaying serum CA19-9 levels. Serum CEA levels were higher in the PNHCC and SHC groups than in the PHCC and BHSOL groups ($P < 0.01$). It has been reported that serum levels of CEA might be elevated significantly in patients with digestive tract tumors 2-18

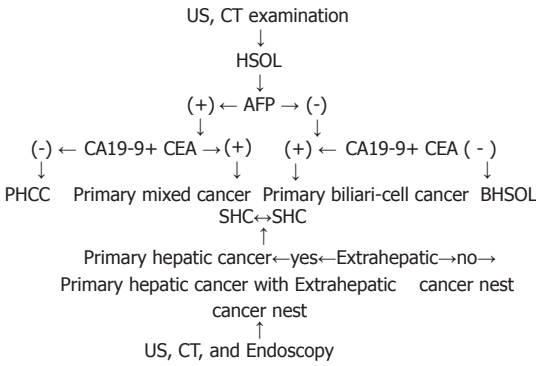


Figure 1 A flow chart for preoperative and differential diagnosis of hepatic carcinoma.

mo before the lesions were found clinically by X-ray examination^[6,7]. CEA is an important marker for the diagnosis of liver metastasis. Sometimes the level of CEA is elevated by 100% in patients with hepatic metastasis. CEA may also be a marker of intestinal tumors. Therefore, we can assay serum CEA levels to differentiate between SHC and PNHCC, and BHSSOL and PHCC.

As shown in Table 2, negative-AFP and positive CA 19-9 + CEA occurred in 90% of SHC and primary biliary cell cancer (96.7%) among PNHCC. Both positive AFP and CA19-9 + CEA occurred in 10% of SHC and mixed cancer (3.3%) among PNHCC. SHC usually originated from the tumors of lower organs, *i.e.*, stomach, colon, pancreas, biliary tree, *etc.* As some of the tumors of the digestive system belong to hepatoid adenocarcinomas in SHC, AFP levels were positive^[8]. Nagai *et al*^[9] reported that serum AFP was elevated in 5.4% of gastric carcinoma, and liver metastasis occurred in 72% of these patients. The appearances of SHC and PNHCC intersect, making differentiation between the two difficult. Our study indicates that extrahepatic cancer nests (OTCN) are more common in SHC than in PNHCC ($P < 0.01$). In general, patients with OTCN discovered by US, CT, X-ray, and endoscopy may be considered to have SHC, while those without OTCN may be considered to have PNHCC. Strictly speaking, however, OTCH transferred from primary hepatic cancer should be differentiated from primary OTCN by pathologic examination alone. Based on the above results, the procedure of early diagnosis and differential diagnosis of hepatic carcinoma is shown by the Figure 1. By detecting serum levels of AFP, CA19-9, and CEA in patients with BHSSOL, preoperative and differential diagnosis of PHCC, PNHCC, SHC, and BHSSOL might be improved.

REFERENCES

- 1 Ma ZC, Tang BH, Tang JY and Ye KL. Studies on diagnostic criteria of hepatocellular carcinoma with positive AFP. *Zhonghua Xiaohau Zazhi* 1993; **13**: 286
- 2 Li WD. Deliberation to diagnostic criteria of the formula: "AFP+SOL=HCC". *Zhonghua Xiaohau Zazhi* 1994; **14**: 262
- 3 Filella X, Fuster J, Molina R, Grau JJ, García-Valdecasas JC, Grande L, Estapé J, Ballesta AM. TAG-72, CA 19.9 and CEA as tumor markers in gastric cancer. *Acta Oncol* 1994; **33**: 747-751 [PMID: 7993641 DOI: 10.3109/02841869409083943]
- 4 Satake K, Takeuchi T. Comparison of CA19-9 with other tumor markers in the diagnosis of cancer of the pancreas. *Pancreas* 1994; **9**: 720-724 [PMID: 7846015 DOI: 10.1097/00006676-199411000-00008]
- 5 Pasquali C, Sperti C, D'Andrea AA, Costantino V, Filipponi C, Pedrazzoli S. CA50 as a serum marker for pancreatic carcinoma: comparison with CA19-9. *Eur J Cancer* 1994; **30A**: 1042-1043 [PMID: 7946572 DOI: 10.1016/0959-8049(94)90154-6]
- 6 Guadagni F, Roselli M, Cosimelli M, Spila A, Cavaliere F, Arcuri R, Abolito MR, Greiner JW, Schlom J. Biologic evaluation of tumor-associated glycoprotein-72 and carcinoembryonic antigen expression in colorectal cancer, Part I. *Dis Colon Rectum* 1994; **37**: S16-S23 [PMID: 8313787 DOI: 10.1007/bf02048426]
- 7 Koizumi F, Odagiri H, Fujimoto H, Kawamura T, Ishimori A. [Clinical evaluation of four tumor markers (CEA, TPA, CA50 and CA72-4) in colorectal cancer]. *Rinsho Byori* 1992; **40**: 523-528 [PMID: 1507478]
- 8 Chang YC, Nagasue N, Abe S, Taniura H, Kumar DD, Nakamura T. Comparison between the clinicopathologic features of AFP-positive and AFP-negative gastric cancers. *Am J Gastroenterol* 1992; **87**: 321-325 [PMID: 1371637]
- 9 Nagai E, Ueyama T, Yao T, Tsuneyoshi M. Hepatoid adenocarcinoma of the stomach. A clinicopathologic and immunohistochemical analysis. *Cancer* 1993; **72**: 1827-1835 [PMID: 7689918 DOI: 10.1002/1097-0142(19930915)72:6<1827::AID-CNCR2820720606>3.0.CO;2-8]



Published by **Baishideng Publishing Group Inc**
8226 Regency Drive, Pleasanton, CA 94588, USA
Telephone: +1-925-223-8242
Fax: +1-925-223-8243
E-mail: bpgoffice@wjgnet.com
Help Desk: <http://www.wjgnet.com/esps/helpdesk.aspx>
<http://www.wjgnet.com>



ISSN 1007-9327

